

**The unfolded protein response pre and post
methanol induction of *Komagataella (Pichia)*
pastoris producing secretory Insulin precursor**

**Von der Naturwissenschaftlichen Fakultät
der Gottfried Wilhelm Leibniz Universität Hannover**

zur Erlangung des Grades
Doktor der Naturwissenschaften
Dr. rer. nat.

genehmigte Dissertation

von

Gustavo Roth,
Mestre em Biologia Celular e Molecular (Brasilien)

geboren am 25.09.1986 in Caxias do Sul/RS, Brasilien

2015

Referentin: Prof. Dr. rer. nat. Ursula Rinas

Korreferent: Prof. Dr. rer. nat. Thomas Scheper

Tag der Promotion: 21.09.2015

Erklärung

Hiermit erkläre ich, dass ich meine Dissertation mit dem Titel „*The unfolded protein response pre and post methanol induction of Komagataella (Pichia) pastoris producing secretory Insulin precursor*“ selbständig verfasst und die benutzten Hilfsmittel und Quellen sowie gegebenenfalls die zu Hilfeleistungen herangezogenen Institutionen vollständig angegeben habe. Die Dissertation wurde nicht schon als Masterarbeit, Diplomarbeit oder andere Prüfungsarbeit verwendet. Alle Stellen der Arbeit, die anderen Werken dem Wortlaut oder dem Sinn nach entnommen wurden, sind kenntlich gemacht.

Hannover, July 2015

Gustavo Roth

Declaration

The work described in this thesis was carried out in the period from October 2012 to July 2015. One part of the experimental work was carried out in the Helmholtz-Zentrum für Infektionsforschung, Braunschweig; the majority of the experimental and theoretical work was performed at the Leibniz University of Hannover, under the supervision of Prof. Dr. Ursula Rinas at the Institute of Technical Chemistry, Hannover. I hereby declare that this submission is my own work and that, to the best of my knowledge and belief, it contains no material previously published or written by another person nor material which has been accepted for the award of any other degree or diploma of the university or other institute of higher learning, except where due acknowledgment has been made in the text.

Hannover, July 2015

Gustavo Roth

Acknowledgements

This Doctoral Thesis was developed in the Institut für Technische Chemie (TCI) of the Gottfried Wilhelm Leibniz Universität Hannover (LUH) in collaboration with the Helmholtz-Zentrum für Infektionsforschung GmbH (HZI) in Braunschweig by means of the National Council of Technological and Scientific Development (CNPq - Brazil) and the Brazilian



Figure 1.1 – Fellowship sponsors.

Federal program Science without Borders (CsF), Doctorate fellowship number 200661/2012-4, with duration of 36 months, starting in October 2012 up to September 2015. CsF is a program that seeks to promote the consolidation, expansion and internationalization of science and technology, innovation and Brazilian competitiveness through the exchange and international mobility.

I would like to express my deepest appreciation to my supervisor Prof. Dr. Ursula Rinas. I also express my sincere gratitude towards my co-supervisor Prof. Dr. Thomas Scheper. Thank you both for providing all the necessary resources to complete my thesis. I am also very grateful to the HZI Braunschweig personal for their valuable technical support: Dr. Heinrich Lünsdorf, Dr. Manfred Nimtz, Dipl.-Ing Wolfgang Kessler, Dipl.-Ing. Steffen Bernecker, Andrew Perreth, Axel Schulz, Burkhard Ebert and Reinhard Sterlinski. During my project I have been fortunate to work with other highly qualified persons from the TCI Hannover, my sincere thanks to: Dr. David Bulnes Abundis, Dr. Zhaopeng Li, Dr. Sascha Beutel, Dr. Tim Lücking, Dr. Satish Kumar Nemani, Dr. Ana Letícia de Souza Vanz, Dr. Steffen Henkel, M. Sc. Daniel Marquard, M. Sc. Anne Stamm, M. Sc. Christoph Busse, Dipl.-Chem. Bettina Carstensen, M. Sc. André Jochums, M. Sc. Gesa Nöhren, M. Sc. Philipp Grünert, Maxi Bär and Martina Weiß. I would like to express my heartfelt gratitude to Dr. Diogenes S. Santos for encouraging me on pursuing the Doctoral thesis abroad. Finally, I would like to express my most sincere gratitude to my wife Dra. Candida Deves Roth and family for constant motivation, love and support. I dedicate this thesis to our lovely coming son, Antônio.

Abstract

The methylotrophic yeast *Pichia pastoris* is an established eukaryotic expression system for the production of heterologous proteins of biopharmaceutical or industrial interest, due to its stable cheap production processes and the good protein secretion abilities. Endoplasmic reticulum (ER)-resident or secretory heterologous protein production usually leads to an unfolded protein response (UPR), through augmented level of chaperones such as Kar2, and to formation of reactive oxygen species (ROS). To improve product titers in an efficient manner, cellular stress responses before and after methanol-induced recombinant proteins production has to be attended in a comprehensive way. Monitoring the main UPR marker Kar2 during the defined medium glycerol growth batch phase, allowed the identification of a sudden and strong ~20 fold downregulation of this ER-resident chaperone from exponential growth phase to stationary phase. High Kar2 levels in exponentially growing cells were observed in culture media with initial glycerol concentrations ranging from 30 to 125 g/L and were suggested to be caused due to an overlapped effect of high osmolarity and high specific growth rates. Additionally, high Kar2 levels prior to methanol induction presented no positive correlation with the secretory Insulin precursor (IP) production assessed by inducing the cells at different glycerol batch time points. Although no clear relation between UPR prior induction and product titer was identified, intracellular and extracellular Kar2 was produced exclusively due to recombinant protein production since after induction no Kar2 was detected in either fraction of the control host strains. Furthermore, methanol induction of *Pichia pastoris* IP producing cells at stationary growth phase resulted in the highest amounts of *de novo* synthesized Kar2 and, under industrial relevant bioreactor conditions, increasing methanol concentrations applied during fed-batch hastened the chaperone secretion. Further results pointed out to a positive correlation of recombinant protein production and augmented ROS levels during the methanol fed-batch phase and to an independence of phase of glycerol growth at induction time and ROS levels for the secretory IP producing strain. Moreover, cells presented high viability during the entire fed-batch process (> 93 %). A deeper comprehension of the nature of UPR is fundamental to improve *P. pastoris* strains performance in various biotechnological processes. Therefore, the herein presented results are a valuable contribution which could be used to guide general models for protein secretion and used for engineering design of new cell factories.

Keywords: *Komagataella (Pichia) pastoris*, recombinant protein production, unfolded protein response

Zusammenfassung

Die methylothrophe Hefe *Pichia pastoris* ist ein bewährtes eukaryotisches Expressionssystem für die Produktion von heterologen Proteinen, welche interessant für biopharmazeutische und industrielle Anwendungen sind, da dieses Expressionssystem einen stabilen und günstigen Produktionsprozess ermöglicht und gute sekretorische Eigenschaften besitzt. Die am endoplasmatischen Reticulum (ER) ansässige Proteinfaltung oder die sekretorische heterologe Proteinproduktion führen normalerweise zu einer ungefalteten Proteinantwort (*unfolded protein response, UPR*) durch eine erhöhten Spiegel an Chaperonen, wie Kar2, und auch zu der Bildung von reaktiven Sauerstoffspezies (*reactive oxygen species, ROS*). Um den Produkttiter effizient zu erhöhen, muss die zelluläre Stressantwort vor und nach der Methanol-induzierten rekombinanten Proteinproduktion umfassend betrachtet werden. Durch die Beobachtung des Hauptindikators für eine UPR, Kar2, während der Glycerin Batch-Wachstumsphase in definiertem Medium, konnte die plötzliche und sehr starke ca. 20-fache Herabregulation dieses ER-ansässigen Chaperones beim Übergang der exponentiellen Wachstumsphase zur stationären Phase festgestellt werden. Ein hoher Kar2 Level in exponentiell wachsenden Zellen konnte in Kulturmedien mit einer Anfangsglycerinkonzentration von 30 bis 120 g/L beobachtet werden. Es wird angenommen, dass dieser hohe Kar2 Level auf einen überlappenden Effekt von hoher Osmolarität und hohen spezifischen Wachstumsraten zurückzuführen ist. Zusätzlich hat ein hoher Kar2 Spiegel vor der Induktion mit Methanol keine positive Korrelation mit der Produktion des sekretorischen Insulinvorläufers gezeigt, unabhängig davon zu welchem Zeitpunkt der Glycerin Batch-Phase die Zellen induziert wurden. Trotzdem, dass keine Relation zwischen der UPR vor Induktion und des Produkttiters festgestellt wurde, trat intrazelluläres und extrazelluläres Kar2 nur aufgrund der rekombinanten Proteinproduktion auf, da nach Induktion Kar2 in keiner der Fraktionen des Kontrollwirtsstammes detektiert werden konnte. Desweiteren führte die Methanolinduktion von Insulinvorläufer produzierenden *Pichia pastoris* Zellen während der stationären Wachstumsphase zu der höchsten Menge an *de novo* synthetisiertem Kar2. Zudem hatte unter industriell relevanten Reaktorbedingungen eine erhöhte Methanolkonzentration während der Fed-Batch-Phase eine beschleunigte Chaperonsekretion zur Folge. Weitere Ergebnisse lassen auf eine positive Korrelation zwischen rekombinanter Proteinproduktion und eines erhöhten Spiegels an ROS während der Methanol Fed-Batch Phase schließen. Zusätzlich lassen sie Rückschlüsse auf eine Unabhängigkeit des Induktionszeitpunktes während der Glycerin Wachstumsphase und der Menge der ROS im Produktionsstamm des sekretorischen Insulinvorläufers zu. Außerdem zeigten die Zellen eine hohen Viabilität (> 93 %) während des gesamten Fed-Batch-Prozesses. Ein tiefgehendes Verständnis der Eigenschaften der UPR ist entscheidend um die Leistung des *P. pastoris* Stammes in den unterschiedlichsten biotechnologischen Prozessen zu verbessern. Aus diesem Grund sind die hier dargestellten Ergebnisse ein wertvoller Beitrag, der dazu genutzt werden kann, allgemeine Modelle für Proteinproduktion zu schaffen und zudem können die Erkenntnisse für eine konstruktive Entwicklung von sogenannten „cell factories“ genutzt werden.

Stichwörter: *Komagataella (Pichia) pastoris*, Rekombinante Proteinproduktion, ungefalteten Proteinantwort

Table of contents

| | |
|--|------------|
| Abstract | VI |
| Zusammenfassung | VII |
| 1. Introduction | 11 |
| 2. Theoretical background | 12 |
| 2.1. Diabetes..... | 12 |
| 2.2. Insulin | 13 |
| 2.3. <i>Pichia pastoris</i> as expression system..... | 16 |
| 2.4. Regulation of protein folding and ER stress | 17 |
| 2.4.1. The ER-resident protein folding machinery..... | 20 |
| 2.4.1.1. Immunoglobulin heavy chain binding protein – Kar2..... | 21 |
| 2.4.2. The unfolded protein response (UPR) | 23 |
| 2.5. Environmental stresses..... | 25 |
| 2.6. Oxidative stress..... | 27 |
| 3. Aim of this work | 29 |
| 4. Methods | 30 |
| 4.1. Water and sterile work | 30 |
| 4.2. Strain and vector | 30 |
| 4.3. Optical density and determination of cell concentration | 30 |
| 4.4. <i>Pichia pastoris</i> cultures..... | 31 |
| 4.4.1. Shake flask cultivations | 31 |
| 4.4.2. Bioreactor cultivations | 32 |
| 4.4.3. Bioreactor batch and shake flask fed-batch protocol..... | 34 |
| 4.5. Calculations..... | 34 |
| 4.6. Analytical methods | 34 |
| 4.6.1. Determination of purified IP concentration | 35 |
| 4.6.2. SDS polyacrylamide gel electrophoresis (SDS-PAGE) | 35 |
| 4.6.3. Western blotting..... | 36 |

| | | |
|------------|---|-----------|
| 4.6.4. | Kar2 normalized quantification | 37 |
| 4.6.5. | Identification of protein bands by MALDI TOF | 38 |
| 4.7. | Purification of Insulin precursor | 38 |
| 4.8. | Quantification of Insulin precursor by RP-HPLC | 39 |
| 4.9. | Flow cytometry | 39 |
| 5. | Results | 41 |
| 5.1. | The unfolded protein response (UPR) in <i>Pichia pastoris</i> cultures | 41 |
| 5.1.1. | Downregulation of UPR during bioreactor glycerol batch phase | 42 |
| 5.1.1.1. | High Kar2 abundance in exponentially growing cells | 43 |
| 5.1.2. | Independence of prior to induction Kar2 levels on secretory IP production | 46 |
| 5.1.3. | Influence of methanol concentration on Kar2 secretion during bioreactor feedback controlled fed-batches | 49 |
| 5.2. | Reactive oxygen species (ROS) and cellular viability monitoring | 52 |
| 5.2.1. | Augmented ROS in recombinant <i>P. pastoris</i> strains | 52 |
| 5.2.2. | General ROS increase in <i>P. pastoris</i> X33-IP cells induced at different growth times | 55 |
| 6. | Discussion..... | 57 |
| 7. | Conclusions and outlook..... | 63 |
| 8. | References | 65 |
| 9. | Appendix I | 76 |
| 9.1. | Composition of inoculum culture media..... | 76 |
| 9.2. | Application of a two-phase fed-batch process for Insulin precursor production | 78 |
| 9.3. | Insulin precursor purification..... | 82 |
| 9.4. | Insulin precursor quantification | 83 |
| 10. | Appendix II..... | 84 |
| 10.1. | <i>Pichia pastoris</i> X33 host strain cultivation..... | 84 |
| 11. | Appendix III | 86 |
| 11.1. | Identification of proteins bands..... | 86 |
| 12. | Appendix IV | 88 |
| 12.1. | Bioreactor feedback controlled fed-batches..... | 88 |

| | |
|---|------------|
| 13. Appendix V | 91 |
| 13.1. Images employed in the Kar2 relative quantification | 91 |
| 14. Appendix VI | 94 |
| 14.1. ROS fluorescence histograms of control experiments | 94 |
| 15. Appendix VII | 96 |
| 15.1. Materials | 96 |
| 15.1.1. Strains | 96 |
| 15.1.2. Chemicals, media components, kits and other consumables | 96 |
| 15.1.3. Equipments and laboratory tools | 99 |
| 15.2. List of figures | 101 |
| 15.3. List of tables | 103 |
| 15.4. Abbreviations | 104 |
| 16. Curriculum Vitae | 108 |

1. Introduction

Biopharmaceuticals are considered the future of the pharmaceutical industry. Nowadays, there are more than 300 biopharmaceutical products including therapeutic proteins and antibodies in the market with world sales exceeding USD 165 billion in 2012, and growth expectation of 15 % per year. In Brazil, the Ministry of Health spends around USD 10 billion annually on these highly expensive imported products; even though this stands for ~45 % of the budget allocated to medicines, it represents only 5 % of the purchased drugs volume [1]. Due to governmental intervention, Brazil is willing to put up some of the financing to try to reduce its expenses for buying drugs by encouraging more domestic production of key biopharmaceuticals with patents about to expire.

Along the last decades, improvements in the production of heterologous proteins have been achieved, however the strategies sometimes are strain and/or protein specific and cannot be generally implemented. The methylotrophic yeast *Pichia pastoris* is among the most favored microbial eukaryotic expression systems for production of recombinant proteins of biopharmaceutical or industrial interest, due to its stable cheap production processes and the good protein secretion abilities. To study the physiology of *Pichia pastoris* producing recombinant products in fed-batch bioreactor cultures has been part of the group research focus for some years now [2-4]. The interest arises because there is limited knowledge existing on how stress responses during the production of proteins such as Insulin, vaccines or others are affecting the final productivities and the recombinant product quality. Furthermore, surprisingly little attention has been given to the yeast physiological state prior to induction, independent of the production of aberrant proteins. This work, therefore, aims for the interdisciplinary integration of strong science and robust technical excellence consolidated through international exchange, seeking to deepen the knowledge which underlies the sophisticated biopharmaceuticals production process.

2. Theoretical background

In the first section of this work, topics which are required for a better general comprehension of the studied thesis are introduced. At first, a brief presentation, prevalence data and estimation of the chronic disease for which the recombinant protein here produced can be applied, as well as, a brief historical background, characterisation of the hormone itself and some market projections together with its research outlook. Thereafter, the microbiological platform in which the biopharmaceutical was produced is presented, jointly with some specific properties of the biotechnological process employed. Finally, the most relevant background for this work is presented – regulation of protein folding and stress responses. A general idea of the cellular folding process is presented, focusing afterwards in the specifics of the folding machinery and its regulation, stress due to heterologous protein production and the effect of the environment on cells.

2.1. Diabetes

The scientific term "diabetes mellitus" describes a metabolic disorder of multiple aetiology characterized by chronic hyperglycaemia with disturbances of carbohydrate, fat and protein metabolism resulting from defects in Insulin secretion, Insulin action, or both. Diabetes is a chronic disease that occurs either when the pancreas does not produce enough Insulin or when the body cannot effectively use the Insulin it produces. Insulin is a hormone that regulates blood sugar [5]. Hyperglycaemia, or raised blood sugar, is a common effect of uncontrolled diabetes and over time leads to serious damage to many of the body's systems, especially the nerves and blood vessels.

In 2014 the global prevalence of diabetes was estimated to be 9% among adults 18 years and older [6]. In 2012 diabetes was the direct cause of estimated 1.5 million deaths [7]. More than 80% of diabetes deaths occur in low- and middle-income

countries [7]. The World Health Organization projects that diabetes will be the 7th leading cause of death in 2030 [8].

There are two main types of diabetes. Type 1 diabetes (previously known as Insulin-dependent, juvenile or childhood-onset) is characterized by deficient Insulin production and requires daily administration of Insulin. The cause of type 1 diabetes is not known and it is not preventable with current knowledge. Type 2 diabetes (formerly called non-Insulin-dependent or adult-onset) results from the body's ineffective use of Insulin. Type 2 diabetes comprises 90% of people with diabetes around the world [5], and is largely the result of excess body weight and physical inactivity. Other categories of diabetes include gestational diabetes (a state of hyperglycaemia which develops during pregnancy) and "other" rarer causes (genetic syndromes, acquired processes such as pancreatitis, diseases such as cystic fibrosis, and exposure to certain drugs, viruses, and unknown causes). Intermediate states of hyperglycaemia (impaired fasting glucose or impaired glucose tolerance) are conditions at high risk of progressing to type 2 diabetes.

2.2. Insulin

Insulin is produced by the pancreatic beta-cells essential for normal glucose homeostasis and therefore useful in treating diabetes. Insulin therapy is essential to the survival of those with type 1 diabetes and is used to control the symptoms/progression of a minority of those with the more commonly occurring type 2 diabetes. Projections estimate that by 2030 the global diabetes prevalence will lay around 328 million cases [8]. According to the latest market report the global Insulin market was valued at USD 19.99 billion in 2012 and is expected to grow at a geometric progression ratio of 6.1 % from 2013 to 2019 to reach USD 32.24 billion in 2019 [9]. Novo Nordisk A/S (Denmark), Eli Lilly & Co. (USA) and Sanofi S.A. (France) represent the major global Insulin manufacturers.

Insulin has become one of the most thoroughly studied molecules in scientific history. Such importance is exemplified by its involvement in several Nobel Prizes. The first one in 1923, was awarded jointly to Frederick Grant Banting and John

James Rickard Macleod "for the discovery of Insulin". Early commercial Insulin preparations were generally produced by an acid-alcohol precipitation of pancreatic extracts from slaughterhouse bovine and porcine animals. The initial preparations contained so many impurities, that the first patient treated with an injection of Insulin suffered severe allergic reaction. Successful purification occurred through the discovery of a zinc promoted Insulin crystallization [10], followed by a re-crystallization step. This process allowed the production of highly pure animal Insulins called "conventional Insulins" which were commercialized for many years.

The second Nobel Prize involving Insulin was the one in Chemistry awarded to Frederick Sanger in 1958. His work on the structure of proteins culminated with the first protein ever to be sequenced – bovine Insulin. In time, different animals had their Insulin sequence determined and it turned out that the amino acid sequence of Insulin is almost exactly the same for hundreds of different species, explaining the reason for successful application of animal Insulin in human in the early 1920's. Looking at the enzyme in more detail, the sequence of porcine Insulin and human Insulin differ by one amino acid, whereas bovine Insulin is different by three amino acids from human (Figure 2.2.1). Human Insulin is a two-stranded hormone of 51 amino acids (aa) containing two polypeptide chains, α (21 aa) and β (30 aa), with three disulfide bonds. Two of these interlink the α - and β -chains, while the additional disulfide bond is an intra α -chain bond important for the tertiary structure and the physiological efficacy of the molecule [11].

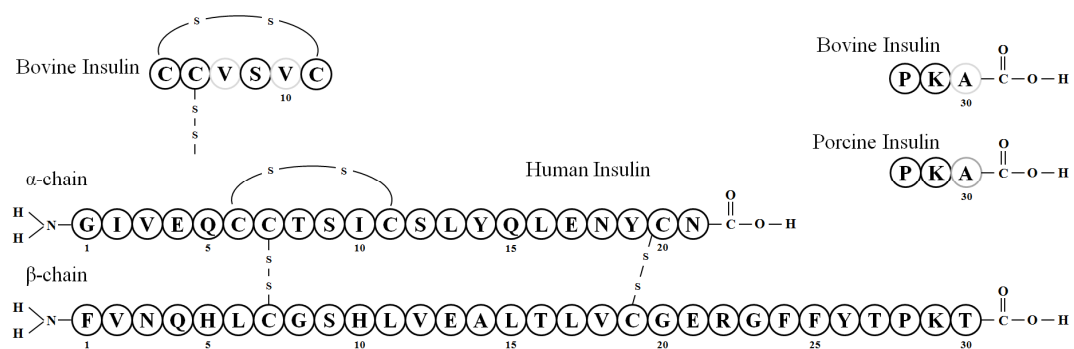


Figure 2.2.1 – Amino acid sequences of human, bovine and porcine Insulin.

The advent of recombinant DNA technology in the early 1980's provided an obvious step towards the growing requirement for Insulin, gradually replacing the slaughterhouse supplied animal Insulin for synthesized nucleotide sequences coding for the human Insulin. Biosynthesized Insulin was the first recombinant product approved by the U.S. Food and Drug Administration (FDA) for human application [12, 13]. This first approach developed by scientists at City of Hope National Medical Center, USA, in collaboration with Genentech Inc., USA, was based on two parallel fermentation and purification processes, one for each Insulin chain [14]. The procedure termed "chain combination", fused the α and β chains to carrier proteins, expressed in two different *Escherichia coli* strains and the purified chains were co-incubated under reactions conditions to form intact Insulin. Nowadays, there are two economically viable "proinsulin routes" employed. Both produce a Insulin precursor (IP) polypeptide from which mature Insulin is derived via *in vitro* proteolytic excision of the "C" or "connecting" peptide. One approach continues to apply the bacterial expression system *E. coli*, producing inclusion bodies containing IP, however in a single fermentation protocol, with subsequent solubilization and refolding procedures [15]. The other commercially applied route, involves the utilization of the yeast *Saccharomyces cerevisiae* as expression system, producing an engineered construct consisting of the Insulin α chain, a 29 amino acid β chain (lacking the C terminal β -30 threonine, Figure 2.2.1) linked via a short synthetic (often AAK) C peptide, and a fused *S. cerevisiae* α -mating factor pre-pro-peptide signal leader sequence [16-18], which facilitates soluble extracellular secretion, and is itself enzymatically removed during the process.

In time, the ability to chemically synthesize genes of altered nucleotide sequence was mastered and several Insulin analogues have been engineered to display either an accelerated or prolonged duration of action and many have been approved for general medical use [12]. Current Insulin-based diabetes research is increasingly focused not on the Insulin molecule per se, but upon areas such as the development of non-parenteral Insulin delivery systems, as well as organ-/cell-based and gene therapy-based approaches to control the disease. In June 2014, the FDA approved Afrezza[®] from MannKind Co., USA, which is an inhaler with pre-measured rapid-acting Insulin for type 1 and type 2 diabetes.

2.3. *Pichia pastoris* as expression system

Commensurate with the projected escalation in the prevalence of diabetes in the coming decades [8], there will be an increased demand for Insulin estimated on approximately more than 16000 kg/year [19]. Though *S. cerevisiae* is still the main yeast system for Insulin production, numerous alternative yeast hosts have become available in recent years [20-22]. Among these microbial factories, the methylotrophic yeast *Pichia pastoris* has emerged as a very useful expression host with superior features [23-25] and has been successfully employed for the high-level production of Insulin precursor [2].

Recently, the commonly used recombinant protein production *Pichia pastoris* strains, such as X-33 and GS115, were classified as *Komagataella sp.* [26]. Since at the time this work was performed all the data banks used the *Pichia pastoris* name as well, the earlier denomination (*P. pastoris*) is used when referring to the strain X-33 and GS115.

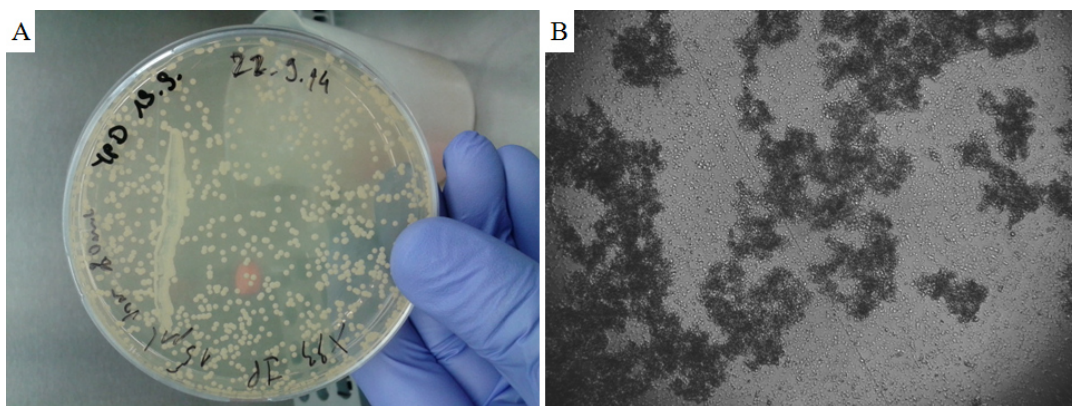


Figure 2.3.1 – *Pichia pastoris* X33-IP (A) isolated colonies grown in agar plates and (B) In situ microscopy image of high cell density culture in 10 L bioreactor.

Pichia pastoris is a single-celled eukaryote which possesses remarkable prokaryote-like characteristics. These notable features include the easiness of genetic manipulation and rapid growth on relatively inexpensive media similar to *E. coli* [23]. On the other hand, *P. pastoris* also present unique advantages

exclusive to eukaryotes. Among others features, post-translational modifications, such as glycosylation and disulfide bridges formation, stand out [24]. As a consequence, heterologous proteins are more likely to be correctly processed, folded and assembled into functional molecules when produced in *P. pastoris* compared with *Escherichia coli* [27]. The preference of *P. pastoris* for respiratory growth is a key physiological trait that greatly facilitates its culturing at high-cell densities relative to fermentative yeasts (*Saccharomyces cerevisiae*). Furthermore, as a methylotrophic yeast *P. pastoris* possesses two alcohol oxidase genes, *AOX1* and *AOX2*, the first has a highly inducible and tightly regulated promoter (PAOX1) [28]. The Aox1 promoter is strongly repressed in cells grown on most carbon sources; such as glycerol, but it is induced over 1000-fold when cells are shifted to a medium containing methanol as a sole carbon source, which is an advantage regarding expression control of recombinant proteins which can be toxic to the producing cell [23]. In addition, *P. pastoris* shows a stable integration of expression plasmids into the genome and the ability to grow to high cell densities ($> 100 \text{ g L}^{-1}$ dry cell mass) in bioreactor cultures [29]. Other important characteristics that make this expression system an attractive choice are its capacity of high level secretion of heterologous protein and the relative low levels of endogenous proteins that are secreted to the medium, which facilitates purification [30]. Generally in *P. pastoris*, the entry of heterologous proteins into secretory pathway is mediated by the *Saccharomyces cerevisiae* α -mating factor pre-peptide signal leader sequence (MF α). The use of this secretion signal peptide can lead to recombinant protein concentration in the culture supernatant exceeding 10 g/L [31].

2.4. Regulation of protein folding and ER stress

The extensive use of *Pichia pastoris* as a platform for recombinant protein expression has been providing the opportunity for deeper understanding of cellular physiological responses in diverse extreme environments. It is well established today that heterologous overexpression of proteins is connected with different stress reactions [32, 33]. In its wider definition, stress is the response of any system

to perturbations of its “normal state”. Regarding a living organism these disturbances can be either life-enhancing changes, e.g. feeding, or life-threatening changes, e.g. starvation. High-level expression of a foreign protein may either directly limit other cellular processes by competing for their substrates, or indirectly interfere with metabolism, if their manufacture is blocked, thus induce a metabolic stress reaction of the cell [32]. The protein folding process and subsequent secretion is a rather complex process involving many interacting participants. Due to this interdependence, genetically increasing the rate of one step can lead to rate-limitation of another one, which can then become the bottleneck of the expression system. Moreover, in most cases the rate limiting step in the eukaryotic secretion pathway has been identified to be the exit of proteins from the Endoplasmic Reticulum (ER) [34].

It should be noted, however, that most of the knowledge on the *Pichia pastoris* folding machinery is derived from similarity to other yeasts (mainly *Saccharomyces cerevisiae*) and that detailed functional characterization is largely missing.

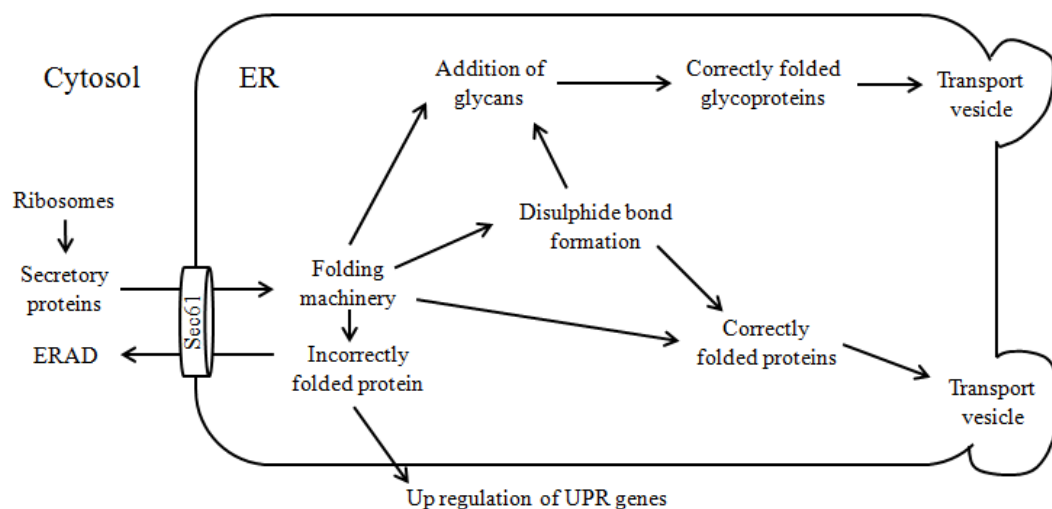


Figure 2.4.1 – Schematic representation of protein folding and secretion in ER. Modified based on [35].

The ER is the first compartment in the secretory pathway and is a major protein folding compartment in a eukaryotic cell, second only to the cytosol. All secretory

proteins enter the secretory pathway through the ER [36]. After synthesis on the ribosomes, proteins are translocated through the Sec61 complex translocon pore into the ER lumen for modification and delivery to their proper target sites within the secretory pathway and the extracellular space. In the ER, proteins fold into their native conformation and undergo a multitude of post-translational modifications, including signal sequence processing, disulfide bond formation and glycosylation. In a process termed quality-control (QC) only correctly folded proteins are exported to the Golgi complex, while incompletely folded or misfolded proteins are retained in the ER to complete the folding process or in extreme cases to be targeted for degradation [37]. Specialized cargo vesicles that selectively incorporate these proteins bud from the ER and are targeted to the Golgi membrane by the activity of the coat protein complex II (CopII). In the Golgi network proteins undergo additional post-translational modifications and are subjected to sorting mechanisms that finally target them to their final destination. The accumulation of mis/unfolded proteins in the ER lumen results in activation of ER-Nucleus signaling pathway called as unfolded protein response (UPR). Upon strong or prolonged ER stress, an ubiquitin mediated pathway mechanism called ER-associated protein degradation (ERAD) is responsible for the retention of misfolded or unmodified nonfunctional proteins in the ER and their subsequent removal, schematic representation in Figure 2.4.3 [38]. Curiously, in higher eukaryotic organisms, when these mechanisms do not remedy the stress situation, apoptosis is initiated presumably to eliminate unhealthy or infected cells [39, 40].

Several efforts on overcoming protein folding stress for improved recombinant protein production had been attempted [41-43]. Promising expectations emerged that increased level of secretion helpers, such as PDI, Ero1, Sso2, Kar2 and Hac1, would result in increased folding capacity in the ER, and thus improved secretion rates, however the findings were rather inconsistent and unpredictable. It seems that the effect of co-expression strongly depends on the properties of the target protein and, moreover, it seems that fine-tuned overexpression of these genes are required to generate a functional secretory network to improve foreign protein overproduction, recently reviewed in [44].

2.4.1. The ER-resident protein folding machinery

The endoplasmic reticulum (ER) harbors a protein folding machinery that folds client proteins, quality controls the folding process, and, when necessary, activates the unfolded protein response [36]. The folding demand arises from nascent polypeptide chains entering the ER in a mis/unfolded conformation. Misfolded proteins containing cytoplasmic, intramembrane or endoplasmic reticulum (ER)-luminal lesions are recognized by cytoplasmic and luminal chaperones and associated factors (listed in [36]) which can facilitate protein translocation, protein folding, and, when necessary, protein degradation. The ER-resident protein folding machinery consists of: foldases (e.g., thiol oxidoreductases), molecular chaperones (e.g., Hsp70, Hsp40), the ER lectins (e.g., calnexin, calreticulin), and the AAA ATPase proteins.

Foldases can present thiol oxidase, disulfide isomerase, and chaperone activities. The most prominent example of protein foldase families are protein disulfide isomerases (PDIs) and *cis-trans* peptidyl prolyl isomerases (PPIs). These proteins catalyze the formation and isomerization of disulfide bonds and the *cis-trans* isomerization of peptidyl prolyl bonds, respectively. To catalyze disulfide bond formation and present thiol oxidoreductase activity, PDI must be maintained in an oxidized state which is accomplished by oxidoreductin 1 (Ero1), an ER membrane protein [45, 46]. In the oxidative environment provided by the ER, Ero1 passes electrons to molecular oxygen via FAD, potentially creating reactive oxygen species (ROS).

Molecular chaperones are found in endoplasmic reticulum (ER), cytosol and mitochondria and play a vital role in protein biogenesis, translocation and degradation [47]. They interact with hydrophobic surfaces on unfolded proteins, thereby shielding them from engaging in non-productive interactions with other polypeptide chains [48]. They do not enhance the rate of protein folding. The major classes of chaperones include, the helper proteins Hsp70, the Hsp40 (co-chaperones), the nucleotide exchange factors (NEF), the Hsp90 and the Hsp110. The most important chaperones are those that belong to the Hsp70 family, having a molecular weight of about 70 kDa and are upregulated due to changes in

temperature, oxidative stress, among others. Whereas in *Escherichia coli* Hsp70 is termed DnaK, in eukaryotes as in yeast cells, which expresses several slightly different Hsp70 proteins, the chaperones located in the ER are called BiP/Grp78, and in yeast, Kar2 [49]. Chaperone activity of Hsp70 is ATP dependent and includes cycles of ATP hydrolysis and protein binding [50]. Hsp70s play a vital role in protein folding, translocation, disassembly of aggregates and targeting proteins to the ER-associated protein degradation pathway. Hsp40s, in *E. coli* DnaJ, act as co-chaperone and enhance the ATPase activity of Hsp70 [51]. NEFs help in release of ADP from ATPase binding domain, a rate limiting step in the Hsp70 cycle [52]. Hsp110s are distantly related to Hsp70s and can act as NEF stimulating ATPase activity and also act as holdase preventing protein aggregation [52].

N-glycosylation has a major initial role in signaling of protein folding steps involving many proteins that enter the ER. The recognition of monoglucosylated species is performed by the ER lectin chaperones calnexin, and its homologue calreticulin [37]. After removal of two terminal glucose residues, calnexin binds to specific oligosaccharides, exhibiting its chaperone function. Removal of the last glucose residue releases calnexin from the glycoprotein, thus enabling further folding or targeting towards degradation. While *S. cerevisiae* lacks the gene for UGGT (the mammalian enzyme re-adding glucose to the glycan and thus recycling proteins to calnexin binding [53]), a homolog was identified in *P. pastoris* [54]. In *Saccharomyces cerevisiae* nascent glycoproteins are bound by Cne1, a homologue of the mammalian calnexin [55].

2.4.1.1. Immunoglobulin heavy chain binding protein – Kar2

The accumulation of unfolded proteins in the ER lumen triggers the transcription of a large set of stress responsive genes encoding ER resident chaperones and foldases, including the main UPR marker, Kar2 [38, 56]. The most prominent ER molecular chaperone Kar2, in yeast, (also known as BiP/Grp78/HspA5 in other organisms) belongs to Hsp70 family of heat shock proteins and it is present in the lumen of the ER of all eukaryotes. In addition to relieve stress by chaperoning

protein folding, relying on a number of interaction partners, including Hsp40 co-chaperones, nucleotide exchange factors, and signal transducers, Kar2 also acts as: sensor protein for the presence of un-/misfolded proteins, import and export of protein in the ER, protein degradation and calcium homeostasis [57]. Kar2 also takes part in protein quality control, upon persistent misfolding, N-glycosylated polypeptides are slowly released from calnexin/Cne1 and enter a second level of retention-based ER quality control by aggregating with the Kar2 chaperone complex [53]. The first identified Kar2 homolog was in fibroblasts, whose rate of synthesis is increased when cells are starved of glucose, hence its name glucose-regulated protein, Grp78 [58]. The origin of the other Kar2 homolog BiP comes from its identification as a cofactor of immunoglobulin assembly, hence the name immunoglobulin heavy chain binding protein BiP [59]. Kar2 has ~74 kDa and is the product of a karyogamy gene, *KAR2* [49], hence the terminology, whereas in *Escherichia coli* it is homolog to the bacterial DnaK. Kar2 has an N-terminal ATPase and a C-terminal substrate binding domain. When bound to substrates the ATPase activity of Kar2 is stimulated, cycling ADP–ATP by folding polypeptide chains, consuming energy (Figure 2.4.2) [48]. These reactions are regulated by co-chaperones, also called J-proteins in reference to the *E. coli* enzymes [51], and can be inhibited by depleting cellular ATP [60, 61]. ER-resident family members such as Kar2 have a C-terminal tetrapeptide ER retention signal, usually KDEL in animal cells and HDEL in yeast [62]. The HDEL motif is recognized by Erd2, a membrane protein in yeast, which is responsible for indicating the retention of these ER-resident proteins in the ER lumen [63, 64], or the motif is recognized by the respective receptor in the Golgi apparatus, leading to packaging of the ER-protein into CopI vesicles and retrograde transportation to the ER [65-67].

Over the last decade Kar2 protein has attracted even more attention due to the involvement of UPR in progression of critical human diseases, such as metabolic disease, neurodegenerative disease, inflammatory disease, and cancer [68]. In cancer, due to environmental changes such as poor vascularization and the resulting hypoxia and glucose starvation, tumor cells are prone to ER stress and UPR. Endoplasmic reticulum storage diseases are listed in [36] and were recently reviewed in [69].

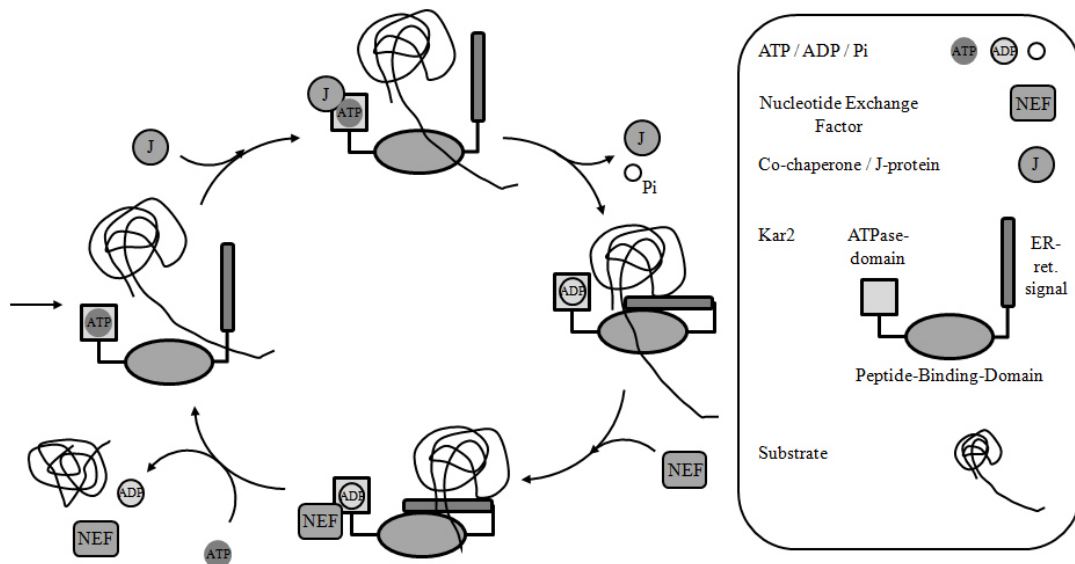


Figure 2.4.2 – The folding cycle of Kar2, a chaperone belonging to the Hsp70 family. Figure modified based on [47].

2.4.2. The unfolded protein response (UPR)

To maintain ER homeostasis the quality control systems ensure that only correctly folded, modified and assembled proteins travel further along the secretory pathway of the Golgi apparatus. Overproduction of recombinant proteins and other disturbances may overload the ER folding and secretion capacity, resulting in the accumulation of misfolded or unfolded proteins, and ER stress as a consequence. This triggers the activation of the unfolded protein response (UPR) pathway, which aims at reducing ER stress conditions by induction of genes involved in protein folding and the ER-associated degradation (ERAD) pathway [36, 47, 56]. The initial description and major progress in understanding the molecular mechanisms of the UPR was done using the yeast *S. cerevisiae* [70, 71]. Specifically, this yeast was used for the molecular cloning of the UPR transducer Ire1 and the UPR-specific transcription factor Hac1 [72].

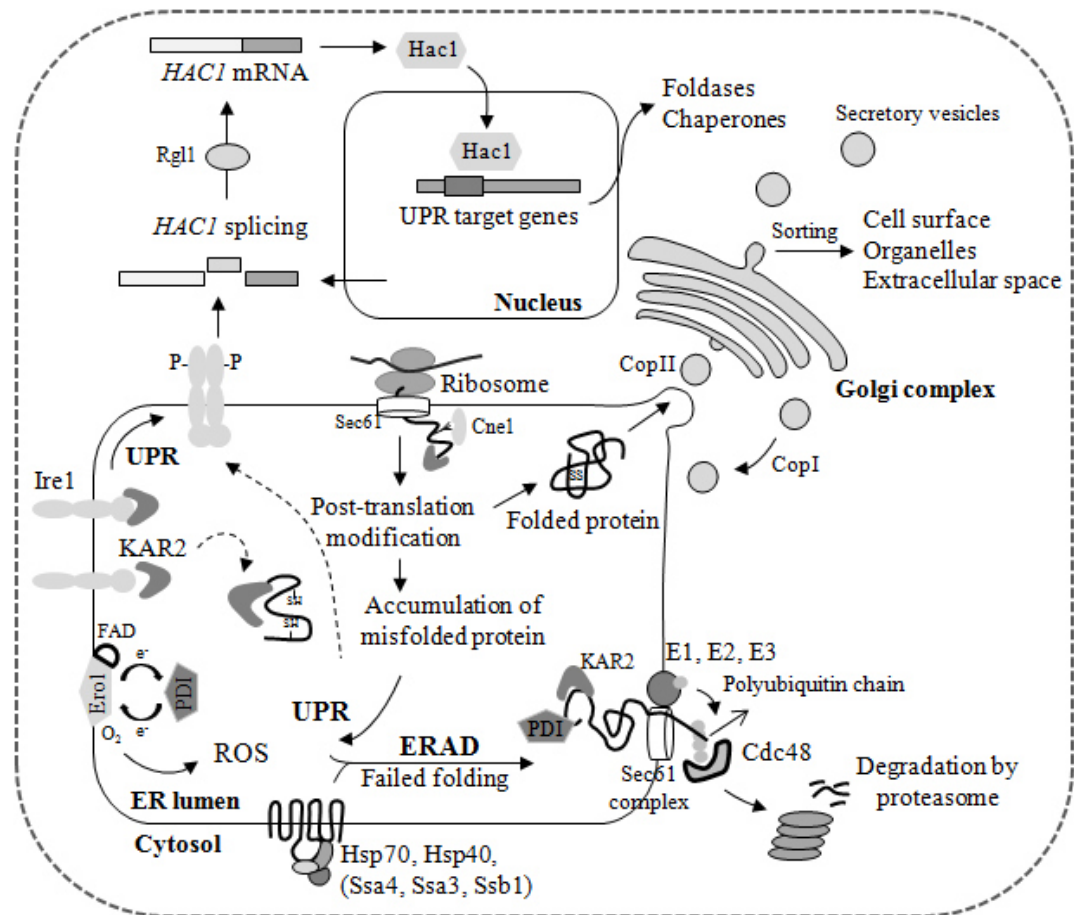


Figure 2.4.3 – Diagram representing the protein folding, secretion, UPR and ERAD in yeast. Modified based in [73].

In yeast UPR, represented in Figure 2.4.3, misfolded proteins in the ER are sensed by the Ire1-bound Kar2. Ire1 is a transmembrane protein oriented with the N-terminal in the ER lumen and the C-terminal in the cytosol [74]. Ire1, when activated promotes the splicing of the message for the Hac1 transcription factor. Hac1 activity is regulated by an unconventional splicing event of *HAC1* messenger RNA (mRNA), removing an intron that prevents its translation in the absence of ER stress. If unfolded proteins accumulate in the ER, Kar2 dissociates from monomeric Ire1 to perform its chaperone function, and Ire1 dimerizes and gets activated. After removing the intron from precursor *HAC1_u* mRNA (*HAC1* splicing), the exons are joined by tRNA ligase Rgl1 to form translation-competent *HAC1_i* mRNA. The encoded Hac1 protein then locates to the nucleus and activates target genes with UPR elements (UPREs) in their promoters [71, 72]. Hac1 is known to activate or repress over 100 genes, including *KAR2*, *PDI* and *ERO1* in *S.*

cerevisiae [75]. The induced transcriptional response aims at restoring ER homeostasis by increasing the ER lumen and surface area as well as the ER folding machinery.

The *HAC1* gene and splice event was recently characterized in *Pichia pastoris* [76]. *P. pastoris HAC1* contains a 322 bp intron, flanked by splicing sites, similar to homologs from other species. As in *S. cerevisiae*, *HAC1* splicing is dependent on Ire1 in *P. pastoris*, and the last five amino acids of the newly generated C-terminus of *P. pastoris* Hac1 are required for UPR activation [77]. *HAC1* mRNA is constitutively expressed in *P. pastoris* independent of externally applied ER stress conditions or recombinant protein production [76], but because of the secondary structure of the intron, no protein is produced when the mRNA remains unspliced [78]. Regarding this matter, the occurrence of UPR activity in “unstressed” cells was implicated in nutrient sensing and control of cellular responses to fluctuations in nutrient levels, extending the physiological functions of the UPR [79-82]. Furthermore, recent studies on a *P. pastoris* strain secreting human serum albumin at $\mu = 0.015$ to 0.15 h^{-1} in glucose-limited chemostat cultivations illustrated that the yeast reacts to different growth rates by tuning genes involved not only in carbon and nitrogen sources but also those regulating stress responses, e.g. the UPR [83].

2.5. Environmental stresses

The impact of environmental factors on *P. pastoris* cells has been investigated in the past years and the changes in the proteins involved in folding and degradation were always object to better understand their effect on the final recombinant product yield [32, 33]. In order to achieve heterologous protein overexpression cells usually undergo typical high cell density fermentation processes which exert growth conditions that deviate far from their natural environment. Temperature, pH, solute concentration, oxygenation, metal ion concentration, or high levels of organic compounds are typical environmental stress factors. Overlapping global expression programs in response to a diverse set of stresses, including their specific

features and a common response to all of the stressful conditions, are generally termed “environmental stress response” (ESR) pathway.

A study on the responses of *Saccharomyces cerevisiae* to a variety of environmental stresses concluded that a common program for genome wide transcriptional changes exists as a reaction to diverse environmental changes, encompassing roughly 900 genes [84]. Generally, it was observed that the ESR genes are up- or downregulated transiently as a reaction to a shift to stressful conditions, and return to the near normal level after adaptation to the new conditions. Studies with *Pichia pastoris* in which the cultivation temperature was decreased from 30 to 20 °C led to a 3 fold increase in specific productivity of recombinant protein in spite of downregulation of chaperones from the Hsp70 family, such as Ssa4 and Ssb1, as well Hsp60 and Hsp82; Kar2 was also downregulated while the PDI did not show any change at lower temperatures [85]. Regarding environmental oxygen availability, very little is known about its impact on the physiology of recombinant *Pichia pastoris* in comparison to other yeasts. Recent studies on *P. pastoris* report that under steady state conditions, low oxygen availability strongly affected among others, the stress responses, particularly the unfolded protein response [86, 87]. Additionally, a beneficial effect of hypoxia on recombinant protein secretion in *P. pastoris* chemostat cultivations has been reported [88].

In biotechnological processes, hyperosmotic stress is regarded as a typical problem, as in high cell density bioreactor cultivations, media initially contain high concentrations of major nutrients (e.g., carbon sources such as glucose or glycerol) and salts. Osmotically active compounds may either be ionic (dissociated salts or organic acids) or uncharged (e.g., sugars, sugar alcohols, or undissociated organic acids). Depending on the severity of the osmotic change to which *S. cerevisiae* is submitted, it presents usually the induction of the environmental stress response (ESR) and of the high osmolarity glycerol (HOG) pathway [84, 89, 90]. These metabolic fine-tuning allow the yeast cells to cope with external ionic hyperosmolarity by producing compatible solutes, generally glycerol, osmoregulating internal cellular environment, inducing, among a multitude of cellular readjustments, the transcription of glycerol-3-phosphate dehydrogenase (*GPDI*) and repression of the plasma membrane glycerol efflux channel (*FPSI*)

[91-94]. While so far there is no evidence that UPR triggers an osmoresponse such as production of compatible solutes or confers resistance to salt, adaptation to hyperosmotic conditions has been shown to activate an UPR-like response including upregulation of chaperones (e.g., Kar2) in *Pichia pastoris*, whereas in strains already having UPR activation due to recombinant protein overproduction, the effect of elevated osmolarity is less pronounced [95].

Environmental nutrient sensing and control of cellular responses to fluctuations in nutrient levels have been suggested to be a second physiological function for the UPR in yeast and mammals [36, 96]. Observations uncover that in addition to keeping the biosynthetic burden and biosynthetic capacity of the ER in line, the UPR also monitors the biosynthetic activity of the ER to inform the cell about its overall metabolic state. In diploid budding yeast, high nitrogen concentrations in the medium are responsible for an increased influx of nascent unfolded polypeptide chains into the ER and activation of Ire1, regulating *HAC1* mRNA splicing [79].

2.6. Oxidative stress

Oxidative stress can be simply defined as a state where there is a relative imbalance within cells between generation and removal of reactive oxygen species (ROS). It has been shown that some classical markers of the UPR pathway have an important role in attenuating oxidative stress in yeast and in mammals [75, 82]. ROS adversely affect cell viability and possibly the quality of the protein product, trigger apoptosis, and function as signaling molecules in the UPR [97]. Regarding methylotrophic yeasts, oxidative stress caused by methanol degradation is a relevant issue. Methanol is first oxidized inside the peroxisomes by alcohol oxidase (Aox1) to form formaldehyde (CH_2O) and hydrogen peroxide (H_2O_2), which are both highly toxic compounds that increase the intracellular ROS levels (Figure 2.6.1) [98]. Formaldehyde is a central intermediate situated at the branch point between assimilation and dissimilation pathways [99], and is promptly metabolized. On the other hand, H_2O_2 despite having no unpaired electrons and thus is not a radical, it is often qualified as ROS since it can easily convert itself

into the highly reactive hydroxyl radical ($\cdot\text{OH}$), thus generating oxidative stress. Another central source of reactive oxygen species with consequent UPR activation is the oxidative protein folding [97, 100, 101]. PDI and other foldases are responsible for the correct formation of disulfide bonds during oxidative folding and the isomerisation of incorrectly folded disulfides [46, 47]. Therefore, the rate of ROS generation is dependent upon the complexity of the protein to be folded, heterologous or not, the availability of chaperones to assist folding and ATP used by chaperones [97, 101]. As already mentioned, in the oxidative environment provided by the ER, Ero1 passes electrons to molecular oxygen via FAD, potentially creating ROS [45, 46]. The yeast ER has one Ero1 and mammals have two isozymes, Ero1 α and Ero1 β . Ero1 α is induced by hypoxia and may play a role in ERAD [102, 103], whereas Ero1 β is induced by the unfolded protein response [104]. The relevance of this oxidative-stress-generating process can be illustrated by the estimation that the Ero1-mediated oxidation could account for up to 25% of cellular ROS produced during protein synthesis [97].

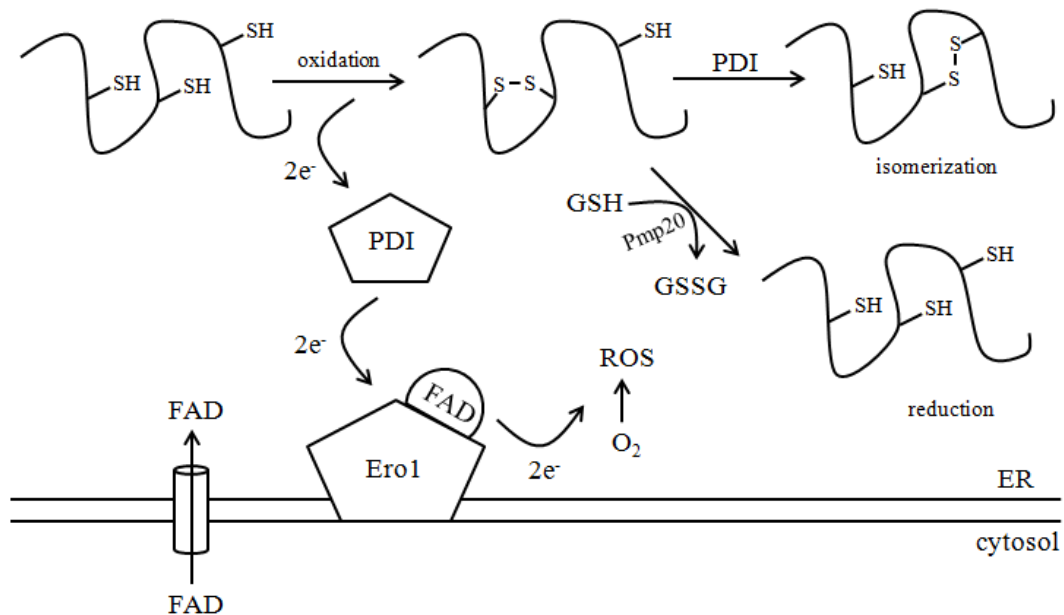


Figure 2.6.1 –Oxidative protein folding in the yeast ER diagram. Modified from [97].

FAD-bound Ero1 oxidizes PDI, which then subsequently oxidizes folding proteins directly, thereafter passing electrons to molecular oxygen, presumably resulting in the production of ROS. FAD, which is synthesized in the cytosol, can readily enter the ER lumen and stimulate the activity of Ero1. Disulfide isomerization and reduction may be performed by PDI. Reduced glutathione (GSH) may also assist in disulfide reduction mediated by Pmp20, resulting in the production of oxidized glutathione (GSSG).

3. Aim of this work

The main goal of the work presented here was to perform a comprehensive analysis of the unfolded protein response (UPR) pre and post methanol induction of the yeast *Pichia pastoris* producing and non-producing an Insulin precursor (IP) in bioreactor cultures under control of the tightly methanol-regulated promoter (PAOX1). The cellular folding response during pre-induction glycerol batch phase, the transition to methanol induction medium and the post-induction methanol fed-batch phase were studied in detail. Additionally, the IP producing yeast's unfolded protein response under industrially-relevant bioreactor fed-batch conditions were investigated, allowing a wide comparison of the UPR related results.

A further stress response - the oxidative stress - was analyzed through flow cytometry by monitoring reactive oxygen species (ROS). The effect of methanol metabolism and recombinant protein production on ROS levels was studied. Finally, the role of methanol induction at different phases of glycerol batch growth of IP producing cells on ROS levels was monitored.

4. Methods

4.1. Water and sterile work

For all experiments ultrapure water, purified with Arium Pro VF (Sartorius, Germany), was used. Aseptic operations, which required sterility to avoid contaminations, were performed under a clean bench (Herasafe KS, Thermo Scientific, Germany). All solutions for the cultivations were sterilized by filtration (0.2 μm filter) or autoclaving at 121 °C for 20 min (Systec V-150, Systec GmbH, Germany).

4.2. Strain and vector

The X-33 Insulin producer *Pichia pastoris* strain Mut⁺ phenotype used for the experiments in this work is described previously [2]. The constructed expression vector pPICZ α -IP contains a synthetic codon-optimized gene encoding the IP under the control of the PAOX1 promoter, in-frame with the α -factor secretory signal sequence of *Saccharomyces cerevisiae*. The *P. pastoris* GS115 strain carrying 8-copies of the *HBsAg* gene under the control of the *AOX1* promoter has been described before [105].

4.3. Optical density and determination of cell concentration

The cell concentration (biomass) of suitably diluted culture samples was measured by optical density (OD₆₀₀) at 600 nm using a Multiskan GO UV-Vis spectrophotometer (Thermo Fisher Scientific, Germany), previously zero-calibrated with 1x PBS [8 % (w/v) sodium chloride, 0.2 % (w/v) potassium chloride, 1.42 % (w/v) disodium hydrogen phosphate and 0.245 % (w/v) potassium

phosphate]. The measurements were performed with disposable plastic cuvettes with a path length of 1 cm. For dry cell mass (DCM) determination, 1 mL aliquots of the culture broth were pelleted (13,000 rpm for 15 min at room temperature using an Eppendorf microcentrifuge, Germany) in pre-weighed tubes, re-suspended in 50 mmol/L phosphate buffer (pH 7.2), re-centrifuged and the resultant pellets dried at 80 °C to constant mass.

4.4. *Pichia pastoris* cultures

Three different protocols were employed to cultivate the yeast cells. Cells were submitted either to an entire glycerol batch and methanol induction phase in the shake flasks protocol, or both phases exclusively in bioreactor, or employed in a bioreactor glycerol batch and methanol shake flask fed-batch mixed alternative scheme.

4.4.1. Shake flask cultivations

A starter culture was set up by inoculating 100 mL containing yeast extract (1 % w/v), peptone (2 % w/v) and dextrose (2 % v/v) in 500 mL sterile baffled shake flasks with initial OD₆₀₀ of 0.03 from glycerol stock cultures and grown at 30 °C, under constant shaking in an orbital shaker at 160 rpm for 18 h to an OD₆₀₀ 10. About 1 % of starter culture was used to inoculate 500 ml of buffered glycerol complex medium (BMGY) containing 1 % (w/v) yeast extract, 2 % (w/v) peptone, 100 mmol/L potassium phosphate (pH 6.0), 1.34 g/L yeast nitrogen base with ammonium sulfate and without amino acids, 0.4 mg/L biotin and 5 % (v/v) glycerol in a 2 L baffled shake flask. The culture was incubated at 30 °C, under constant shaking in an orbital shaker at 150 rpm until an OD₆₀₀ ~20 was reached. Subsequently, cells were pelleted by centrifugation (3347 × g), washed with sterile 1x PBS, re-centrifuged and re-suspended in buffered methanol complex medium (BMMY), as above described but containing methanol 1 % (v/v) instead of

glycerol, to an $OD_{600} \sim 100$ and incubated at 30 °C under shaking at 150 rpm. Recombinant protein production was induced through the addition of 1 % (v/v) methanol twice a day at 12 h intervals for a total period of 96 h. Finally, cells were harvested by centrifugation, washed with 1x PBS, and the cells were stored at -80°C until use.

4.4.2. Bioreactor cultivations

To achieve more reproducibility between batch-to-batch experimental results, a single colony upscaling approach was employed for bioreactor cultures and the undesired production of the byproduct ethanol was avoided. Instead of directly transferring frozen cells into pre-cultures medium, as employed for the shake flask cultures, cryo bank pellets were diluted, cells were cultured in agar plates, colonies were isolated, only then transferred to complex media pre-cultures, thereafter to the inoculum containing the 25 g/L glycerol defined medium and finally into the bioreactor. X33 and X33-IP cryo cell banks were diluted and cultured in 2 % (w/v) agar plates containing: yeast extract (1 % w/v), peptone (2 % w/v) and dextrose (2 % v/v) medium in order to grow isolated single colonies. One single colony of either strain was transferred to a 100 mL sterile baffled shake flask containing 25 mL of medium with 1.34 g/L sterile yeast nitrogen base with ammonium sulfate and without amino acids, 5 g/L sterile glycerol and 0.4 mg/L biotin. This starter culture was grown in an orbital shaker at 30 °C and 160 rpm until an $OD_{600} \sim 5$ was reached. Thereafter, the pre-inoculum culture was prepared with 1 % (v/v) of the starter culture in one 500 mL sterile baffled shake flask filled with 100 mL of the same complex medium described above and cultured until $OD_{600} \sim 5$. Subsequently, the pre-inoculum was used to inoculate the inoculum, at an initial OD_{600} of 0.5, two 2 L sterile baffled shake flasks filled with 500 mL of defined growth media containing per liter: glycerol, 25 g; potassium dihydrogen phosphate, 9.4 g; yeast trace metal (YTM) solution, 4.56 g; ammonium sulfate, 15.7 g; magnesium sulfate heptahydrate, 4.6 g; calcium chloride dihydrate, 0.28 g; and biotin, 0.4 mg. The YTM solution contained per liter: potassium iodide, 207.5 mg; manganese sulfate, 760.6 mg; disodium molybdate, 484 mg; boric acid, 46.3 mg; zinc sulfate

heptahydrate, 5.032 g; ferric chloride hexahydrate, 12.0 g; and sulfuric acid, 9.2 g. The inoculum cultures contained, when mentioned, the previously described complex media. All shake flask cultures were grown at 30 °C and 160 rpm with starting OD₆₀₀ of 0.1. The cellular growth was monitored by optical density measurements at 600 nm in a Multiskan GO UV-Vis spectrophotometer (Thermo Fisher Scientific, Germany). For details on the composition of the inoculum culture media refer to Appendix I item 10.1.

The controlled batch cultivations were performed in 2 L Biostat[®] B plus or 10 L Biostat[®] C systems and the feed-back controlled fed-batch cultures in 5 L Biostat[®] B (Sartorius, Germany). Bioreactor cultivations were started with an initial OD₆₀₀ of 0.5. The application of the two-phase fed-batch process for Insulin precursor production is described in detail in Appendix I item 9.2. During the cultivation, the temperature and pH were kept constant at 30 °C and pH 5.5. For maintaining the pH, 12.5 % (v/v) ammonium hydroxide and 1 mol/L phosphoric acid were used. In case of foaming, 1 mL antifoam Ucolub N115 per 1 L culture media was manually supplemented into the bioreactor. The aeration rate was set to 1,75 vvm and the stirrer speed was regulated between 400 and 2000 rpm gaining constant dissolved oxygen (DO) concentration of 20 % air saturation. The concentrations of oxygen and carbon dioxide in the exhaust gas were determined by BlueInOne gas sensors (BlueSens, Germany). The same above described defined media was employed with either glycerol or glucose as carbon source. Complete consumption of glycerol or glucose in the medium was recognized by a massive decline in stirrer speed, which correlates to reduced oxygen uptake of the cells due to nutrient depletion. Production of recombinant Insulin precursor was initiated by addition of a methanol solution [96 % (w/w) methanol and 4 % (w/w) YTM] to the mentioned final methanol concentration, which was maintained constant throughout the remainder of the induction period based on *on-line* measured methanol concentrations determined from the methanol vapor in the off-gas using a flame ionization detector (Ratfish Instruments, Germany). Based on the gas liquid phase equilibrium methanol concentrations were determined in the off-gas using two point calibrations directly before and after induction (detailed FID calibration values and operation are described on Appendix I item 9.2).

4.4.3. Bioreactor batch and shake flask fed-batch protocol

The alternative shake flask fed-batch protocol was employed with cells were harvested sterile from the 10 L defined medium glycerol batch during different growth phases, centrifuged, washed with 1x PBS and re-suspended to a final $OD_{600} \sim 100$ in buffered methanol complex media containing 1 % (w/v) yeast extract, 2 % (w/v) peptone, 100 mmol/L potassium phosphate (pH 6.0), 1.34 g/L yeast nitrogen base with ammonium sulfate and without amino acids, 0.4 mg/L biotin and 1 % (v/v) methanol. Cultures were grown in 150 mL sterile baffled shake flasks with 25 % filling volume in an orbital shaker at 30 °C and 160 rpm. Recombinant protein production was induced through the addition of 1 % (v/v) methanol twice a day at 12 h intervals for a total period of 96 h.

4.5. Calculations

The estimation procedure to calculate the specific growth rate (μ_{max}) was performed by using suitable smoothing routines and mass balances that permitted to supply complete data sets with coincident off-line biomass and substrate values. Carbon dioxide production rate (CPR), oxygen uptake rate (OUR) and the respiratory quotient (RQ) were calculated as described elsewhere [106].

4.6. Analytical methods

Ethanol concentrations were determined by gas chromatography (Shimadzu 14B GC, Kyoto, Japan) using a Supelcowax 10 column (Sigma-Aldrich, Germany), injector temperature 180 °C, column temperature 70 - 160 °C, detector temperature 280 °C, n-Propanol (8 g/L) internal standard, injection volume of 0.2 μ L and a flame ionization detector. The osmolarity of the culture supernatant samples was measured by freezing-point depression with an Osmomat 3000 (Gonotec,

Germany). The glucose concentration of supernatants samples was measured by YSI 2950 Biochemistry Analyzer (YSI Life Sciences, UK). Supernatants glycerol concentration was determined by high performance liquid chromatography Chromaster system (Hitachi, USA) with an Aminex HPX-87H column (Bio-Rad Laboratories, USA) at 60 °C using 0.005 mol/L H₂SO₄ as the mobile phase at a flow rate of 0.6 mL/min and monitored by a refractor index detector.

4.6.1. Determination of purified IP concentration

The purified IP protein contents were measured by PierceTM bicinchoninic acid (BCA) protein assay kit with bovine serum albumin (BSA) as standard. The total protein was quantified identically as described in protocol provided with kit [107]. For all standard curves a minimal linear regressive coefficient of 0.99 was considered. In addition, protein concentrations were reconfirmed by dry-weight protocol. Determined volumes of purified IP solution dialyzed against 1x PBS buffer and solely 1x PBS buffer solution were separately lyophilized in pre-weighed and clean weighing conical centrifuge tubes. After freeze-drying was completed, the resulting powders were weighed and protein concentration was determined by discounting the mass difference per unit of volume between the IP/1x PBS solution and the 1x PBS solution.

4.6.2. SDS polyacrylamide gel electrophoresis (SDS-PAGE)

Culture broth was harvested, centrifuged at 13,000 rpm for 5 min; cell pellets and supernatants were separated and stored at -80 °C until use. The intracellular and extracellular fractions were analyzed by SDS-PAGE 12 or 16 % and Western blot. The formulation of stacking and separation gels mixture for 12 and 16 % SDS-PAGE is given in Table 4.6.1. Cell pellets were washed with ice-cold 1x PBS, re-suspended in cell lysis buffer (25 mmol/L potassium phosphate buffer pH 8.0, 5

mmol/L EDTA, 8 % (w/v) glycerol, 500 mmol/L sodium chloride), and normalized to a final OD₆₀₀ of 50. After 1:1 dilution with loading buffer (20 mmol/L Tris-HCl pH 8.0, 2 mmol/L EDTA, 5 % (w/v) SDS, 0.02 % (w/v) bromophenol blue, 5.5 % (v/v) glycerol, 20 % (v/v) 2-Mercaptoethanol), samples were boiled for 1 h at 96 °C and aliquots were loaded into the 12 or 16 % SDS-PAGE gel. The extracellular samples were 1:1 diluted with modified loading buffer (as described before however with 10 % (v/v) 2-Mercaptoethanol) and boiled at 96 °C for 5 min and loaded into the SDS-PAGE gels. The gel lanes were loaded with 7 µL sample (intra-/extracellular) and run at 60 V during the stacking and 110 V during the separation. The separated proteins were either stained with Coomassie brilliant blue solution (8.5 % (v/v) phosphoric acid, 10 % (w/v) ammonium sulfate, 0.1 % (w/v) Coomassie Blue G-250 and 20 % (v/v) methanol) or electroblotted onto a PVDF membrane (Bio-Rad Laboratories, USA).

Table 4.6.1 – Composition of resolving and stacking SDS-PAGE gels

| | Resolving gel 12 % (mL) | Resolving gel 16 % (mL) | Stacking gel 6 % (mL) |
|---|----------------------------|----------------------------|--------------------------|
| NF-Acrylamide/Bis-solution 40 % (29:1) | 3.00 | 3.75 | 0.75 |
| Resolving buffer 1.5 mol/L Tris HCl pH 8.8 | 3.20 | 3.20 | - |
| Stacking buffer 1.5 mol/L Tris HCl pH 6.8 | - | - | 0.63 |
| 1 % (w/v) SDS | 1.00 | 1.00 | 0.30 |
| Ultrapure water | 2.80 | 2.05 | 3.77 |
| 25 % (w/v) APS | 0.02 | 0.02 | 0.01 |
| TEMED | 0.02 | 0.02 | 0.01 |

4.6.3. Western blotting

Proteins separated on SDS-PAGE were electrotransferred using Bio-Rad Semi-dry Western blot apparatus onto polyvinylidene difluoride (PVDF) membrane. Prior to transfer PVDF membrane was soaked in methanol for a short time and then soaked in transfer buffer (25 mmol/L Tris, 200 mmol/L glycine and 20 % (v/v) methanol) along with thick filter pads for 5 min. The transfer was carried out at constant voltage of 15 V for 45 min at room temperature. After transfer, the membrane was

removed and incubated in blocking solution (5 % (w/v) skim milk, 2 % (w/v) polyvinylpyrrolidone, 1 % (v/v) Tween 20 in 1x PBS pH 7.2) for 2 h on a shaker at room temperature. Subsequently, the membrane was washed thrice with PBS-T (1x PBS containing 1 % (v/v) Tween 20) and incubated for 1h on a shaker at room temperature with mouse monoclonal primary antibody anti-HDEL (2E7) (sc-53472; Santa Cruz Biotechnology, USA), diluted to 1:1000 in PBS-T containing 5% skimmed milk and 2 % (w/v) polyvinylpyrrolidone. After incubation blots were washed thrice with PBS-T and incubated for 1h in a shaker at room temperature with secondary antibody (goat anti-mouse IgG H and L chain specific peroxidase conjugate (Calbiochem, USA), diluted 1:5000). Thereafter blots were again washed thrice with PBS-T and developed with TMB (3,3',5,5'-tetramethylbenzidine, Sigma-Aldrich, Germany) substrate until the bands were clearly visualized. All steps in immunoblotting were carried out on an orbital shaker. Each wash step was carried out for 5 minutes.

4.6.4. Kar2 normalized quantification

A normalized abundance analysis of Kar2 was performed during the entire thesis, allowing a representative comparison between different experimental conditions. Kar2 abundance changes were measured by densitometry analysis of Western blot membranes and SDS-PAGE gel images with ImageJ software (National Institutes of Health, USA). To enable representative analysis between conditions, the compared intracellular lysate or extracellular samples were prepared, loaded and run in two 12 % SDS-PAGE gels. One gel was stained with Coomassie for later analysis and the separated proteins in the other gel were electrotransferred onto Western blot PVDF membranes with subsequent anti-HDEL antibody incubation. The 12 % SDS-PAGE gels were either loaded with intracellular lysate samples previously normalized by optical density corresponding to an OD₆₀₀ of 50 and/or directly with extracellular supernatant fractions. Densitometry analysis allowed the determination of the Kar2 band area in the Western blot PVDF membrane image and the determination of the total intracellular/extracellular protein lane area from the corresponding time point sample in the Coomassie stained SDS-PAGE 12 %

gel image. The division of both estimated area values resulted in a normalized quantification of detectable Western blot Kar2 levels in the SDS-PAGE intracellular and/or extracellular *Pichia pastoris* fractions, termed Kar2 Western blot relative abundance.

4.6.5. Identification of protein bands by MALDI TOF

The SDS-PAGE band containing proteins were excised from the gels, washed thrice with Milli-Q water and additional two wash steps alternatively with Milli-Q water and acetonitrile by keeping in thermomixer for 5 mins at 300 rpm (Eppendorf, Germany). Thereafter a drying step in a speed vacuum centrifuge (Eppendorf, Germany) for 1 hour at 30 °C was performed, followed by freezing the samples at -80 °C. The spots were processed as follows. Identification of proteins bands were performed as described elsewhere [4]. Briefly, peptide mass fingerprints obtained by the MALDI TOF MS were processed using FlexAnalysis 2.0 (Bruker Daltonics GmbH, Germany) and used to search the NCBI database by using Mascot 2.10 software (<http://www.matrixscience.com>). The parameters used for searching were as follows: taxonomy: other Fungi, tryptic digestion, modifications were allowed for carbamidomethylation of cysteine (fixed modification) and methionine oxidation. Proteins with MASCOT score (probability based MOWSE scores) greater than 78 were considered significant ($P < 0.05$) as described elsewhere [4, 73].

4.7. Purification of Insulin precursor

Culture broth was first centrifuged, filtrated with 0,22 µm filters and frozen at -80° C. The supernatant was diluted 1:4 with sterile ultrapure water with 1% Tween 20 (pH 2.0, 4.7 mS/cm) to reduce the salt content (conductivity of culture broth was 24.2 mS/cm), the pH and the viscosity for more efficient binding to the Streamline SPXL resin (GE Healthcare, USA). The ultrapure H₂O with 1 % Tween 20 and

supernatant solution were mixed with 32.5 mL sediment bed of StreamLine SPXL resin and left overnight for interaction under agitation and 4 °C. After loading, the column was packed and washed with ultrapure water (pH 5.8) until the absorbance at 280 nm returned to base line in elute. Following, the bound IP was eluted using conventional chromatography using 1 mol/L sodium chloride (pH 7.5, conductivity ~100 mS/cm). Protein containing fractions (absorbance at 280 nm) were pooled. The pool was dialyzed against 1x PBS in Centricon falcon with MWCO of 3000 kDa. Lyophilisation was performed for storage and future quantification analysis.

4.8. Quantification of Insulin precursor by RP-HPLC

Filtered aliquots of *Pichia pastoris* cell-free supernatants and purified Insulin precursor powder, in several concentrations, were mixed 1:1 with solution A [0.15 % (v/v) TFA in ultrapure water] and analyzed by reversed-phase high performance liquid chromatography (RP-HPLC) using a 3 µm SUPELCOSIL™ LC-304 column (3.3 cm × 4.6 mm) with a Chromaster liquid chromatography system (Hitachi, USA), equipped with an autoinjector (model 5210), UV-VIS detector (model 5420), pumps A and B (model 5110), and a column oven whose temperature was maintained at 24 °C (HPLC column oven, model 5310). Elution was performed with a gradient formed by mixing solutions A and B [0.15 % (v/v) TFA in acetonitrile] as follows: 10 % B (0 - 6 min), 10 – 43 % B (6 - 41 min), 43 – 100 % B (41- 43 min), 100 – 10 % B (43 - 53 min), 10 % B (53 - 60 min). The flow rate was maintained at 1 mL/min and the column effluent was monitored at 214 nm and 280 nm.

4.9. Flow cytometry

Cell viability was determined by flow cytometry as described in [108]. The formation of intracellular ROS was measured employing 2',7'-dichlorofluorescein diacetate (DCFH-DA), as described in [109, 110]. Cells were analyzed on an Epics

XL-MCL (Beckman Coulter Inc., USA) with a 488 nm Argon laser. Using BD FACSFlow as the sheath fluid, 2×10^4 cells (events) were measured per analysis. Propidium iodide (PI) dye could penetrate only cells with leaky membranes and bind to DNA, exhibiting fluorescence with excitation at 480 nm and an emission maximum at 630 nm. Viable cells are able to deacetylate DCFH-DA to 2',7' - dichlorfluorescein (DCFH), which is not fluorescent. Upon activation of the cell oxidative burst, DCFH is rapidly oxidized to highly fluorescent 2',7' - dichlorfluorescein (DCF) in the presence of the generated ROS. DCF remains trapped within the cell and emits a green fluorescent signal that is measured to provide an index of intracellular ROS formation. Harvested cells were centrifuged to remove the supernatant. Afterwards, 5 μ L DCFH-DA (20 mmol/L in DMSO, stored at -20 °C) was added to 1 mL of the cell suspension diluted with PBS and incubated with continuous shaking at 37 °C for 30 min. Then the sample was placed on ice to stop any reactions. At 2 min before reading, 6 μ L PI (1 mg/mL) was added in the sample and analyzed. Samples were treated with heat over a flame to generate positive dead cells. To create ROS positive controls, oxidative activity was stimulated with Di-tert-butyl peroxide (DTBP) to a final concentration of 100 μ M, incubating cells suspension at 37 °C for 1 hour. The labeled cells were excited at 488 nm and the emitted light was collected through a 520/30 nm band-pass filter (FL1, for DCF) and a 630/30 nm BP filter (FL3, for PI).

5. Results

5.1. The unfolded protein response (UPR) in *Pichia pastoris* cultures

The unfolded protein response (UPR) of *Pichia pastoris* cells containing the Insulin precursor insert (X33-IP) and host strain (X33) during the execution of a two-stage fed-batch process was the focus of the investigation in this thesis section. For a detailed study, the first and the second cultivation stages - glycerol batch and methanol fed-batch phase, respectively - were initially investigated separately and afterwards jointly for a comprehensive understanding. The first stage, known as glycerol batch phase (GBP), consisted of a batch process with high initial glycerol concentration in low salt defined medium where *Pichia pastoris* cells were allowed unlimited growth until depletion of carbon sources. The second stage, the methanol induction phase (MIP), consists of a fed-batch process in which the secretory production of Insulin was induced. UPR investigations during the MIP were performed employing a shake flask fed-batch protocol where methanol was induced at an every 12 h interval for a period of 96 h. This protocol enabled the study of three parallel methanol induced culture conditions started, however, from the same bioreactor glycerol batch. Afterwards, cells UPR was investigated in bioreactor methanol feedback controlled fed-batches in order to study the physiological response of the producing strain in industrial relevant culture scale. Cells were grown in a glycerol batch, induction with different methanol concentrations were performed at the “DO-spike”, and the feedback fed-batches were controlled in closed loop by a proportional-integral-derivative (PID) controller in response to a flame ionization detector (FID).

Refer to Appendix I, section 9.2, 9.3 and 9.4 for parameter details of an entire two-stage fed-batch cultivation, purification and HPLC quantification, respectively, performed to obtain Insulin precursor lyophilized powder employed in the entire thesis as standard for IP quantification curves.

5.1.1. Downregulation of UPR during bioreactor glycerol batch phase

Non-carbon limited batch cultivations with *P. pastoris* producing and non-producing strains were studied, monitoring cellular physiological response, with special focus to the unfolded protein response (for details on the host strain cultivation, refer to section 10.1). The metabolic state of the cells was accessed by examining small fluctuations of proteins containing the HDEL ER retention peptide using an anti-HDEL antibody, which is present in the main UPR response target protein Kar2. Figure 5.1.1– A shows the SDS-PAGE gel with samples normalized by OD₆₀₀, collected during the entire glycerol batch phase and Figure 5.1.1 – B illustrates the same lysate samples electro-blotted onto a PVDF membrane, stained for a controlled time period after incubation with specific antibodies. These images were employed in the Kar2 relative quantification densitometry analysis described in detail in the Methods section 4.6.4. For a comprehensive analysis of the batch process, after the end of the exponential phase cells were allowed to enter the stationary phase and the intracellular amount of Kar2, the main marker for UPR, was monitored during the entire process (Figure 5.1.1 – C). The growth related protein aggregation prevention phenomenon seems to be differently regulated during the applied non-carbon limited batch cultures. After early adaptation (Lag phase), cells start consuming glycerol and the growth related Kar2 biosynthesis gets fully activated by cells entering the exponential growth phase (Figure 5.1.1 – B and C). In time, cellular growth declines and is followed by a decrease in the Kar2 amount. When compared to initial exponential growth phase values, intracellular Kar2 presented a ~5 fold and ~20 fold decrease in the declining growth phase and stationary phase, respectively, (Figure 5.1.1 – C). No Kar2 could be detected in the extracellular fraction of the producing or non-producing strain during the entire batch growth in glycerol (for the host strain SDS gels refer to Figure 10.1.1 – B and D).

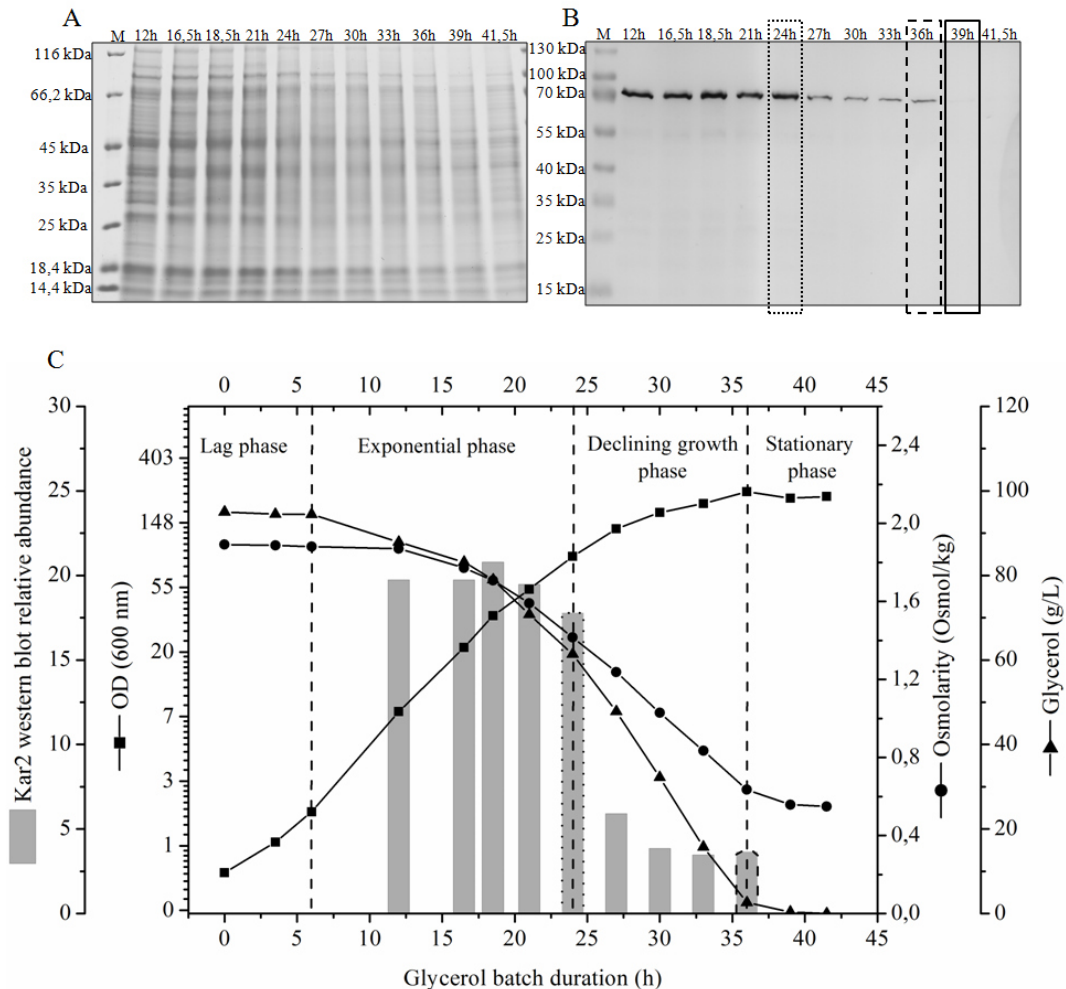


Figure 5.1.1 – Time course analysis of the bioreactor glycerol batch from *Pichia pastoris* X33-IP cells.

(A) Intracellular lysates fractions from *P. pastoris* X33-IP analyzed by 12 % SDS-PAGE. (B) Intracellular lysates fractions from *P. pastoris* X33-IP probed for proteins containing the endoplasmic reticulum retention signal peptide HDEL (e.g. Kar2, 74 kDa) by Western blot analysis. All lysate loaded samples were normalized at OD₆₀₀ 50 and extracellular fractions were directly applied. (C) Abundance changes of UPR related protein Kar2 are given in relative units corresponding to Western blot densitometry analysis, the optical density, and extracellular glycerol concentrations and osmolarity during glycerol batch. The sample at 12h was the first with enough cell pellet which allowed intracellular fraction examination. The vertical dashed lines highlight the growth phases during glycerol batch process. The M lane denotes the molecular weight marker. The highlighted Kar2 relative abundance quantification dotted and dashed bars in (C) stand for the respective time points Western blot bands in (B).

5.1.1.1. High Kar2 abundance in exponentially growing cells

The burden of growth in a recombinant-protein-free environment was further investigated in *Pichia pastoris* X33-IP cells employing the same low salt defined medium containing four different glycerol concentrations, as indicated in Table

5.1.1. Considering that glycerol is a trihydroxy sugar alcohol, the increase in media osmolarity, measured by a freezing point osmometer, correlates positively with increasing glycerol concentrations (Figure 5.1.2 and Table 5.1.1). It is important to report that media osmolarity values decreased during the batch phase parallel to glycerol decline, caused via cellular consumption (Figure 5.1.2). Furthermore, it is viable to speculate that lower glycerol concentrations favored cellular growth, since the highest maximal specific growth rate (μ_{\max}) was achieved under the lowest initial glycerol concentration (30 g/L) (Table 5.1.1).

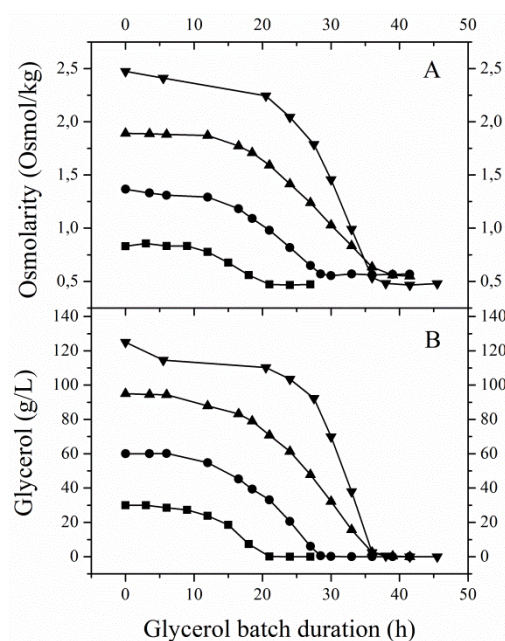


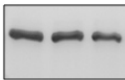
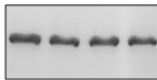
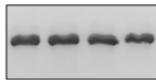
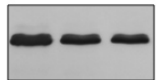
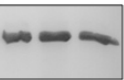
Figure 5.1.2 – Media osmolarity decreases concomitant to glycerol reduction.

Time course analysis of media osmolarity (A) and glycerol concentrations (B) during *Pichia pastoris* X33-IP batch phase cultivations. Identical symbols in Figure A and B correspond to the same batch conditions.

Although promising expectations emerged that increased medium osmolarity would result in increased biosynthetic capacity, through the presence of augmented Kar2 levels, the findings pointed rather to other conclusions. It seems that the UPR is equally highly activated in exponentially growing cells regardless of strain and the initial glycerol concentrations employed, ranging from 30 to 125 g/L. For better comprehension, the Western blot bands in Table 5.1.1, from the respective exponential growth phase (as defined in Figure 5.1.1 – C) of each different glycerol concentration applied and strain, were quantified for Kar2 relative abundance as

previously. The *Pichia pastoris* culture conditions studied, presented very similar relative intracellular Kar2 abundance during exponential growth phase (Table 5.1.1), further illustrated by the proximity of each Kar2 relative amount to the calculated average of 19. Moreover, identical UPR downregulation time profile observed during X33-IP 95 g/L glycerol batch growth (Figure 5.1.1) was detected for all the glycerol conditions and producing or non-producing strains described in Table 5.1.1 (detailed X33 host strain UPR downregulation: Figure 10.1.1).

Table 5.1.1 – Comparison of *Pichia pastoris* batches with different glycerol concentrations

| <i>Pichia pastoris</i> Strain | X33-IP | X33-IP | X33-IP | X33 | X33-IP |
|--|---|---|--|---|---|
| Initial glycerol (g/L) | 30 | 60 | 95 | 95 | 125 |
| Maximal specific growth rate μ_{\max} (h⁻¹) | 0.26* | 0.20* | 0.18 | 0.18 | 0.18 |
| Initial medium osmolarity (osmol/kg) | 0.83* | 1.36* | 1.85 | 1.81 | 2.47 |
| Exponential phase Kar2 |  |  |  |  |  |
| Kar2 WB relative abundance | 17* | 19* | 20 | 21 | 18 |

* Results are an average of duplicate experiments.

5.1.2. Independence of prior to induction Kar2 levels on secretory IP production

So far, the observations have illustrated that exponentially growing cells present UPR activation prior to recombinant protein induction, regardless of initial medium osmolarity, glycerol concentration and strain, and that this folding response is downregulated during growth time course. The synthesis of UPR related proteins prior to induction have been suggested to precondition *P. pastoris* cells for more effective IP secretion [4]. To investigate if this “more constitutive” UPR induction influenced the recombinant protein production, 10 L glycerol bioreactor batch cultivations of *P. pastoris* X33-IP and X33 (host strain culture details in section 10.1) were performed, harvesting the X33-IP cells at three different growth moments corresponding to high, medium and low constitutive Kar2 (highlighted rectangles in Figure 5.1.1 – B whose relative Kar2 band abundance are represented by the bars in the left side of the dashed line in Figure 5.1.3 – B) and shifting them directly to methanol induction phase in shake flasks. This protocol enabled the study of three parallel cultures induced with different initial intracellular Kar2 amount, grown, however, in the same original 10 L glycerol batch. The induction with 1% (v/v) methanol at every 12 h intervals for a period of 96 h was performed to simulate a fed-batch process.

In line with previous results [4], an expected decline in Kar2 intracellular levels, until almost undetectable amounts, occurred right after methanol induction in both strains (X33-IP and X33 Figure 5.1.3 – A). An immediate UPR decrease was even observed in exponentially growing cells, which presented at induction time (0h methanol feed) the highest amount of batch produced intracellular Kar2 (abundance bar in the left side of the dashed line in Figure 5.1.3 – B). Furthermore, concomitant to the Kar2 intracellular drop after methanol induction, increase of the chaperone detected levels in the extracellular fraction of the producing strain (X33-IP) occurred simultaneously to the uprising secretion of Insulin precursor (IP) (Figure 5.1.3 – A and C). The increasing levels of extracellular Kar2 in the X33-IP producing strain are represented by the relative abundance quantification shown in Figure 5.1.3 – B.

The Kar2 relative abundance analysis allowed the further observation that after methanol induction the biosynthesis of freshly produced Kar2 takes place. Considering the respective amount of batch produced intracellular Kar2 at induction time as an initial reference for each growth phase, the upper part of the abundance bars above the horizontal dotted lines in Figure 5.1.3 – B represent the *de novo* synthesized Kar2 during methanol induction phase. It is viable to speculate that all freshly produced Kar2 was able to fold the Insulin precursor correctly, however failed to unbind from the zymogen and both were secreted as a Kar2/IP complex, as already reported [111].

Additionally, the time course production of secretory Insulin precursor in shake flasks was analyzed for the differently UPR preconditioned cultures (Figure 5.1.3 – C). Cells from the bioreactor batch culture harvested at the stationary growth phase, where the lowest batch related intracellular Kar2 amount was detected, presented the highest secretory Insulin precursor production in shake flasks (Figure 5.1.3 – C), not evidencing a positive correlation between the batch-produced Kar2 and secretory IP production.

Taken together, these observations and the fact that the non-producing strain presented no Kar2 expression neither in the intracellular or extracellular fraction after methanol induction (Figure 5.1.3 – A and Figure 10.1.1), indicate that Kar2 is not needed for cellular maintenance on methanol containing media during the 96 hours observed. Hence, for the IP producing strain, it seems that independently of the level of UPR prior to induction, the secretory IP production reactivates the biosynthesis of Kar2 and all fresh chaperones were directed to recombinant proteins folding.

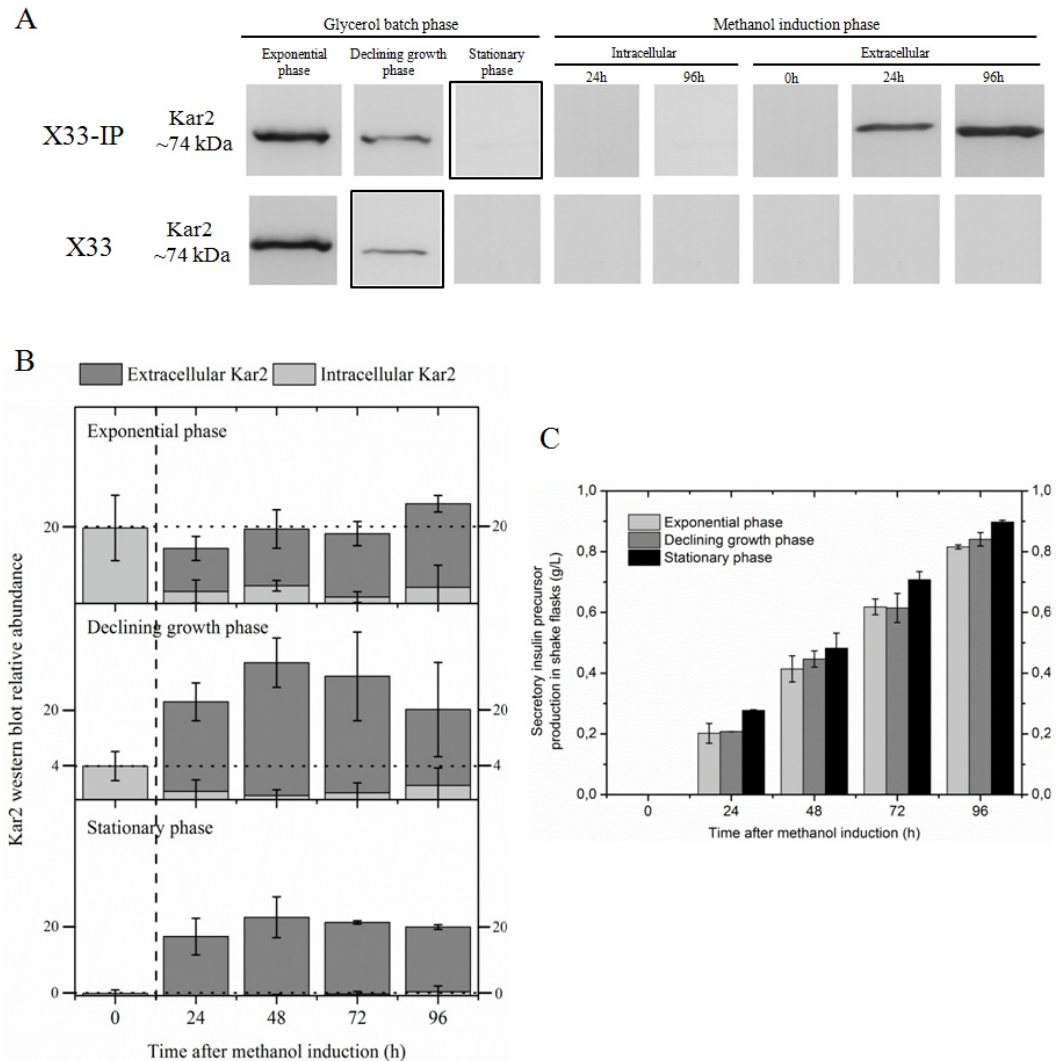


Figure 5.1.3 – Monitoring Kar2 in the intracellular and extracellular fractions of methanol fed-batch phase in shake flasks of *P. pastoris* cells harvested at different glycerol growth phase and time course analysis of secretory Insulin precursor production.

(A) Sections of Western blot analysis of intracellular crude cell lysate and extracellular supernatant from producing and non-producing cells probed for proteins containing the endoplasmic reticulum retention signal peptide HDEL (e.g. Kar2, 74 kDa). Samples were taken at the indicated glycerol batch phase and at 0, 24, 96 hours after methanol induction. The bands inside the highlighted rectangles indicate the intracellular Kar2 amount at methanol induction time. All lysate loaded samples were normalized at OD₆₀₀ 50 and extracellular fractions were directly applied. (B) Intracellular and extracellular abundance changes of the UPR related protein, Kar2, are given in relative units corresponding to an average of the resulting values from duplicate gels images. All Kar2 amounts above the dotted horizontal line stand for freshly synthesized chaperone. The abundance bars at the left side of the dashed vertical line indicate the intracellular Kar2 amount present during glycerol batch. (C) Time course analysis of secretory Insulin precursor production in shake flasks quantified by HPLC from cells harvested at different glycerol growth phase. The average and standard error from two independent experiments are shown.

5.1.3. Influence of methanol concentration on Kar2 secretion during bioreactor feedback controlled fed-batches

Pichia pastoris X33-IP cells were grown employing the two-stage bioreactor fed-batch procedure. Initially cells were grown in the 95 g/L glycerol and low salt defined medium batch procedure followed by the FID feedback controlled methanol induced fed-batch phase, under different inducer concentrations: 1.7, 5.0, 6.8 g/L methanol. The feedback controlled methanol fed-batches were induced at the end of each exponential growth phase, when the batch carbon sources were depleted and the “DO-spike” was observed. Before evaluating how Kar2 was regulated during the different methanol induction phase conditions, its state was monitored during the glycerol batches and at induction time. All glycerol batch phases from the later methanol induced fed-batches presented the same growth related UPR downregulation as described in section 5.1.1 and exemplified by Figure 9.2.4. Figure 5.1.4 illustrates that at methanol induction moment all glycerol growth phases from the four fed-batch conditions presented comparable intracellular Kar2 amounts and complete absence of the chaperone in the extracellular fraction.

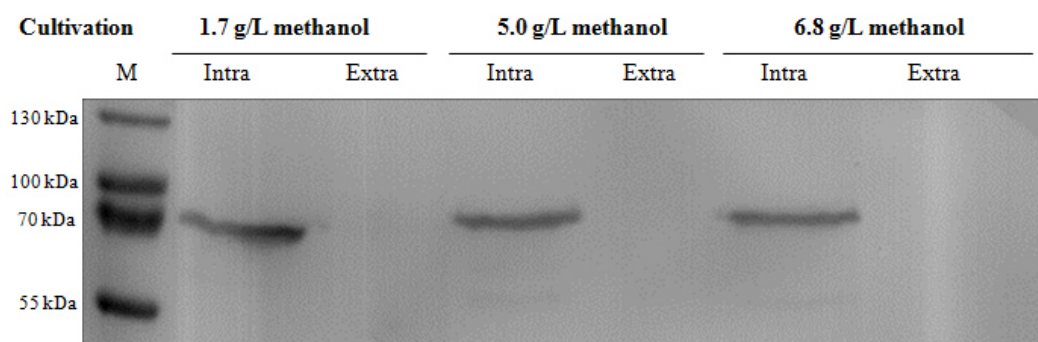


Figure 5.1.4 – Comparison of intracellular and extracellular Kar2 at fed-batch methanol induction time.

Kar2 was analyzed in the intracellular and extracellular fraction of *Pichia pastoris* X33-IP cells at glycerol batch DO-spike – moment of methanol induction – for all four different methanol concentration fed-batches. All lysate loaded samples were normalized at OD₆₀₀ 50 and extracellular fractions were directly applied. The M lane denotes the molecular weight marker.

Thereafter, the evaluation of Kar2 expression level and cellular location during the secretory IP producing fed-batch phase was performed. To illustrate the results, the previously applied Kar2 relative quantification densitometry technique was once again employed, comparing three different bioreactor cultivations, respectively with 1.7, 5.0 and 6.8 g/L methanol. Figure 5.1.5 – A demonstrates that during the feedback controlled methanol fed-batch phases employed the intracellular abundance of Kar2 decreases until no more chaperone was detected, as observed for the producing and non-producing strains in the shake flask fed-batches (Figure 5.1.3 – A). In addition, it was possible to identify one other protein in the intracellular fraction that was recognized by the anti-HDEL antibody in the intracellular fraction, possibly protein disulfide isomerase (PDI), ~55 kDa or degradation of Kar2 (Figure 13.1.3 – B). The next step was to monitor Kar2 secretion in the feedback controlled fed-batches. As previously observed for the shake flask fed-batches, the extracellular abundance of Kar2 increased with time during the feedback controlled methanol fed-batch phases until complete detectable intracellular absence was observed (Figure 5.1.5 – A). In all fed-batch conditions the extracellular Kar2 increase occurs concomitantly with its intracellular decrease and parallel to increasing Insulin precursor secretion (Figure 5.1.5 – A and B). Moreover, it seems that the increase of methanol concentration in the methanol fed-batch phase accelerated Kar2 secretion process (Figure 5.1.5 – A). However, since foaming was observed at the highest methanol fed-batch concentration (6.8 g/L) applied any correlation between methanol concentration and Kar2 secretion should be made cautiously. Furthermore, the comparable intracellular Kar2 amounts at induction time (Western blot presented in Figure 5.1.4) were reconfirmed by the relative Kar2 quantification technique in Figure 5.1.5 – A (bars in the left side of the dashed vertical line). Summarized, these results from the feedback controlled fed-batches point out that *Pichia pastoris* X33-IP cells presented comparable physiological response, monitored by intracellular and extracellular Kar2 quantification, during secretory Insulin production regardless of the cultivation procedure employed, shake flask or bioreactor.

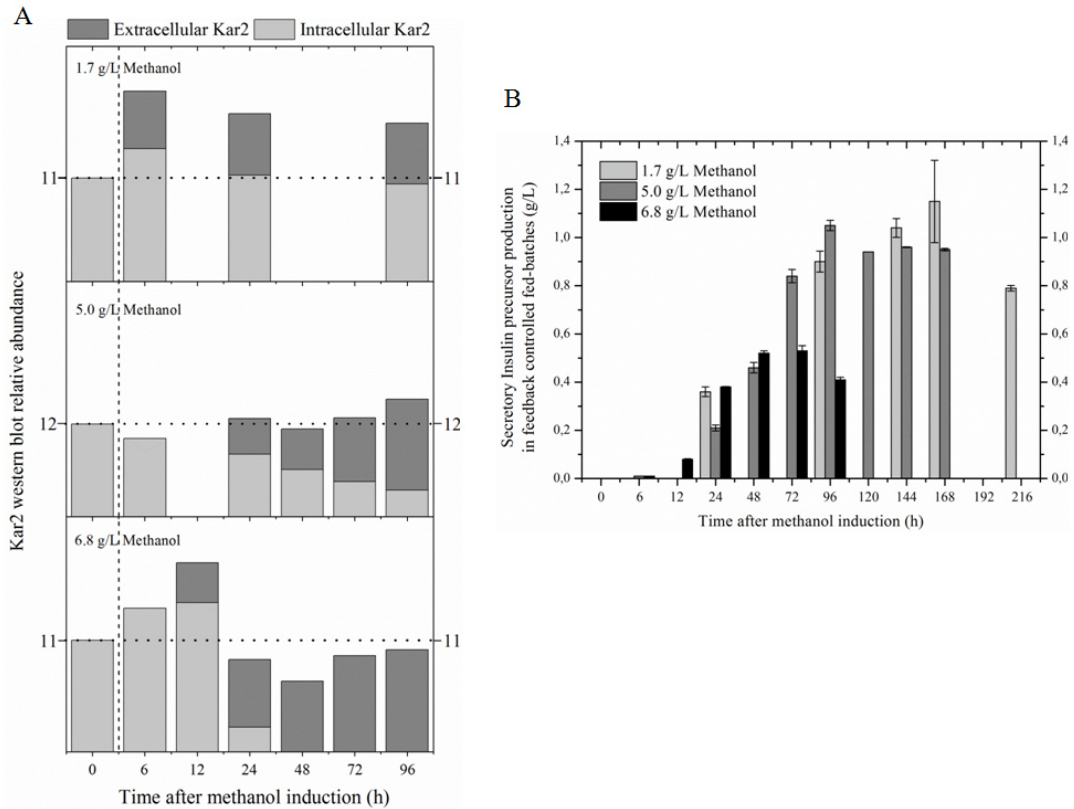


Figure 5.1.5 – Effect of different fed-batch methanol concentrations on intracellular and extracellular Kar2 and on secretory Insulin precursor production.

(A) Intracellular and extracellular abundance changes of the UPR related protein, Kar2, are given in relative units. All Kar2 amounts above the dotted horizontal line stand for freshly synthesized chaperone. The abundance bars at the left side of the dashed vertical line indicate the intracellular Kar2 amount produced during glycerol batch at induction time. (B) Time course analysis of secretory Insulin precursor production quantified by HPLC from cells under different methanol fed-batch concentrations. The average and standard error from two independent HPLC analyses are shown.

5.2. Reactive oxygen species (ROS) and cellular viability monitoring

The time course study of reactive oxygen species (ROS) and cell viability during the *Pichia pastoris* methanol shake flask fed-batch was performed by flow cytometry, firstly comparing two producing and two non-producing strains: the intracellular Hepatitis B surface antigen (HBsAg) and the secretory Insulin precursor (X33-IP) producing strains and the respective GS115 and X33 host strains. Thereafter, the effect of growth related UPR induction on ROS formation was studied, employing the X33-IP producing strain grown in 10 L defined medium glycerol bioreactor batch harvested at different growth moments: exponential phase, declining growth phase and stationary phase.

5.2.1. Augmented ROS in recombinant *P. pastoris* strains

The comparison between 4 *Pichia pastoris* strains grown under identical shake flask containing complex media conditions enabled the analysis of the effect of methanol metabolism and recombinant protein production on cellular oxidative stress through ROS formation. The producing strains applied here have been successfully employed for the heterologous production of intracellular Hepatitis B surface antigen (6 g/L) and the secretory Insulin precursor (3 g/L) [2, 112], where proteomic studies showed that the ER-resident production of HBsAg submitted *P. pastoris* cells to higher activation of ERAD and UPR stress responses, when compared to the secretory IP [3, 4]. As control, the non-producing *his4* auxotroph GS115 and the host strain X33 were employed.

Flow cytometry results indicated that the secretory IP and the intracellular HBsAg producing strains presented increased ROS formation under the conditions tested. X33-IP and HBsAg cells presented increasing FL1 (ROS) mean fluorescent signal intensity during the methanol induction phase, reaching the highest values at 96 h after methanol induction (Figure 5.2.1 – A). Since both host strains at 96 h of

methanol feeding showed lower FL1 fluorescence signal under the same culture conditions, it is clear that the effect of heterologous protein production on ROS formation is higher than methanol metabolism, in spite of its basal increase over time. Unexpectedly, despite of having to cope with a larger and complex product, the HBsAg producing strain presented slightly higher FL1 mean signal intensities than the GS115 host strain in both cultivation repetitions, whereas the X33-IP producing strain showed ~3.5 fold average fluorescence signal increase relative to the X33 non-producing strain, indicating augmented ROS formation throughout secretory heterologous protein production. Furthermore, the strains presented high viability (> 93 %) and relatively constant OD₆₀₀ values during the entire methanol induction phase (Figure 5.2.1 – B and C).

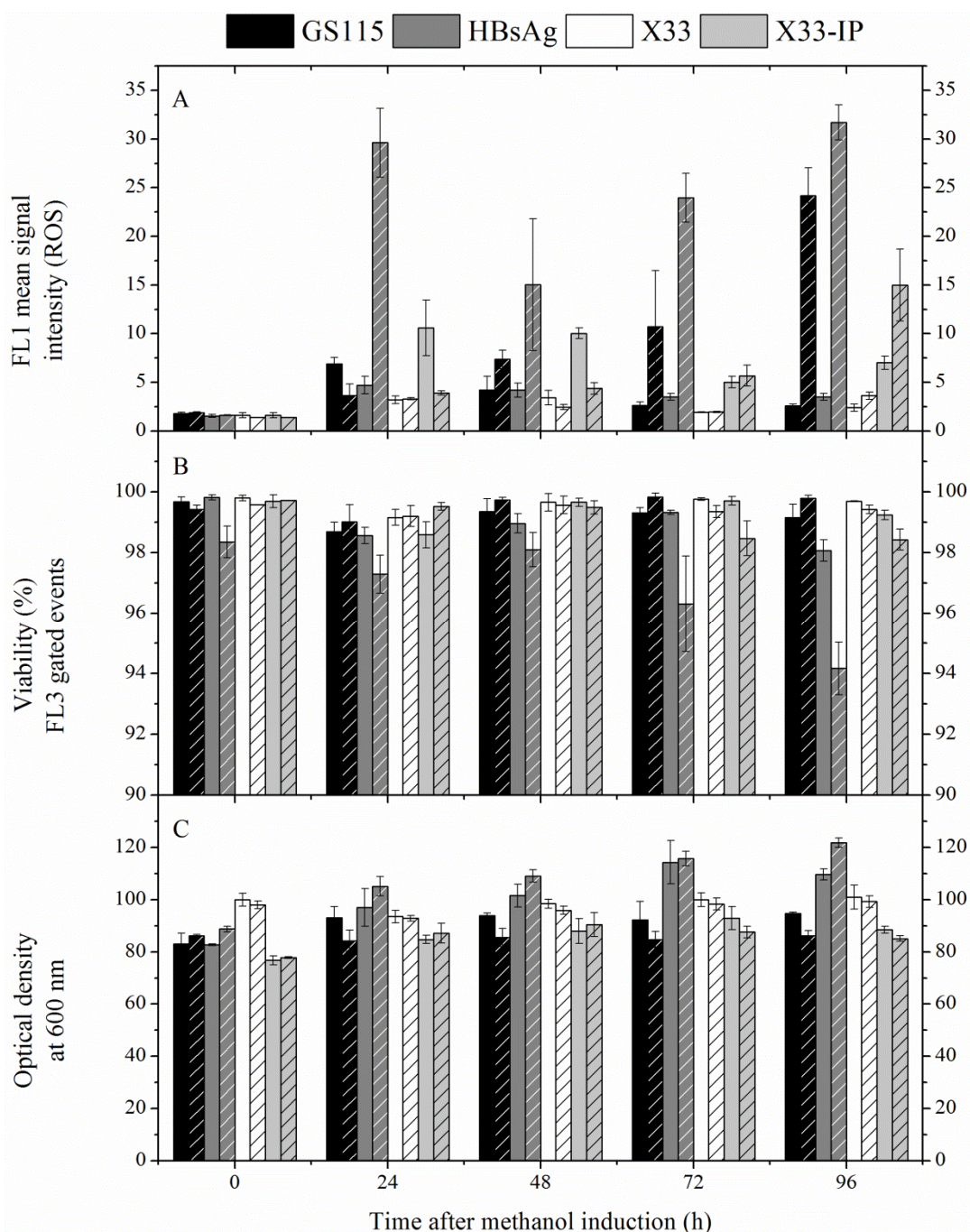


Figure 5.2.1 – ROS, viability and optical density of 4 different *Pichia pastoris* strains.

Pichia pastoris shake flask fed-batch cultures of GS115, X33, HBsAg and X33-IP cells were monitored and compared during the methanol induction phase for reactive oxygen species (ROS) formation (A), cellular viability (B) and optical density at 600 nm (C). Fluorescence signal intensity for ROS (FL1) and viability (FL3), monitored by flow cytometry, were carried out by double staining with DCF and PI, respectively. Cells were first grown in complex media containing glycerol to generate sufficient biomass, harvested, centrifuged and re-suspended in three shake flasks with fresh methanol containing media. Cultivations with the 4 strains were performed two times independently and the pattern inside the bars indicates repetition experiments. The average and standard error from the methanol induction phase of each strain's triplicate shake flasks experiments are shown.

5.2.2. General ROS increase in *P. pastoris* X33-IP cells induced at different growth times

The study of ROS formation of *Pichia pastoris* X33 secreting Insulin precursor (X33-IP) was performed employing the previously described methanol shake flask fed-batch protocol, with cells harvested from a 10 L defined medium glycerol batch at different growth moments. Induction with 1% (v/v) methanol at every 12 h intervals for a period of 96 h was performed to simulate a fed-batch process. A general FL1 mean fluorescence signal (ROS) increase was observed during the methanol induced secretory IP production shake flask fed-batch independent of the different glycerol growth moment which they were induced (Figure 5.2.2 – A). Results point out that augmented ROS is equally increased independently of the UPR activation during glycerol batch prior to methanol induction. During the entire shake flask fed-batch process cells presented very high viability values, > 98 % (Figure 5.2.2 – E). At time point 0 h cells presented the lowest ROS amounts (Figure 5.2.2 – A). In time, cells adapt to the methanol containing media, arresting growth, (stabilizing OD₆₀₀, Figure 5.2.2 – D), metabolizing the substrate through the dissimilation pathway and the secretory production of Insulin precursor (Figure 5.2.2 – F). In the first 24 h the highest residual methanol was found (Figure 5.2.2 – B), thereafter cells consume it per shake flask (~37 mL culture medium) in a rate of ~15 g/day (Figure 5.2.2 – C). It should be noted that the shake flask protocol employs the induction of 1 % (v/v) methanol at every 12 h intervals for a period of 96 h. The highest ROS formation was detected, as expected, after 96 h, the end of the methanol shake flask fed-batch cultivation (Figure 5.2.2 – A). At this point, the highest levels of secretory Insulin were also detected (Figure 5.2.2 – F).

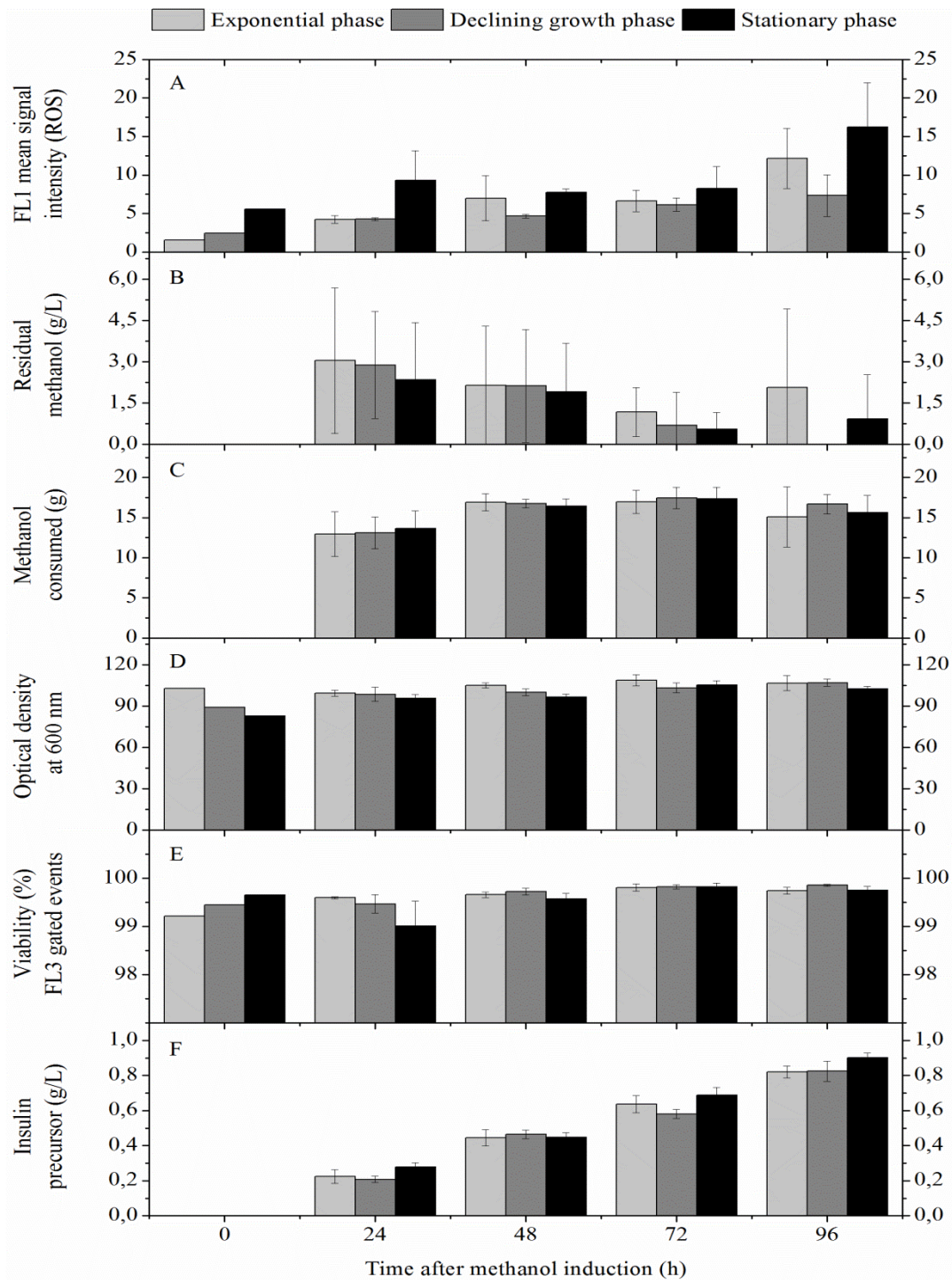


Figure 5.2.2 – Methanol shake flask fed-batches time course monitoring and comparison of X33-IP cells.

Pichia pastoris X33-IP shake flask fed-batch cultures of cells harvested at exponential growth, declining growth and stationary growth phases were monitored and compared during the methanol induction phase for reactive oxygen species (ROS) formation (A), supernatant residual (B) and consumed (C) methanol concentration, optical density at 600 nm (D), cellular viability (E) and secretory Insulin precursor production by HPLC (F). Fluorescence signal intensity for ROS (FL1) and viability (FL3), monitored by flow cytometry, were carried out by double staining with DCF and PI, respectively. Cells were firstly grown in complex media containing glycerol to generate sufficient biomass, harvested, centrifuged and re-suspended in three shake flasks with fresh methanol containing media. The average and standard error from the methanol induction phase of each condition's triplicate shake flasks experiments are shown.

6. Discussion

The increasing need for biopharmaceuticals is a fact which is represented by its every year growing market. This ever rising demand has to be attended with state of the art technique. *Pichia pastoris* has a remarkable success story over the past three decades due to its unique characteristics; among them its high secretory capacity, the ability to grow into high biomass, possibility of human like glycosylation, controllable recombinant protein promoter. In spite of all this advantages, there is still limited knowledge on how stress responses during the production of proteins such as Insulin, vaccines or others are affecting the final productivities and the recombinant product quality. Stress responses are a broad subject which demands careful attention. The study of physiological responses of *Pichia pastoris* has been the interest of our research group for some years now. Firstly, the biotechnological process development was performed for intracellular production of Hepatitis B surface antigen (HBsAg) and thereafter for the secretory production of Insulin precursor (IP) employing two-stage fed-batch bioreactor cultivation with *Pichia pastoris* GS115 and X33, respectively [2, 112]. Afterwards, a general study of the cells physiological response was performed employing 2D gels proteomics technique. A difference in the cells response depending on the recombinant protein produced was reported [3, 4]. Interestingly, while producing the small molecule of IP *Pichia pastoris* cells did not present the expected ER stress response as they did during the recombinant HBsAg production. This discrepancy between stress response depending of the product produced and cellular state prior and after induction, rose several questions which were the focus of the work presented in this thesis. Furthermore, surprisingly little attention has been given to the yeast physiological state prior to induction, independent of the production of aberrant proteins. Therefore, to attend these questions, the unfolded protein response in *Pichia pastoris* X33 cells producing and non-producing secretory Insulin precursor was studied in detail. The cultivation phases – the glycerol batch and the methanol fed-batch – were initially studied separately and thereafter in a comprehensive manner where the effect of one phase upon the other was the subject of study.

The commercially available operational manual for fed-batch growth of *Pichia pastoris*, originally developed for the Mut⁻ strain [113], undergoes three different fermentation phases. A glycerol batch phase (GBP), a mixed-feed transition phase (TP) and finally a methanol induction phase (MIP). The alternative fermentation techniques developed by our research group excluded the TP, employed the Mut⁺ strain obtaining high-level protein expression [2, 112]. The modified two-phase fed-batch procedure for the secretory production of Insulin precursor (IP) [2], originally developed for high-level intracellular production of Hepatitis B surface antigen (HBsAg) with *P. Pastoris* GS115 [112], was further optimized by employing the bioreactor defined medium in the pre-cultures, obtaining more reproducible growth curves prior to main culture inoculation (Appendix I, section 9.1). The production of Insulin precursor purified powder, to be used as a reference during the entire thesis, was performed by cultivating the inoculum preconditioned *Pichia pastoris* cells containing the Insulin precursor insert (X33-IP) in the industrial relevant fed-batch approach [2]. In this system, usually applied for large scale production of recombinant proteins, cells were initially transferred into batch defined medium containing high glycerol concentrations and low to moderate salt, resulting in high initial osmolarities, and grown until high biomass prior to induction of recombinant proteins (Figure 5.1.1 and Appendix I, section 9.2). The successful production and purification of IP enabled its use as a quantification standard during the entire thesis (Appendix I, Figure 9.2.2, Figure 9.2.3, Figure 9.3.1 and Figure 9.4.1).

Downregulation of Kar2 throughout glycerol batch phase

The occurrence of inherent protein misfolding incidents during cellular growth [38] requires quality control systems. As an integral part of the ER surveillance machinery, Kar2 binds more persistently to misfolded or unassembled proteins and prevents them from exiting the ER [36]. In spite of the attenuation of the immediate osmotic stress, which can cause temporary growth arrest [93], by preconditioning cells in defined medium pre-culture, metabolic adaptation results were obtained monitoring the UPR marker Kar2 intracellular levels. The growth related unfolded protein response seems to be differently regulated during the applied non-carbon limited glycerol batch cultures independently if the *Pichia pastoris* strain X33 carried or not the secretory Insulin precursor insert (Figure 5.1.1 and Figure 10.1.1)

or on how high the initial defined medium glycerol concentrations were (Table 5.1.1). Taking in account that studies demonstrated that UPR markers (e.g. Kar2) in *Pichia pastoris* wild type strains were ~3 fold upregulated in ionic compounds induced high osmolarity when compared to low osmolarity conditions [95], thus the high Kar2 amount for both strains in this work during exponential growth phase was thought to be related to the elevated initial osmolarity caused by high glycerol concentration in culture medium. This hypothesis however was ruled out by the results obtained from the batch cultures containing different initial glycerol concentrations. Indeed, employing variable glycerol concentrations different osmolarity values were obtained (Figure 5.1.2), however the same initial relative abundance of Kar2 at exponential phase and UPR decrease during batch cultivation time course were observed for all glycerol conditions employed (Table 5.1.1). This could mean that cells present an equal and maximal biosynthetic capacity, measured by monitoring Kar2, to undergo growth in defined medium containing glycerol. On the other hand, recent reports account for UPR induction, by upregulation of *HAC1*, also a UPR marker, and its primary targets, with increasing specific growth rate (μ) as one major regulatory reaction to increasing cellular proliferation [83]. Therefore the observed high relative abundance of Kar2 for all glycerol conditions during the initial exponential phase hours presented in Table 5.1.1 would be due to an overlapped effect caused by osmolarity and specific growth rate. Since, while under low initial glycerol concentrations, consequently low medium osmolarity, cells achieve a higher maximal specific growth rate (μ_{\max}), and vice-versa, the effect of osmolarity on UPR could be masked due to the effect of growth rate in UPR. Furthermore, the disappearance of intracellular Kar2 during the stationary growth phase could indicate a phenomenon called ER-phagy [114-116]. Autophagy is a normal physiological process to maintain cellular homeostasis that occurs during extended cultivation periods and under other conditions, and Ribophagy – degradation of ribosomes - and Pexophagy – degradation of peroxisomes - have been already observed in *Pichia pastoris* growing under different conditions [3, 114, 117-119]. The process of engulfing the ER and target it to degradation, would explain the disappearance of the ER-resident chaperone Kar2 during the batch stationary phase of growth, as observed by Zhong et al. [114], however this phenomenon has to be further investigated to avoid any early conclusions.

Independence of prior to induction Kar2 levels on secretory IP production

There is some evidence that exposure to osmotic stress can have a beneficial effect on recombinant protein production in bacterial, yeast and mammalian host organisms, however this effect, at least in mammalian cells, is often cell line specific [90, 95, 120-122]. Additionally, it is already known that extrapolation of environmental conditions, such as cellular nutritional state [36], methanol concentration in the MIP [4] and temperature [85], could force the yeast cells into high levels of ER stress through the activation of the unfolded protein response (UPR) and Endoplasmic-reticulum-associated protein degradation (ERAD). Regarding the methanol induction phase different levels of stress on the host cell may be exerted, depending on the specific features of the overexpressed secreted mutant or foreign protein. Not only elevated intracellular levels [3, 111, 123] but also increased extracellular secretion of Kar2 [41, 111] have been reported. In the case of methanol-induced secretory Insulin precursor production in *Pichia pastoris* X33 there is a decrease of the UPR activity in the intracellular fraction [4]. Since, little attention has been given to the cells physiological state prior to induction and how relevant is its effect over the production phase, the shake flask fed-batch protocol was employed harvesting cells at different growth moments during glycerol batch phase and inducing them for the secretory production of Insulin precursor. In spite of expectations that UPR preconditioned cells, induced with methanol during the exponential growth phase, would favor recombinant protein production due to augmented relative Kar2 abundance, results pointed out to other conclusions. It seems that the generated UPR during glycerol batch phase does not influence the secretion of Insulin precursor (Figure 5.1.3 – C). Actually, *Pichia pastoris* X33-IP cells induced at the stationary phase, which were growth related Kar2 absent, produced high amounts of fresh chaperone, and elevated IP production and Kar2 secretion during the methanol phase (Figure 5.1.3). Furthermore results indicate that this ER chaperone secretion phenomenon is solely due to recombinant production since the *Pichia pastoris* host strain X33 presented after methanol induction intracellular and extracellular absence of Kar2 (Figure 10.1.1). These unexpected results corroborate with the previously reported decrease of UPR and ERAD pathways during methanol induced secretory IP production [4], as well as, with the non-essentiality for growth of retained Kar2 by the HDEL

system [63], as producing and non-producing cells presented high viability values (> 98 %) during the entire shake flask fed-batch procedure (Figure 5.2.2 – E). The Insulin precursor gene is preceded by the *Saccharomyces cerevisiae* α -mating factor pre-pro-peptide signal leader sequence. This secretion signal seems to work fine given that IP has been successfully detected in the culture supernatant during the shake flask and feedback controlled fed-batches (Figure 5.1.3 – C, Table 12.1.1 and Figure 9.2.2 – F). However, this could also be causing Kar2 extracellular translocation, given that it has been shown that the Erd2-mediated retention can be saturated by overexpression of an HDEL-tagged pro- α -factor or Kar2, and by other conditions that activate the UPR (e.g., treatment with β -mercaptoethanol or tunicamycin) [63, 64, 111, 124, 125]. These results indicate that the retention of ER luminal proteins is a complicated and still unsolved mechanism, which does not strictly depend only on HDEL/KDEL sequences, but is likely a combination of several factors.

Augmented ROS throughout recombinant protein production

Studies on *Saccharomyces cerevisiae* showed that in addition to upregulate the known UPR targets, the Ire1-*HAC1* pathway also activated some anti-oxidative stress genes, possibly in order to reduce reactive oxygen species produced during the cellular response to ER stress, suggesting a protective “side-effect” action of this pathway on oxidative stress [75, 126]. Considering that recombinant protein production may also induce ER stress, an imbalance between heterologous protein folding and disulfide bond formation rates in *S. cerevisiae* were proposed to lead to production of augmented ROS, through many glutathione peroxidase (Pmp20) mediated futile redox cycles [101]. Indeed, augmented ROS was observed solely in the IP and HBsAg producing strains (Figure 5.2.1 – A), indicating a clear higher effect of heterologous protein production compared to methanol metabolism on ROS. Nevertheless, in the work of Vanz et al. [3] after methanol induction in HBsAg and IP production a strong upregulation of Cta1, an enzyme involved in the removal of H₂O₂, was observed for both strains, whereas Pmp20 increase was only observed for the first. Thus, illustrating the importance of correct detoxification function of these enzymes involved in methanol metabolism, considering that ROS can give rise to a significant degree of oxidative stress and even induce UPR if the level of PDI substrates is sufficiently high [75, 82]. Furthermore, other studies have

also demonstrated an unexpected protective effect of UPR over oxidative stress. Higher ROS levels were detected in *P. pastoris* cells with activated UPR expressing intracellular recombinant human interleukin-10 cultivated at 30 °C compared to ER-phagy absent cells grown at 20 °C [114]. A similar defensive effect of UPR on ROS formation was suggested by flow cytometry results in this thesis. A stronger increase in reactive oxygen species during the methanol induced shake flask fed-batch protocol independently of UPR activation prior to induction solely in the secretory Insulin precursor producing strain was observed when compared to the HBsAg producing strain and to their respective host strains, X33 and GS115 (Figure 5.2.1 – A and Figure 5.2.2 – A). The HBsAg producing strain unexpectedly presented slightly increased ROS levels compared to the non-producing strain. Concerning stress responses of HBsAg and IP producing strains, published studies under similar conditions pointed out for different cellular physiological responses. While producing high amounts of ER-resident HBsAg cells presented high intracellular ERAD and UPR activation [3]. On the other hand, during IP secretion an intracellular decrease of UPR- and ERAD-related proteins was observed [4], in accordance with results presented here, however with the additional observation of Kar2 presence in the extracellular fraction (Figure 5.1.3). Moreover, since both strains did not significantly grow after methanol induction Figure 5.2.1 – C, the reported unfolded protein response can be assumed exclusively due to recombinant protein production. These results allow the speculation that since IP producing cells secrete Kar2 during methanol induction phase, they lose their intracellular protein folding capacity, which in turn reduces their ability to cope with ROS formation, however the HBsAg producing cells produce high amounts of intracellular recombinant protein, activating the folding machinery and ultimately the UPR, but since Kar2 remains intracellular [127], cells can cope with folding, matching the disulfide bonds formation therefore protecting cells and not generating ROS.

7. Conclusions and outlook

The unfolded protein response in *Pichia pastoris* X33 cells producing and non-producing secretory Insulin precursor was studied primarily by analyzing the Kar2 relative abundance independently in each phase of the bioreactor cultivation, the glycerol batch and the methanol fed-batch. Later on the impact of the first on the second phase was the object of investigation. Collectively the results point out that *Pichia pastoris* Kar2 chaperone participates in two distinguishable cellular functions. Under biotechnological relevant batch growth, where high initial extracellular osmolarity due to elevated concentrations of the non-fermentative carbon source glycerol, the host cell and the producing strain presented an overlapped constitutive activation of the UPR machinery prior to induction of recombinant proteins. The need to overcome the inherent misfolding caused by rapid growth in the hyperosmotic environment applied fully activates the cellular biosynthetic capacity at early exponential growth phase. After initial growth arrest and adaptation to batch environment, both strains undergo identical time course downregulation of the main UPR marker, Kar2. After methanol induction, host cells and IP strain undergo different UPR regulation regardless of identical biosynthetic response caused by growth in glycerol batch. The absence of intracellular and extracellular Kar2 in the host strain reveals the unneeded chaperone presence for cellular maintenance during methanol cultures. On the other hand, all freshly synthesized Kar2 by the producing strain was directed to folding of secretory Insulin precursor. Moreover, the batch UPR constitutive preconditioning had no positive correlation with the secretory Insulin precursor production. Taken together, these observations lead to the conclusion that cells undergo two different UPR related activations. One is a time course decrease occurring prior to the production of recombinant proteins throughout the glycerol batch phase, where at initial exponential growth phase high Kar2 levels were detected supposedly due to an overlapped effect of rapid growth and osmolarity. The other folding response happens when cells are shifted to methanol-induced secretory Insulin precursor production, where Kar2 is freshly synthesized and secreted together with correctly formed Insulin precursor. Furthermore, studies

carried out monitoring ROS levels of secretory IP and intracellular HBsAg producing strains and their respective host strains indicated a stronger effect of heterologous protein production compared to methanol metabolism on reactive oxygen species.

The future prospects to this work covers firstly the clarification of the mechanisms involved in the Kar2 disappearance during the late stage of the declining growth phase and stationary phase. Further studies should identify, perhaps through electron microscopy images or by identification of an alternative ER marker, whether if during extended batch periods, when nutrients became scarce, cells undergo the selective autophagic process, identified as ER-phagy [114], and if so, how *Pichia pastoris* yeast regulates this autophagic process. Secondly, future studies should concentrate on the ER-resident chaperones translocation during the methanol fed-batch phase. Efforts should contemplate not only the intracellular and extracellular translocation of the HDEL tagged proteins, but also their CopI mediated transport from the Golgi apparatus to the ER. Furthermore, the study of alternative substrates and perhaps, the induction of hyperosmolarity through ionic osmolytes would help to clarify, independently, the relation between growth rate and medium osmolarities results observed in this work for *Pichia pastoris* X33 cells during glycerol batch. Thirdly, the speculated protective “side-effect” of UPR activation due to recombinant protein production should be further investigated. While “unprotected” UPR decreased IP producing cells presented rising ROS levels during the methanol induction phase, the ER-stressed HBsAg producing cells unexpectedly cope with the oxidative stress during fed-batch phase, supposedly due to the ongoing intracellular recombinant protein related UPR. Proteomic studies should perhaps focus on the detection of Pmp20, the glutathione peroxidase, during secretory IP production, and extra effort should be placed on the transcriptional regulation analysis of Yap1, a transcription factor involved in the glutathione redox system [128, 129], applying RT-PCR with specific primer to monitor its anti-oxidative role. Concluding, the summed up current biotechnological relevant yeast data presented here might be used in future strain and bioprocess engineering development considering the diversity in which the *Pichia pastoris* unfolded protein response was studied.

8. References

1. **R\$ 35 bilhões serão investidos na aquisição de medicamentos até 2016 - Ministério da Saúde - Brasil** [<http://www.brasil.gov.br/saude/2013/04/r-35-bilhoes-serao-repassados-para-a-aquisicao-de-medicamentos-ate-2016>]
2. Gurralkonda C, Polez S, Skoko N, Adnan A, Gabel T, Chugh D, Swaminathan S, Khanna N, Tisminetzky S, Rinas U: **Application of simple fed-batch technique to high-level secretory production of insulin precursor using *Pichia pastoris* with subsequent purification and conversion to human insulin.** *Microb Cell Fact* 2010, **9**:31.
3. Vanz AL, Lünsdorf H, Adnan A, Nimtz M, Gurralkonda C, Khanna N, Rinas U: **Physiological response of *Pichia pastoris* GS115 to methanol-induced high level production of the Hepatitis B surface antigen: catabolic adaptation, stress responses, and autophagic processes.** *Microb Cell Fact* 2012, **103**:11.
4. Vanz AL, Nimtz M, Rinas U: **Decrease of UPR- and ERAD-related proteins in *Pichia pastoris* during methanol-induced secretory insulin precursor production in controlled fed-batch cultures.** *Microb Cell Fact* 2014, **13**:23.
5. Alberti KG, Zimmet PZ: **Definition, diagnosis and classification of diabetes mellitus and its complications. Part 1: diagnosis and classification of diabetes mellitus provisional report of a WHO consultation.** *Diabet Med* 1998, **15**:539-553.
6. **Global status report on noncommunicable diseases 2014.** Geneva: World Health Organization; 2014.
7. **Global health estimates: deaths by cause, age, sex and country, 2000-2012.** Geneva: World Health Organization; 2014.
8. Mathers CD, Loncar D: **Projections of global mortality and burden of disease from 2002 to 2030.** *PLoS Med* 2006, **3**:e442.
9. **Insulin market expected to reach USD 32.24 billion globally in 2019 - Transparency Market Research Company** [<http://www.transparencymarketresearch.com/pressrelease/insulin-market.htm>]
10. Scott DA: **Crystalline insulin.** *Biochem J* 1934, **28**:1592-1602.
11. Ahmad B: **Pharmacology of insulin.** *Br J Diabetes Vasc Dis* 2004, **4**:10-14.

12. Walsh G: **Therapeutic insulins and their large-scale manufacture.** *Appl Microbiol Biotechnol* 2005, **67**:151-159.
13. Ferrer-Miralles N, Domingo-Espin J, Corchero JL, Vazquez E, Villaverde A: **Microbial factories for recombinant pharmaceuticals.** *Microb Cell Fact* 2009, **8**:17.
14. Goeddel DV, Kleid DG, Bolivar F, Heyneker HL, Yansura DG, Crea R, Hirose T, Kraszewski A, Itakura K, Riggs AD: **Expression in *Escherichia coli* of chemically synthesized genes for human insulin.** *Proc Natl Acad Sci USA* 1979, **76**:106-110.
15. Nilsson J, Jonasson P, Samuelsson E, Ståhl S, Uhlén M: **Integrated production of human insulin and its C-peptide.** *J Biotechnol* 1996, **48**:241-250.
16. Thim L, Hansen MT, Norris K, Hoegh I, Boel E, Forstrom J, Ammerer G, Fiil NP: **Secretion and processing of insulin precursors in yeast.** *Proc Natl Acad Sci USA* 1986, **83**:6766-6770.
17. Markussen J, Damgaard U, Diers I, Fiil N, Hansen MT, Larsen P, Norris F, Norris K, Schou O, Snel L, et al: **Biosynthesis of human insulin in yeast via single chain precursors.** *Diabetologia* 1986, **29**:568A-569A.
18. Kjeldsen T: **Yeast secretory expression of insulin precursors.** *Appl Microbiol Biotechnol* 2000, **54**:277-286.
19. Baeshen NA, Baeshen MN, Sheikh A, Bora RS, Ahmed MMM, Ramadan HAI, Saini KS, Redwan EM: **Cell factories for insulin production.** *Microb Cell Fact* 2014, **13**.
20. Porro D, Sauer M, Branduardi P, Mattanovich D: **Recombinant protein production in yeasts.** *Mol Biotechnol* 2005, **31**:245-259.
21. Gellissen G, Hollenberg CP: **Application of yeasts in gene expression studies: a comparison of *Saccharomyces cerevisiae*, *Hansenula polymorpha* and *Kluyveromyces lactis*- a review.** *Gene* 1997, **190**:87-97.
22. Hollenberga CP, Gellissenb G: **Production of recombinant proteins by methylotrophic yeasts.** *Curr Opin Biotechnol* 1997, **8**:554-560.
23. Cereghino GP, Cereghino JL, Ilgen C, Cregg JM: **Production of recombinant proteins in fermenter cultures of the yeast *Pichia pastoris*.** *Curr Opin Biotechnol* 2002, **13**:329-332.
24. Li P, Anumanthan A, Gao XG, Ilangovan K, Suzara VV, Düzgüneş N, Renugopalakrishnan V: **Expression of Recombinant Proteins in *Pichia Pastoris*.** *Appl Biochem Biotechnol* 2007, **142**:105-124.
25. Macauley-Patrick S, Fazenda ML, McNeil B, Harvey LM: **Heterologous protein production using the *Pichia pastoris* expression system.** *Yeast* 2005, **22**:249-270.

26. Kurtzman CP: **Biotechnological strains of *Komagataella (Pichia) pastoris* are *Komagataella phaffii* as determined from multigene sequence analysis.** *J Ind Microbiol Biotechnol* 2009, **36**:1435-1438.
27. Wriessnegger T, Sunga AJ, Cregg JM, Daum G: **Identification of phosphatidylserine decarboxylases 1 and 2 from *Pichia pastoris*.** *FEMS Yeast Res* 2009, **9**:911-922.
28. Higgins D, Cregg J: **Introduction to *Pichia pastoris*.** In *Pichia Protocols. Volume 103*. Edited by Higgins D, Cregg J: Humana Press; 1998: 1-15.[*Methods in Molecular Biology*TM].
29. Cereghino JL, Cregg JM: **Heterologous protein expression in the methylophilic yeast *Pichia pastoris*.** *FEMS Microbiol Rev* 2000, **24**:45-66.
30. Sunga AJ, Tolstorukov I, Cregg JM: **Posttransformational vector amplification in the yeast *Pichia pastoris*.** *FEMS Yeast Res* 2008, **8**:870-876.
31. Werten MW, van den Bosch TJ, Wind RD, Mooibroek H, de Wolf FA: **High-yield secretion of recombinant gelatins by *Pichia pastoris*.** *Yeast* 1999, **15**:1087-1096.
32. Mattanovich D, Gasser B, Hohenblum H, Sauer M: **Stress in recombinant protein producing yeasts.** *J Biotechnol* 2004, **113**:121-135.
33. Gasser B, Saloheimo M, Rinas U, Dragosits M, Rodriguez-Carmona E, Baumann K, Giuliani M, Parrilli E, Branduardi P, Lang C, et al: **Protein folding and conformational stress in microbial cells producing recombinant proteins: a host comparative overview.** *Microb Cell Fact* 2008, **7**:11.
34. Shuster JR: **Gene expression in yeast: protein secretion.** *Curr Opin Biotechnol* 1991, **2**:685-690.
35. Krogh AM: **Stability of heterologous protein production by *Saccharomyces cerevisiae* in continuous cultures.** *Ph.D. Thesis*. Technical University of Denmark, Center for Microbial Biotechnology; 2009.
36. Schroder M, Kaufman RJ: **ER stress and the unfolded protein response.** *Mutat Res* 2005, **569**:29-63.
37. Ellgaard L, Molinari M, Helenius A: **Setting the standards: quality control in the secretory pathway.** *Science* 1999, **286**:1882-1888.
38. Travers KJ, Patil CK, Wodicka L, Lockhart DJ, Weissman JS, Walter P: **Functional and genomic analyses reveal an essential coordination between the unfolded protein response and ER-associated degradation.** *Cell* 2000, **101**:249-258.

39. Ma Y, Hendershot LM: **The mammalian endoplasmic reticulum as a sensor for cellular stress.** *Cell Stress Chaperon* 2002, **7**:222-229.
40. Rutkowski DT, Kaufman RJ: **A trip to the ER: coping with stress.** *Trends in Cell Biology* 2004, **14**:20-28.
41. Samuel P, Prasanna Vadhana AK, Kamatchi R, Antony A, Meenakshisundaram S: **Effect of molecular chaperones on the expression of *Candida antarctica* lipase B in *Pichia pastoris*.** *Microbiol Res* 2013.
42. Damasceno LM, Anderson KA, Ritter G, Cregg JM, Old LJ, Batt CA: **Cooverexpression of chaperones for enhanced secretion of a single-chain antibody fragment in *Pichia pastoris*.** *Appl Environ Microbiol* 2006, **74**:381-389.
43. Gasser B, Sauer M, Maurer M, Stadlmayr G, Mattanovich D: **Transcriptomics-based identification of novel factors enhancing heterologous protein secretion in yeasts.** *Appl Environ Microbiol* 2007, **73**:6499-6507.
44. Puxbaum V, Mattanovich D, Gasser B: **Quo vadis? The challenges of recombinant protein folding and secretion in *Pichia pastoris*.** *Appl Microbiol Biotechnol* 2015, **99**:2925-2938.
45. Frand AR, Kaiser CA: **Ero1p oxidizes protein disulfide isomerase in a pathway for disulfide bond formation in the endoplasmic reticulum.** *Mol Cell* 1999, **4**:469-477.
46. Tu BP, Ho-Schleyer SC, Travers KJ, Weissman JS: **Biochemical basis of oxidative protein folding in the endoplasmic reticulum.** *Science* 2000, **290**:1571-1574.
47. Buck TM, Wright CM, Brodsky JL: **The activities and function of molecular chaperones in the endoplasmic reticulum.** *Semin Cell Dev Biol* 2007, **18**:751-761.
48. Flynn GC, Pohl J, Flocco MT, Rothman JE: **Peptide-binding specificity of the molecular chaperone BiP.** *Nature* 1991, **353**:726-730.
49. Rose MD, Misra LM, Vogel JP: ***KAR2*, a karyogamy gene, is the yeast homolog of the mammalian BiP/GRP78 gene.** *Cell* 1989, **57**:1211-1221.
50. McCarty JS, Buchberger A, Reinstein J, Bukau B: **The role of ATP in the functional cycle of the DnaK chaperone system.** *J Mol Biol* 1995, **249**:126-137.
51. Han W, Christen P: **Mechanism of the targeting action of DnaJ in the DnaK molecular chaperone system.** *J Biol Chem* 2003, **278**:19038-19043.
52. Raviol H, Sadlish H, Rodriguez F, Mayer MP, Bukau B: **Chaperone network in the yeast cytosol: Hsp110 is revealed as an Hsp70 nucleotide exchange factor.** *EMBO J* 2006, **25**:2510-2518.

53. Molinari M, Galli C, Vanoni O, Arnold SM, Kaufman RJ: **Persistent glycoprotein misfolding activates the glucosidase II/UGT1-driven calnexin cycle to delay aggregation and loss of folding competence.** *Mol Cell* 2005, **20**:503-512.
54. Delic M, Valli M, Graf AB, Pfeffer M, Mattanovich D, Gasser B: **The secretory pathway: exploring yeast diversity.** *FEMS Microbiol Rev* 2013, **37**:872-914.
55. Xu X, Kanbara K, Azakami H, Kato A: **Expression and characterization of *Saccharomyces cerevisiae* Cne1p, a calnexin homologue.** *J Biochem* 2004, **135**:615-618.
56. Kimata Y, Kimata YI, Shimizu Y, Abe H, Farcasanu IC, Takeuchi M, Rose MD, Kohno K: **Genetic evidence for a role of BiP/Kar2 that regulates Ire1 in response to accumulation of unfolded proteins.** *Mol Biol Cell* 2003, **14**:2559-2569.
57. Dudek J, Benedix J, Cappel S, Greiner M, Jalal C, Muller L, Zimmermann R: **Functions and pathologies of BiP and its interaction partners.** *Cell Mol Life Sci* 2009, **66**:1556-1569.
58. Shiu RP, Pouyssegur J, Pastan I: **Glucose depletion accounts for the induction of two transformation-sensitive membrane proteins in Rous sarcoma virus-transformed chick embryo fibroblasts.** *Proc Natl Acad Sci USA* 1977, **74**:3840-3844.
59. Haas IG, Wabl M: **Immunoglobulin heavy chain binding protein.** *Nature* 1983, **306**:387-389.
60. Dorner AJ, Wasley LC, Kaufman RJ: **Protein dissociation from GRP78 and secretion are blocked by depletion of cellular ATP levels.** *Proc Natl Acad Sci USA* 1990, **87**:7429-7432.
61. Braakman I, Helenius J, Helenius A: **Role of ATP and disulphide bonds during protein folding in the endoplasmic reticulum.** *Nature* 1992, **356**:260-262.
62. Pelham HRB: **The retention signal for soluble proteins of the endoplasmic reticulum.** *Trends Biochem Sci* 1990, **15**:483-486.
63. Semenza JC, Hardwick KG, Dean N, Pelham HRB: **ERD2, a yeast gene required for the receptor-mediated retrieval of luminal ER proteins from the secretory pathway.** *Cell* 1990, **61**:1349-1357.
64. Dean N, Pelham HRB: **Recycling of proteins from the Golgi compartment to the ER in yeast.** *J Cell Biol* 1990, **111**:369-377.
65. Pelham HR, Hardwick KG, Lewis MJ: **Sorting of soluble ER proteins in yeast.** *EMBO J* 1988, **7**:1757-1762.

66. Papanikou E, Glick BS: **Golgi compartmentation and identity.** *Curr Opin Cell Biol* 2014, **29**:74-81.
67. Majoul I, Sohn K, Wieland FT, Pepperkok R, Pizza M, Hillemann J, Soeling HD: **KDEL receptor (Erd2p)-mediated retrograde transport of the cholera toxin A subunit from the Golgi involves COPI, p23, and the COOH terminus of Erd2p.** *J Cell Biol* 1998, **143**:601-612.
68. Kaufman RJ: **Orchestrating the unfolded protein response in health and disease.** *J Clin Invest* 2002, **110**:1389-1398.
69. Wang S, Kaufman RJ: **The impact of the unfolded protein response on human disease.** *J Cell Biol* 2012, **197**:857-867.
70. Cox JS, Walter P: **A novel mechanism for regulating activity of a transcription factor that controls the unfolded protein response.** *Cell* 1996, **87**:391-404.
71. Mori K, Kawahara T, Yoshida H, Yanagi H, Yura T: **Signalling from endoplasmic reticulum to nucleus: transcription factor with a basic-leucine zipper motif is required for the unfolded protein-response pathway.** *Genes Cells* 1996, **1**:803-817.
72. Cox JS, Shamu CE, Walter P: **Transcriptional induction of genes encoding endoplasmic reticulum resident proteins requires a transmembrane protein kinase.** *Cell* 1993, **73**:1197-1206.
73. Vanz AL: **Physiological response of *Pichia pastoris* to recombinant protein production under methanol induction.** *Ph.D. Thesis.* Gottfried Wilhelm Leibniz Universität Hannover, Institut für Technische Chemie; 2013.
74. Shamu CE, Walter P: **Oligomerization and phosphorylation of the Ire1p kinase during intracellular signaling from the endoplasmic reticulum to the nucleus.** *EMBO J* 1996, **15**:3028-3039.
75. Kimata Y, Ishiwata-Kimata Y, Yamada S, Kohno K: **Yeast unfolded protein response pathway regulates expression of genes for anti-oxidative stress and for cell surface proteins.** *Genes Cells* 2006, **11**:59-69.
76. Guerfal M, Ryckaert S, Jacobs PP, Ameloot P, Van Craenenbroeck K, Derycke R, Callewaert N: **The HAC1 gene from *Pichia pastoris*: characterization and effect of its overexpression on the production of secreted, surface displayed and membrane proteins.** *Microb Cell Fact* 2010, **9**:49.
77. Whyteside G, Nor RM, Alcocer MJ, Archer DB: **Activation of the unfolded protein response in *Pichia pastoris* requires splicing of a HAC1 mRNA intron and retention of the C-terminal tail of Hac1p.** *FEBS Lett* 2011, **585**:1037-1041.

78. Rügsegger U, Leber JH, Walter P: **Block of HAC1 mRNA translation by long-range base pairing is released by cytoplasmic splicing upon induction of the unfolded protein response.** *Cell* 2001, **107**:103-114.
79. Schröder M, Chang JS, Kaufman RJ: **The unfolded protein response represses nitrogen-starvation induced developmental differentiation in yeast.** *Genes Dev* 2000, **14**:2962-2975.
80. Scheuner D, Song B, McEwen E, Liu C, Laybutt R, Gillespie P, Saunders T, Bonner-Weir S, Kaufman RJ: **Translational control is required for the unfolded protein response and *in vivo* glucose homeostasis.** *Mol Cell* 2001, **7**:1165-1176.
81. Kuhn KM, DeRisi JL, Brown PO, Sarnow P: **Global and specific translational regulation in the genomic response of *Saccharomyces cerevisiae* to a rapid transfer from a fermentable to a nonfermentable carbon source.** *Mol Cell Biol* 2001, **21**:916-927.
82. Harding HP, Zhang Y, Zeng H, Novoa I, Lu PD, Calton M, Sadri N, Yun C, Popko B, Paules R, et al: **An integrated stress response regulates amino acid metabolism and resistance to oxidative stress.** *Molecular Cell* 2003, **11**:619-633.
83. Rebnegger C, Graf AB, Valli M, Steiger MG, Gasser B, Maurer M, Mattanovich D: **In *Pichia pastoris*, growth rate regulates protein synthesis and secretion, mating and stress response.** *Biotechnol J* 2014, **9**:511-525.
84. Gasch AP, Spellman PT, Kao CM, Carmel-Harel O, Eisen MB, Storz G, Botstein D, Brown PO: **Genomic expression programs in the response of yeast cells to environmental changes.** *Mol Biol Cell* 2000, **11**:4241-4257.
85. Dragosits M, Stadlmann J, Albiol J, Baumann K, Maurer M, Gasser B, Sauer M, Altmann F, Ferrer P, Mattanovich D: **The effect of temperature on the proteome of recombinant *Pichia pastoris*.** *J Proteome Res* 2009, **8**:1380-1393.
86. Baumann K, Dato L, Graf AB, Frascotti G, Dragosits M, Porro D, Mattanovich D, Ferrer P, Branduardi P: **The impact of oxygen on the transcriptome of recombinant *S. cerevisiae* and *P. pastoris* - a comparative analysis.** *BMC Genomics* 2011, **12**:218.
87. Baumann K, Carnicer M, Dragosits M, Graf AB, Stadlmann J, Jouhten P, Maaheimo H, Gasser B, Albiol J, Mattanovich D, Ferrer P: **A multi-level study of recombinant *Pichia pastoris* in different oxygen conditions.** *BMC Syst Biol* 2010, **4**:141.
88. Baumann K, Maurer M, Dragosits M, Cos O, Ferrer P, Mattanovich D: **Hypoxic fed-batch cultivation of *Pichia pastoris* increases specific and volumetric productivity of recombinant proteins.** *Biotechnol Bioeng* 2008, **100**:177-183.

89. O'Rourke SM, Herskowitz I: **Unique and redundant roles for HOG MAPK pathway components as revealed by whole-genome expression analysis.** *Mol Biol Cell* 2004, **15**:532-542.
90. Hohmann S: **Osmotic stress signaling and osmoadaptation in yeasts.** *Microbiol Mol Biol Rev* 2002, **66**:300-372.
91. Larsson K, Ansell R, Eriksson P, Adler L: **A gene encoding sn-glycerol 3-phosphate dehydrogenase (NAD⁺) complements an osmosensitive mutant of *Saccharomyces cerevisiae*.** *Mol Microbiol* 1993, **10**:1101-1111.
92. Mager WH, Siderius M: **Novel insights into the osmotic stress response of yeast.** *FEMS Yeast Res* 2002, **2**:251-257.
93. Norbeck J, Blomberg A: **Metabolic and regulatory changes associated with growth of *Saccharomyces cerevisiae* in 1.4 M NaCl.** *J Biol Chem* 1997, **272**:5544-5554.
94. Tamás MJ, Luyten K, Sutherland FC, Hernandez A, Albertyn J, Valadi H, Li H, Prior BA, Kilian SG, Ramos J, et al: **Fps1p controls the accumulation and release of the compatible solute glycerol in yeast osmoregulation.** *Mol Microbiol* 1999, **31**:1087-1104.
95. Dragosits M, Stadlmann J, Graf A, Gasser B, Maurer M, Sauer M, Kreil DP, Altmann F, Mattanovich D: **The response to unfolded protein is involved in osmotolerance of *Pichia pastoris*.** *BMC Genomics* 2010, **11**:207.
96. Kaufman RJ, Scheuner D, Schroder M, Shen X, Lee K, Liu CY, Arnold SM: **The unfolded protein response in nutrient sensing and differentiation.** *Nat Rev Mol Cell Biol* 2002, **3**:411-421.
97. Tu BP, Weissman JS: **Oxidative protein folding in eukaryotes: mechanisms and consequences.** *J Cell Biol* 2004, **164**:341-346.
98. Aksam EB, de Vries B, van der Klei IJ, Kiel JA: **Preserving organelle vitality: peroxisomal quality control mechanisms in yeast.** *FEMS Yeast Res* 2009, **9**:808-820.
99. Yurimoto H, Kato N, Sakai Y: **Assimilation, dissimilation, and detoxification of formaldehyde, a central metabolic intermediate of methylotrophic metabolism.** *Chem Rec* 2005, **5**:367-375.
100. Khan SU, Schroder M: **Engineering of chaperone systems and of the unfolded protein response.** *Cytotechnology* 2008, **57**:207-231.
101. Tyo KE, Liu Z, Petranovic D, Nielsen J: **Imbalance of heterologous protein folding and disulfide bond formation rates yields runaway oxidative stress.** *BMC Biol* 2012, **10**:16.

102. Gess B, Hofbauer K-H, Wenger RH, Lohaus C, Meyer HE, Kurtz A: **The cellular oxygen tension regulates expression of the endoplasmic oxidoreductase ERO1-Lalpha.** *Eur J Biochem* 2003, **270**:2228-2235.
103. Tsai B, Rapoport TA: **Unfolded cholera toxin is transferred to the ER membrane and released from protein disulfide isomerase upon oxidation by Ero1.** *J Cell Biol* 2002, **159**:207-216.
104. Pagani M, Fabbri M, Benedetti C, Fassio A, Pilati S, Bulleid NJ, Cabibbo A, Sitia R: **Endoplasmic reticulum oxidoreductin 1-lbeta (ERO1-Lbeta), a human gene induced in the course of the unfolded protein response.** *J Biol Chem* 2000, **275**:23685-23692.
105. Vassileva A, Chugh DA, Swaminathan S, Khanna N: **Effect of copy number on the expression levels of hepatitis B surface antigen in the methylophilic yeast *Pichia pastoris*.** *Protein Expr Purif* 2001, **21**:71-80.
106. Anderlei T, Zang W, Papaspyrou M, Büchs J: **Online respiration activity measurement (OTR, CTR, RQ) in shake flasks.** *Biochemical Engineering Journal* 2004, **17**:187-194.
107. **Thermo Scientific Pierce Protein Assay Technical Handbook**
108. Hohenblum H, Borth N, Mattanovich D: **Assessing viability and cell-associated product of recombinant protein producing *Pichia pastoris* with flow cytometry.** *J Biotechnol* 2003, **102**:281-290.
109. Xiao A, Zhou X, Zhou L, Zhang Y: **Improvement of cell viability and hirudin production by ascorbic acid in *Pichia pastoris* fermentation.** *Appl Microbiol Biotechnol* 2006, **72**:837-844.
110. Eruslanov E, Kusmartsev S: **Identification of ROS using oxidized DCFDA and flow-cytometry.** *Methods Mol Biol* 2010, **594**:57-72.
111. Liu YY, Woo JH, Neville DMJ: **Overexpression of an anti-CD3 immunotoxin increases expression and secretion of molecular chaperone BiP/Kar2p by *Pichia pastoris*.** *Appl Environ Microbiol* 2005, **71**:5332-5340.
112. Gurramkonda C, Adnan A, Gabel T, Lunsdorf H, Ross A, Nemani SK, Swaminathan S, Khanna N, Rinas U: **Simple high-cell density fed-batch technique for high-level recombinant protein production with *Pichia pastoris*: Application to intracellular production of Hepatitis B surface antigen.** *Microb Cell Fact* 2009, **8**:13.
113. Brierley RA, Bussineau C, Kosson OR, Melton A, Siegel RS: **Fermentation development of recombinant *Pichia pastoris* expressing the heterologous gene: bovine lysozyme.** *Ann N Y Acad Sci* 1990, **589**:350-362.
114. Zhong Y, Yang L, Guo Y, Fang F, Wang D, Li R, Jiang M, Kang W, Ma J, Sun J, Xiao W: **High-temperature cultivation of recombinant *Pichia***

- pastoris* increases endoplasmic reticulum stress and decreases production of human interleukin-10. *Microb Cell Fact* 2014, **13**:163.
115. Hamasaki M, Noda T, Baba M, Ohsumi Y: **Starvation triggers the delivery of the endoplasmic reticulum to the vacuole via autophagy in yeast.** *Traffic* 2005, **6**:56-65.
 116. Bernales S, Schuck S, Walter P: **ER-Phagy selective autophagy of the endoplasmic reticulum.** *Autophagy* 2007, **3**:285-287.
 117. Kraft C, Reggiori F, Peter M: **Selective types of autophagy in yeast.** *Biochim Biophys Acta* 2009, **1793**:1404-1412.
 118. Till A, Lakhani R, Burnett SF, Subramani S: **Pexophagy: the selective degradation of peroxisomes.** *Int J Cell Biol* 2012, **2012**:512721.
 119. Cebollero E, Reggiori F, Kraft C: **Reticulophagy and ribophagy: regulated degradation of protein production factories.** *Int J Cell Biol* 2012, **2012**:182834.
 120. Wu MH, Dimopoulos G, Mantalaris A, Varley J: **The effect of hyperosmotic pressure on antibody production and gene expression in the GS-NS0 cell line.** *Biotechnol Appl Biochem* 2004, **40**:41-46.
 121. Kim NS, Lee GM: **Response of recombinant Chinese hamster ovary cells to hyperosmotic pressure: effect of Bcl-2 overexpression.** *J Biotechnol* 2002, **95**:237-248.
 122. Blackwell JR, Horgan R: **A novel strategy for production of a highly expressed recombinant protein in an active form.** *FEBS Lett* 1991, **295**:10-12.
 123. Hohenblum H, Gasser B, Maurer M, Borth N, Mattanovich D: **Effects of gene dosage, promoters, and substrates on unfolded protein stress of recombinant *Pichia pastoris*.** *Biotechnol Bioeng* 2004, **85**:367-375.
 124. Čiplys E, Aučynaitė A, Slibinskas R: **Generation of human ER chaperone BiP in yeast *Saccharomyces cerevisiae*.** *Microb Cell Fact* 2014, **13**.
 125. Belden WJ, Barlowe C: **Deletion of yeast p24 genes activates the unfolded protein response.** *Mol Biol Cell* 2001, **12**:957-969.
 126. Haynes CM, Titus EA, Cooper AA: **Degradation of misfolded proteins prevents ER-derived oxidative stress and cell death.** *Mol Cell* 2004, **15**:767-776.
 127. Bötcher J: **Zelluläre Stressregulation während heterologer Proteinproduktion in *Pichia pastoris*.** Gottfried Wilhelm Leibniz Universität Hannover, Institut für Technische Chemie; 2015.

128. Delic M, Graf A, Koellensperger G, Haberhauer-Troyer C, Hann S, Mattanovich D, Gasser B: **Overexpression of the transcription factor Yap1 modifies intracellular redox conditions and enhances recombinant protein secretion.** *Microbial Cell* 2014, **1**:376-386.
129. Yano T, Takigami E, Yurimoto H, Sakai Y: **Yap1-regulated glutathione redox system curtails accumulation of formaldehyde and reactive oxygen species in methanol metabolism of *Pichia pastoris*.** *Eukaryot Cell* 2009, **8**:540-549.

9. Appendix I

9.1. Composition of inoculum culture media

The usual approach applied for controlled cellular bioreactor processes requires a sequence of upscaling pre-cultures. This concept is necessary to generate an adequate number of cells for inoculation of the production bioreactor. Generally, inoculum cultures are composed of complex medium, which contains an undefined mixture of carbon and nitrogen sources, such as yeast extract or casein hydrolysate. The unknown proportion of complex ingredients can interfere in experimental homogeneity, nevertheless it is widely used. On the other hand, to achieve higher reproducibility, media containing defined amount of ingredients can be employed. *Pichia pastoris* cells producing secretory Insulin precursor (X33-IP) were grown in shake flasks in the commonly applied complex medium and its optical density time course was compared to those obtained from cells grown in defined media containing 10, 25, 75 or 126 g/L glycerol as sole carbon source in shake flasks. As the standard error in Figure 9.1.1 illustrates, under the applied conditions all defined media cultures presented lower optical density heterogeneity values when compared to the complex medium culture. Moreover, X33-IP cells in the culture containing 25 g/L glycerol in defined medium (Figure 9.1.1 – B) were able to grow until higher OD₆₀₀ in more suitable time. Taken together, these results point out that the most appropriate composition of inoculum medium which was employed in the bioreactor cultivations was the defined medium with 25 g/L glycerol.

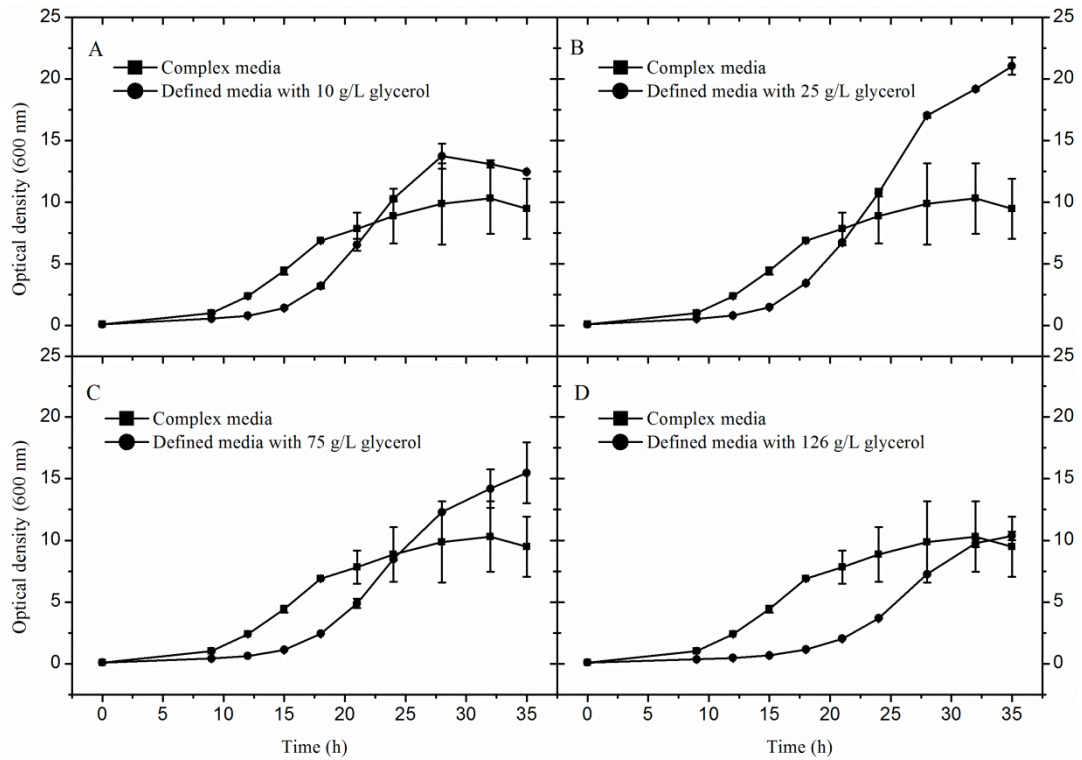


Figure 9.1.1 – Optical density time course comparison of *P. pastoris* X33-IP grown in different inoculum media in shake flasks.

P. pastoris X33-IP cells were grown in commonly used complex medium as well as in defined media containing the indicated glycerol concentrations in shake flasks. The average and standard error from two independent experiments are shown.

9.2. Application of a two-phase fed-batch process for Insulin precursor production

A robust two-phase feedback controlled fed-batch was successfully employed for obtaining secretory Insulin precursor in *Pichia pastoris* X33-IP 5 L bioreactor cultures. Cells grown in the inoculum containing the defined medium described previously were transferred into the bioreactor and the batch phase was initiated. Cells grew exponentially until complete depletion of the carbon source (Figure 9.2.2 – A), indicated by strong drop in the respiration rates, as well as, an expected decrease in the agitation values (Figure 9.2.2 – D and E). Curiously, while cells grew aerobically consuming glycerol, the production of ~0.4 g/L ethanol was detected by the FID (Figure 9.2.2 – B) and confirmed by gas chromatography. Furthermore, at the end of the batch phase a cellular metabolic change takes place indicated by the interruption of ammonia solution addition and sudden increase in phosphoric acid addition (Figure 9.2.2 – C). At this point, the methanol induction phase was started (vertical dashed line in Figure 9.2.2) and ~2 g/L methanol concentration was maintained during the entire fed-batch process (Figure 9.2.2 – B). Successful cellular adaptation to the methanol levels was noticeable by a slight decrease in culture pH followed by base addition for culture pH maintenance and increase in the respiratory activity (Figure 9.2.2 – C and E). The biomass concentration showed only a slight increase after the shift to methanol, increasing from 36 to 40 g/L and starting to decline again after about 150 h growth on methanol (Figure 9.2.2 – A). Aeration was kept at 3.5 L/min throughout the process.

The de-repression of the strong and tightly regulated methanol-inducible alcohol oxidase 1 promoter (PAOX1) was confirmed by 12 % SDS-PAGE analysis (Figure 9.2.3 – A). The presence of alcohol oxidase 1 (Aox1), a major protein required for methanol utilization, which was only present in minor amounts during growth on glycerol, started to increase after 13 h of methanol feeding phase onset, and accumulated until the end of the fed-batch process (Figure 9.2.3 – A). The production and secretion of IP during the methanol induction phase from culture aliquots withdrawn at various time points was confirmed by RP-HPLC and by 16

% SDS-PAGE (Figure 9.2.2 – F and Figure 9.2.3 – B, respectively). As expected, at methanol induction (0 h), there is no Insulin precursor in the cell-free supernatant (Figure 9.2.3 – B). Extracellular IP concentrations increased until 230 h of cultivation, reaching a maximum of 1.15 grams of Insulin precursor per liter of cell-free supernatant. Degradation of IP was not observed during the whole process. Figure 9.2.4 indicates the growth related UPR downregulation during the glycerol batch phase.

The methanol concentration was regulated by a proportional-integrative-derivative (PID) controller in response to the on-line feedback signal of a flame ionization detector (FID) (Figure 9.2.1). For induction, the desired amount of methanol was added to the culture and the FID signal was set. From there on, methanol was automatically pumped into the reactor in a closed loop feedback control. The FID and PID parameters were set-up in order to receive a good response. FID parameters: range = 1000, zero = 3.6 and gain = 9.9. PID controller parameters: pump = 32 rpm, min. output = 0.0, max. output = 100.0, deadband = 0.0, XP = 7.0, TI (s) = 100.0, TD (s) = 0.1, average time (s) = 0.0, output increment (%) = 100.0, set point ramp time (s) = 10.0. The “dead time” from induction until FID stable signal at 20 % was ~25 min. Agitation had no influence on FID signal. These parameters were employed in all fed-batch experiments.

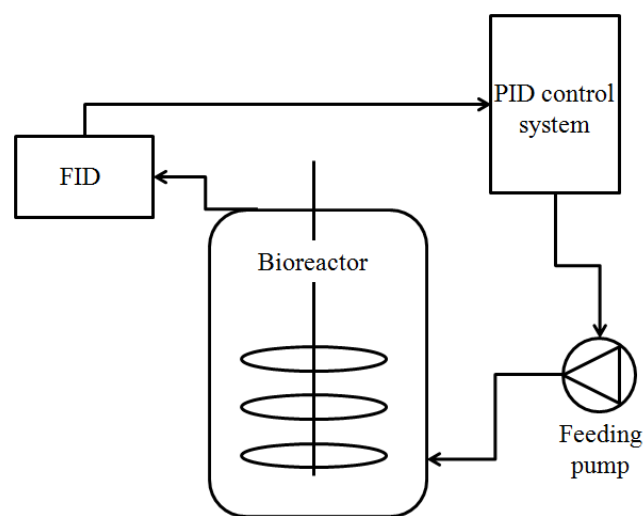


Figure 9.2.1 – Schematic of a closed loop PID feedback controller applied in the fed-batches.

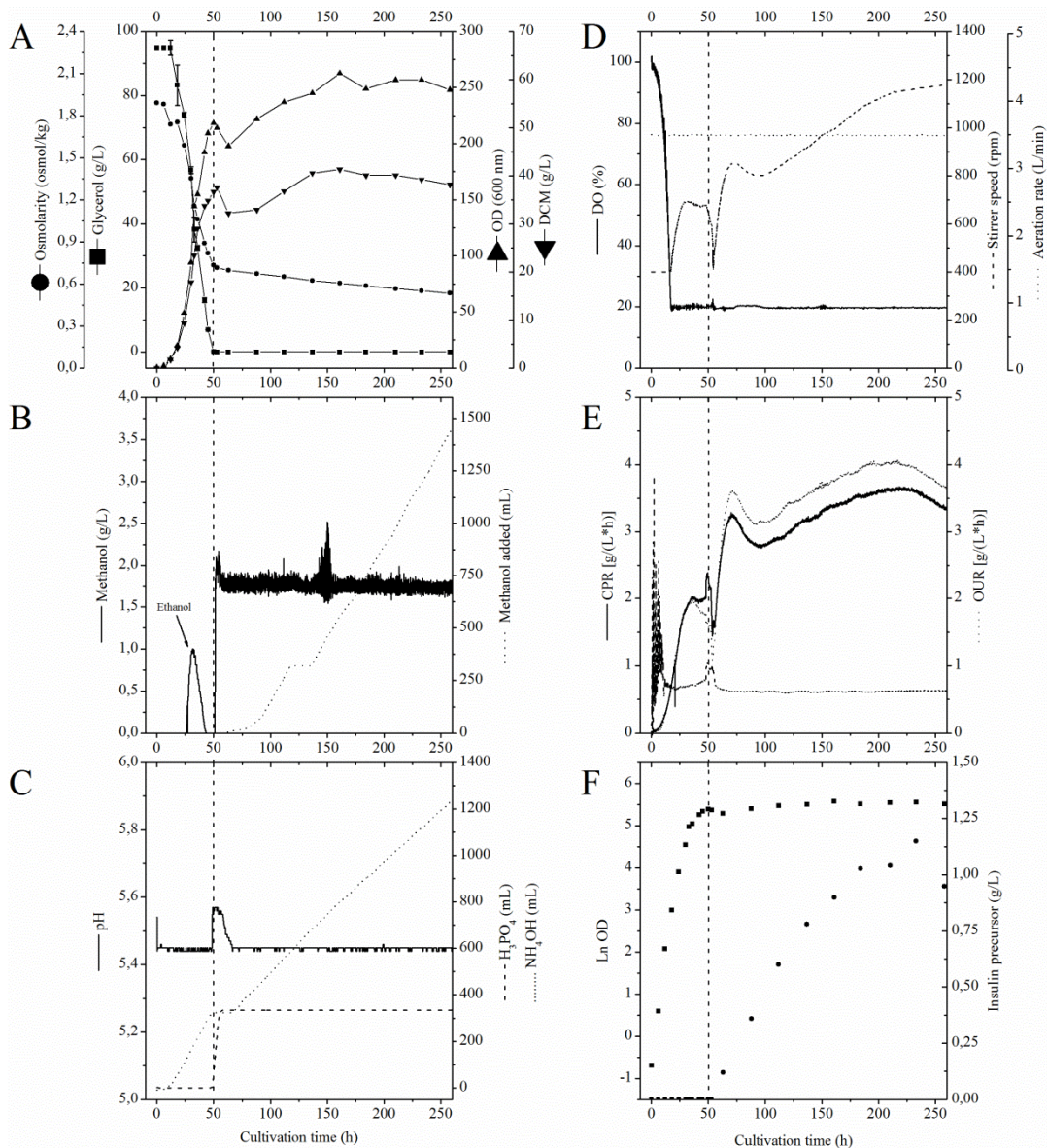


Figure 9.2.2 – Two-phase fed-batch cultivation of *P. pastoris* X-33 secreting Insulin precursor. Cells were first grown in a batch phase with 95 g/L glycerol as carbon source followed by a methanol feeding phase (1.7 g/L) to induce the production of IP. (A) Concentrations of glycerol and biomass (optical density; DCM) and medium osmolarity. (B) Concentration of methanol and amount of methanol added to the bioreactor. A FID detected peak of ethanol produced during glycerol batch phase is indicated. (C) Medium pH, amount of ammonium hydroxide, and amount of phosphoric acid added to the bioreactor. (D) Dissolved oxygen concentration, aeration rate, and stirrer speed. (E) Carbon dioxide production rate, oxygen uptake rate and respiratory quotient. (F) Cell growth and extracellular accumulation of IP. The dashed vertical line indicates the end of the glycerol batch and the start of the methanol feeding phase.

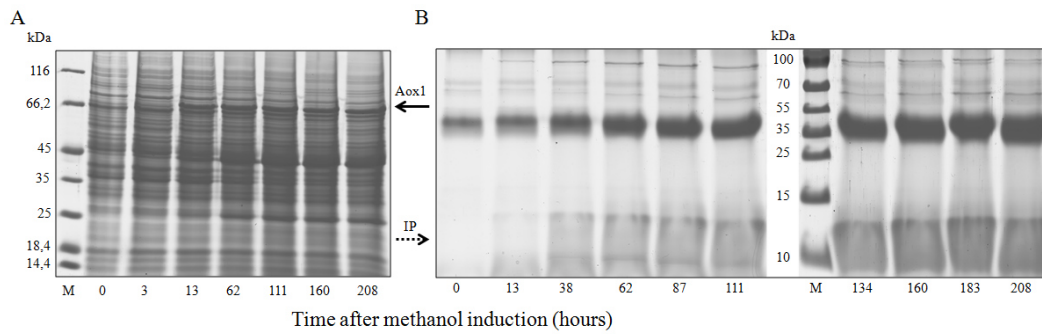


Figure 9.2.3 – SDS-PAGE time course analysis of *Pichia pastoris* X33-IP intracellular and extracellular fractions after methanol induction.

Samples were taken at the indicated time points after the start of methanol feed during bioreactor cultivation. (A) 12 % SDS-PAGE gel Coomassie stained time course analysis of whole intracellular lysates of *P. pastoris* X33-IP. Aox1 is indicated by the solid arrow in the marker height of ~ 70 kDa. All lysate samples were normalized at OD₆₀₀ 50. (B) Time course analysis of secretory Insulin precursor (~10 kDa) expression in extracellular cell-free supernatant in Coomassie stained SDS-PAGE 16 %. All lysate samples were normalized at OD₆₀₀ 50. The dotted arrow denotes the position of IP. The molecular weight marker is indicated by M.

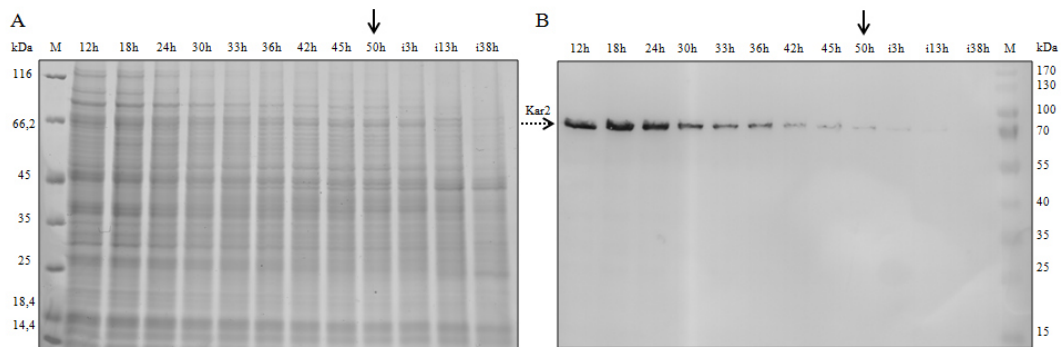


Figure 9.2.4 – SDS-PAGE and Western blot glycerol batch phase time course of the methanol feedback controlled fed-batch.

Samples were taken at the indicated time points during the 95 g/L glycerol batch phase and (i) after methanol induction (1.7 g/L). (A) Intracellular lysates fractions from *P. pastoris* X33-IP analyzed by 12 % SDS-PAGE. (B) Intracellular lysates fractions from *P. pastoris* X33-IP probed for proteins containing the endoplasmic reticulum retention signal peptide HDEL (e.g. Kar2, 74 kDa) by Western blot analysis. All lysate samples were normalized at OD₆₀₀ 50. The solid arrows denote the methanol time of induction and the dotted arrow indicates the height of Kar2. The molecular weight marker is indicated by M.

9.3. Insulin precursor purification

Purification was performed following [2] with modifications. Ion exchange chromatography was employed using a FPLC system. The IP-loaded Streamline SP XL resin was washed with water until the flow through absorbance at 280 nm and conductivity values returned to base line (Figure 9.3.1 – A). Following, the bound IP was isocratically eluted from the resin using 1 mol/L sodium chloride. The column flow through and pooled protein containing fractions, indicated by an absorbance at 280 nm peak, were analyzed by SDS-PAGE (Figure 9.3.1 – B). The eluted 10 mL IP-containing pool was dialyzed against 1x PBS buffer and the final total protein amount in the sample was 2.77 mg/mL, totalizing 34.6 mg of pure IP. Considering that at the time harvested, the cell-free supernatant from the *Pichia pastoris* X33-IP fed-batch cultivation contained ~1000 mg/L Insulin precursor quantified by RP-HPLC, the purification recovery was ~7 %. The pure sample was lyophilized for further quantification use.

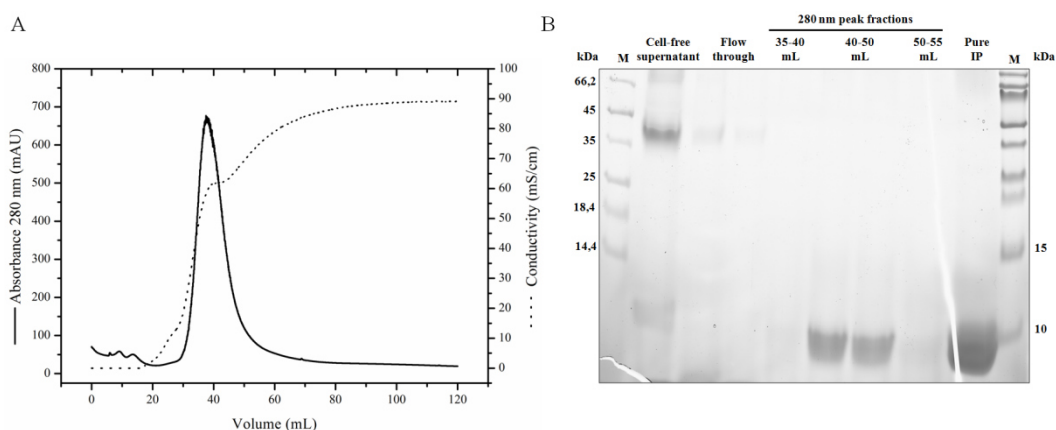


Figure 9.3.1 – Streamline SP XL ion exchange FPLC chromatogram and SDS-PAGE 16 % purification steps.

Purification of secretory Insulin precursor in the cell-free supernatant produced during the two-stage fed-batch process of *Pichia pastoris* X33-IP. (A) Ion exchange chromatogram indicating the milliabsorbance measured at 280 nm and conductivity values of the eluted protein-containing cell-free supernatant. (B) Purification steps analyzed by Coomassie stained SDS-PAGE 16 %. The cell-free supernatant lane stands for the crude extracellular sample, produced during fed-batch, applied for interaction with the ion exchange resin. Flow through lanes state for the unbound eluted proteins. The 280 nm peak fractions indicate the volume in which the protein pool was collected during FPLC elution with 1 mol/L sodium chloride. The concentrated purified Insulin precursor is shown in the lane Pure IP after dialysis against 1x PBS. The molecular weight marker is indicated by M.

9.4. Insulin precursor quantification

Preparations containing different dilutions of the lyophilized powder were used to build a standard curve for Insulin precursor quantification. The Insulin precursor purified powder was re-suspended in ultrapure water and was quantified for total protein content using BCA protein assay kit and BSA as protein reference. Different IP dilutions were prepared and their peak area was analyzed by Reversed-phase HPLC (RP-HPLC). Only one peak was detected by 214 nm absorbance in the dilutions chromatogram which corresponded to the purified Insulin precursor. The Insulin precursor vs. peak area measured at 214 nm standard curve was built and had a linear regressive coefficient of 0.9919 (Figure 9.4.1). The time course analysis of IP production during the methanol induction phase (Figure 9.2.2 – F) was performed employing the peak areas obtained from the withdrawn fed-batch culture aliquots in the linear standard curve equation. To check if none natural proteins has the same retention time as Insulin precursor, negative control runs were performed with samples from the producing strain X33-IP and X33 host strain before and after methanol induction.

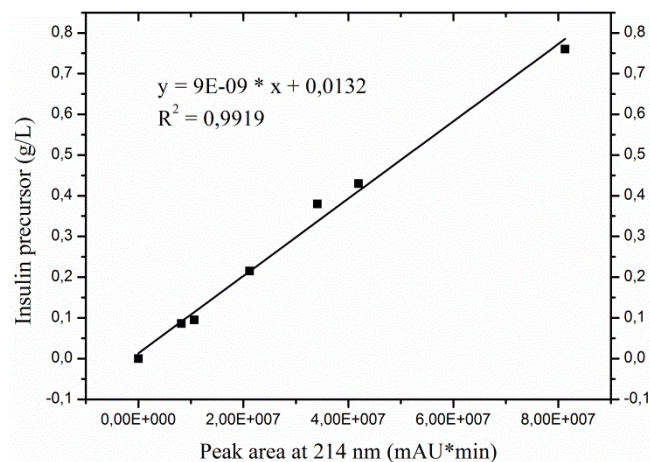


Figure 9.4.1 – Purified Insulin precursor quantification curve by RP-HPLC.

Dilutions of the lyophilized powder from the cell-free supernatant purification produced by *Pichia pastoris* X33-IP fed-batch cultivation versus the integrated peak areas of the purified Insulin precursor detected by 214 nm absorbance RP-HPLC.

10. Appendix II

10.1. *Pichia pastoris* X33 host strain cultivation

Pichia pastoris X33 host strain was cultured in identical conditions as the producing strain X33-IP, allowing its use as a negative control for the physiology studies performed in this thesis. Firstly X33 cells were grown in a 10 L batch phase containing 95 g/L glycerol in the low salt defined medium, afterwards cells were harvested from the bioreactor at the DO-spike, when the carbon source was depleted, to be finally transferred into fresh methanol containing medium employing the shake flask fed-batch protocol. The induction with 1% (v/v) methanol at every 12 h intervals for a period of 96 h was performed to simulate a fed-batch process.

Although the bioreactor harvest was performed at the end of the exponential growth phase (arrow in Figure 10.1.1 – E), X33 cells from the glycerol batch were allowed to grow until the stationary phase to monitor Kar2 levels. The initial high osmolarity caused by elevated glycerol medium concentration decreases during the X33 host strain batch phase (Figure 10.1.1 – E), as observed for the Insulin producing strain under different glycerol conditions (Figure 5.1.2). After harvest and inoculation in fresh methanol containing medium, the host strain cells did not grow significantly during the shake flask fed-batch (Figure 10.1.1 – E), in agreement with that described for the X33-IP producing strain (Figure 5.2.2 – D).

As described previously, the host strain presented during the glycerol batch phase the same growth related UPR downregulation (Figure 10.1.1 – C) as the producing strain X33-IP. No Kar2 could be detected in the extracellular fraction of the non-producing X33 strain at methanol induction time (Figure 10.1.1 – B and D). In spite of the fact that at harvest moment some intracellular Kar2 could be detected in the Western blot analysis (43 h of glycerol batch in Figure 10.1.1 – D), the intracellular and extracellular absence of Kar2 in the X33 non-producing strain during methanol fed-batch (Figure 10.1.1 – D), as published for the other *Pichia pastoris* host strain GS115 [4], indicates that the chaperone secretion phenomena is related to recombinant protein production.

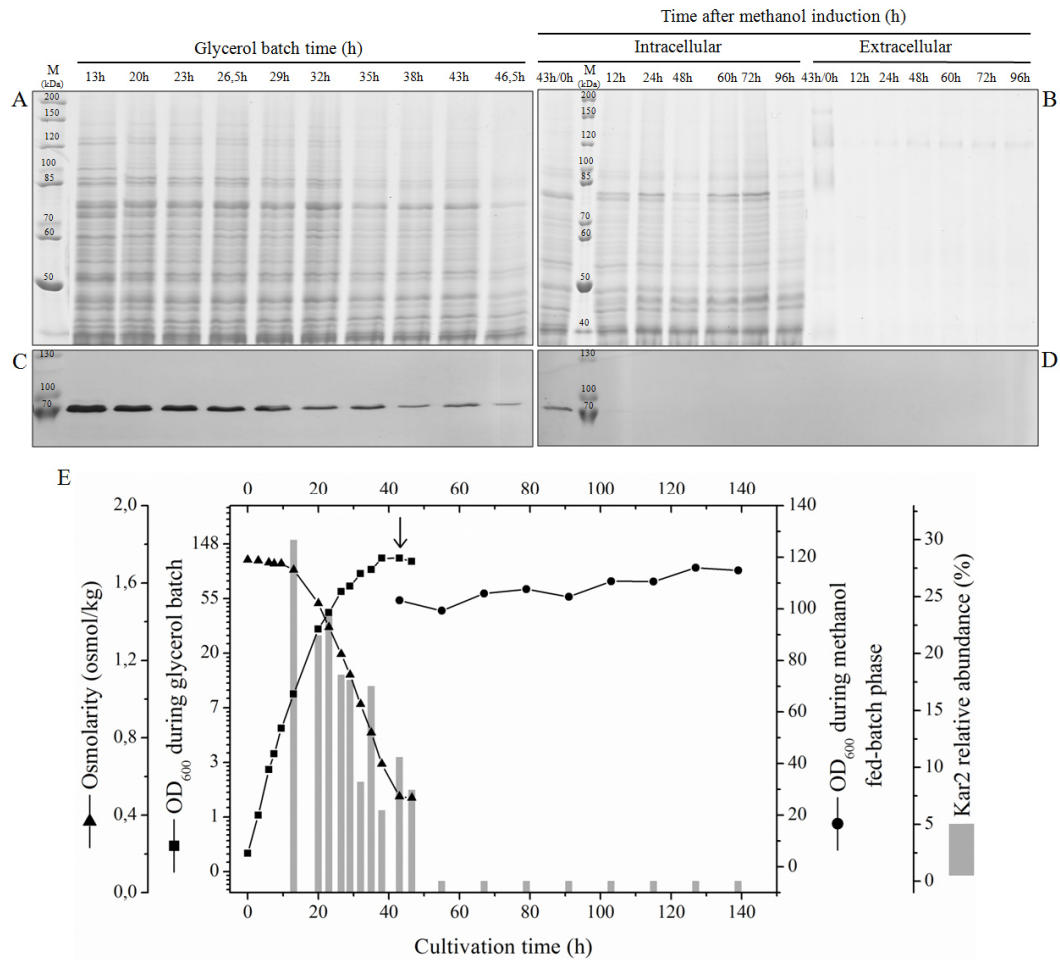


Figure 10.1.1 – Time course analysis of the 95 g/L bioreactor glycerol batch and shake flask fed-batch from *Pichia pastoris* X33 host cells.

P. pastoris X33 12 % SDS-PAGE analysis from the glycerol batch phase intracellular lysates (A) and intracellular and extracellular fractions from methanol shake flask fed-batch (B). Western blot analysis probed for proteins containing the endoplasmic reticulum retention signal peptide HDEL (e.g. KAR2, 74 kDa) from the glycerol batch phase intracellular lysates (C) and intracellular and extracellular fractions from methanol shake flask fed-batch (D). All lysate loaded samples were normalized at OD₆₀₀ 50 and extracellular fractions were directly applied. (E) Abundance changes of UPR related protein Kar2 are given in relative units corresponding to Western blot densitometry analysis, the glycerol batch and methanol fed-batch phase optical density and batch defined medium osmolarity. The sample at 13h was the first with enough cell pellet which allowed intracellular fraction examination and was considered reference for Western blot densitometry analysis. The M lane denotes the molecular weight marker. The arrow indicates the time of cell harvest for shake flask fed-batch inoculation.

11. Appendix III

11.1. Identification of proteins bands

Protein bands from a 12 % SDS-PAGE Coomassie blue stained gel were subjected to MALDI-TOF analysis to confirm their identity (Figure 11.1.1). The gel was loaded with intracellular and extracellular samples from a methanol shake flask fed-batch culture at the indicated time points. The *Pichia pastoris* X33-IP cells were grown in the 10 L glycerol batch and harvested at stationary growth phase (as the period defined in Figure 5.1.1 – C) to start the shake flask fed-batch. Lanes 0 h in Figure 11.1.1 denotes the sampling time before methanol induction, at batch harvest time. Protein bands number 2 and 5 were positively identified, scores 191 and 149 respectively, as alcohol oxidase (Aox1) from *Pichia pastoris* (syn. *Komagataella pastoris*), confirming Aox1 derepression after methanol induction (Figure 11.1.1). Protein bands number 4 and 6 were identified as an ATPase involved in protein import into the ER, also acts as a chaperone to mediate protein folding from *Komagataella pastoris* GS115, scores 85 and 102 respectively. Their identity was positively confirmed by sequence comparison as Kar2 from *Komagataella pastoris*. Kar2 identity was further confirmed when the extracellular fraction lanes of time point 24 h after methanol induction of Figure 11.1.1 and Figure 5.1.3 – A are compared. In the 12 % SDS-PAGE image, the positively identified protein band number 4 lies in the expected molecular weight height of ~74 kDa, whereas in the second figure, an anti-HDEL band in the PVDF Western blot membrane is observed in the same molecular weight height. Furthermore, the anti-HDEL antibody specificity for Kar2 was confirmed by the fact that in Figure 11.1.1 lane 96 h of the extracellular fraction after induction two prominent bands are seen, Aox1 and Kar2 (74.4 and 74.2 kDa, respectively), however when compared to the same time point in the Western blot in Figure 5.1.3 – A, only one band in this molecular weight height was observed. Protein bands number 1 and 3 were identified, scores 202 and 126 respectively, as an ATPase involved in protein folding and the response to stress from *Komagataella pastoris* GS115, which was previously identified in the published work of Vanz et al., 2014 [4], as a heat shock protein/chaperone belonging to the Hsp70 family. These

protein bands were assumed to be Ssa3 by comparing their sequences with the Ssa3 sequence from *Saccharomyces cerevisiae*. Figure 11.1.1 shows a decrease of Ssa3 after methanol induction in the intracellular fraction. In the work of Vanz et al. this same downregulation after methanol induction was observed, however an increase in 2D SDS-PAGE gels of a fragment (~25 kDa) of this protein was reported [4], not observed in the 1D SDS-PAGE gels in this thesis.

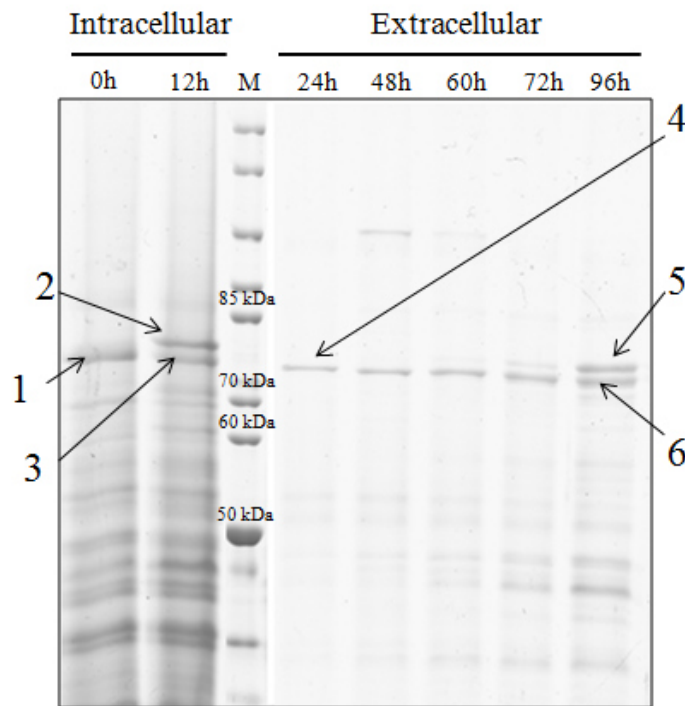


Figure 11.1.1 – 12 % SDS-PAGE Coomassie blue stained gel highlighting the identified protein bands.

Intracellular and extracellular fractions of *Pichia pastoris* X33-IP 1 % (v/v) methanol induction phase in shake flask fed-batch culture. The shake flask culture was started with cells harvested at stationary growth phase during the 10 L glycerol batch and sampling was performed at the indicated time after methanol induction. MALDI-TOF analysis positively identified protein bands numbers 2 and 5 as alcohol oxidase (Aox1), 4 and 6 as Kar2, 1 and 3 as Ssa3. All lysate loaded samples were normalized at OD₆₀₀ 50 and extracellular fractions were directly applied. The M lane denotes the molecular weight marker.

12. Appendix IV

12.1. Bioreactor feedback controlled fed-batches

The bioreactor feedback controlled fed-batches studied in this section were based on the application of a modified two-phase fed-batch procedure employed for the secretory production of Insulin precursor (IP) [2], originally developed for high-level intracellular production of Hepatitis B surface antigen (HBsAg) with *P. Pastoris* GS115 [112]. After *P. pastoris* cells were allowed unlimited growth until depletion of all carbon sources during the glycerol batch phase, methanol was injected in the bioreactor to the desired final concentration and pump feeding was started in order to maintain a constant methanol set-point. The methanol induction phase (MIP) consisted of a feedback controlled fed-batch process, where a flame ionization detector (FID) was employed, in closed loop with a PID controller system, to measure the methanol concentration in the off-gas outlet of the bioreactor (for details, refer to Appendix I, section 9.2, Figure 9.2.2).

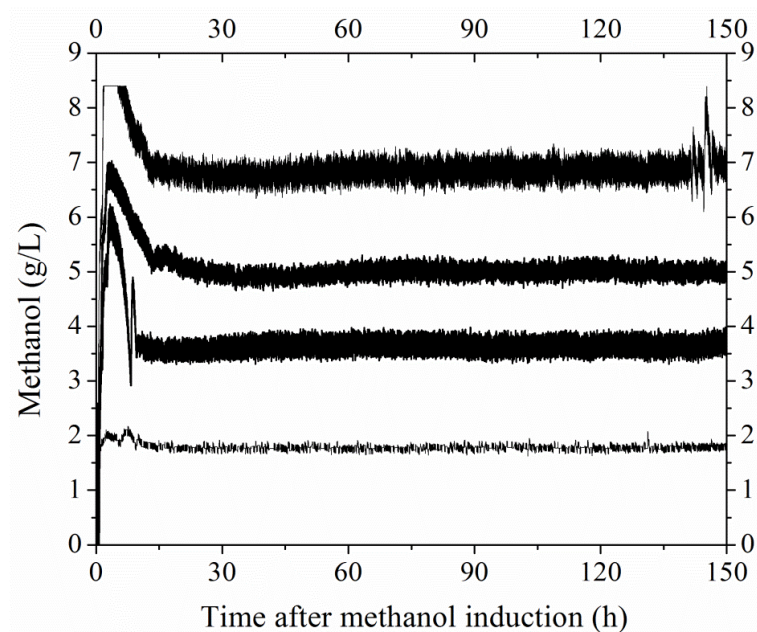


Figure 12.1.1 – Bioreactor FID feedback controlled fed-batches with different methanol concentrations.

After glycerol depletion during batch growth phase, the fed-batch cultures were induced with methanol at four different concentrations. Subsequent to initial cellular adaptation to the new substrate, methanol concentration was kept constant by a feeding pump controlled by a PID system in closed loop with a flame ionization detector (FID).

Methanol derepresses the Aox1 promoter and induces the production of secretory Insulin precursor. After the end of the growth phase – when all carbon sources were depleted and stirring decreases abruptly (DO-spike) - cultivations were induced with different methanol concentrations (Table 12.1.1). As sole carbon source during the production phase, methanol was fed in sufficient and controlled amount and its concentration was kept relatively stable during the entire production phase (Figure 12.1.1). The lowest methanol concentration tested (1.7 g/L) was under similar conditions to the two-phase fed-batch procedure employed for the secretory production of IP [2]. In this condition, the feedback controlled system used in this work was able to pump adequate methanol amounts during the entire fed-batch with the lowest set-point error (Figure 12.1.1). In the other three conditions (3.5, 5.0 and 6.8 g/L methanol), the identical PID controller parameters did not present the same performance, initially over pumping methanol, leading to higher set-point deviations during the entire fed-batch (Figure 12.1.1). In time, however, cells were able to minimize this effect, stabilizing the methanol consumption rate and producing secretory Insulin precursor (Table 12.1.1).

Table 12.1.1 – Parameters of *Pichia pastoris* X33-IP methanol fed-batch cultivations in 5 L bioreactor

| Methanol concentration during production phase (g/L)* | Conversion of methanol into IP $Y_{IP/MeOH}$ (mg/g)* | Methanol consumption rate (g/L.h)* | IP volumetric productivity (mg/L.h)* |
|--|--|---|---|
| 1.7 | 2.5 | 2.5 | 6.3 |
| 3.5 | 2.3 | 4.3 | 9.9 |
| 5.0 | 4.3 | 2.5 | 10.7 |
| 6.8 | 2.9 | 2.4 | 6.9 |

*Values employed in parameters calculations were accounted when the highest amount of IP was reached.

To compare the parameters of the four *Pichia pastoris* X33-IP fed-batch cultivations Table 12.1.1 is presented. As described for the shake flask fed-batches (Figure 5.2.2 – D), biomass production during the feedback controlled bioreactor fed-batches remains approximately constant after methanol induction, therefore the analysis of cellular specific productivity does not play an important role. The

methanol concentration of 6.8 g/L during fed-batch was similar to the conditions applied for the high-level intracellular production of Hepatitis B surface antigen (HBsAg) with *P. pastoris* GS115 [112]. Cells were able to consume and convert into IP this high methanol amount for about 75 hours after induction, presenting foaming afterwards. Since solely under this elevated substrate concentration cells presented foaming, it is viable to speculate that the highest methanol concentration that the cells can tolerate has been reached. The highest productivity was achieved when *Pichia pastoris* cells were submitted to 5.0 g/L of methanol during the fed-batch phase. The secretory Insulin precursor producing cells were able to convert more efficiently the sole substrate into product, 4.3 mg/g $Y_{IP/MeOH}$ (Table 12.1.1). Under this condition as well, cells presented the highest IP volumetric productivity, in the range of 10.7 mg/L.h. For better comparison between the four fed-batches, a plot of IP volumetric productivity vs. methanol concentration was built (Figure 12.1.2). The relation between both variables allows estimating the best methanol concentration for secretory Insulin precursor production in *Pichia pastoris* X33-IP fed-batch cultivations in 5 L bioreactor, which lies around 4.5 g/L.

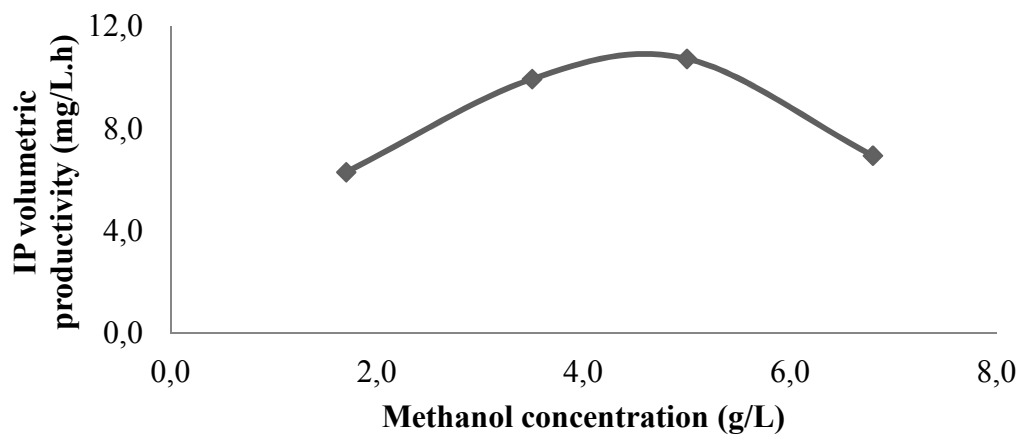


Figure 12.1.2 – Relation between methanol concentration and IP volumetric productivity for *Pichia pastoris* fed-batch cultures.

Indicated methanol concentrations were kept constant during the entire 5 L bioreactor fed-batch culture. Values employed in parameters calculations were accounted when the highest amount of IP was reached.

13. Appendix V

13.1. Images employed in the Kar2 relative quantification

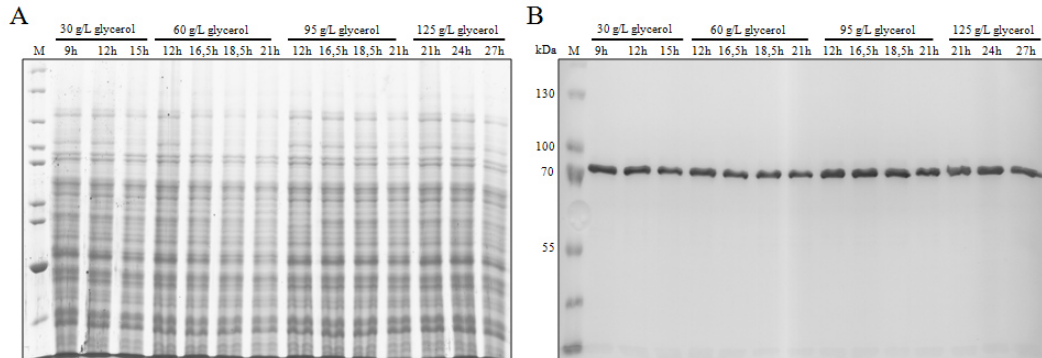


Figure 13.1.1 – SDS-PAGE and Western blot images of *Pichia pastoris* X33-IP bioreactor batches cultivated under different initial glycerol concentrations.

Respectively, the exponential phase intracellular fraction SDS-PAGE (12 %) and Western blot (anti-HDEL) time course images employed for Kar2 relative quantification from cells cultured under different initial glycerol concentrations. Samples were taken at the indicated time points during exponential phase of growth. All lysate loaded samples were normalized at OD_{600} 50 and extracellular fractions were directly applied. The M lane denotes the molecular weight marker.

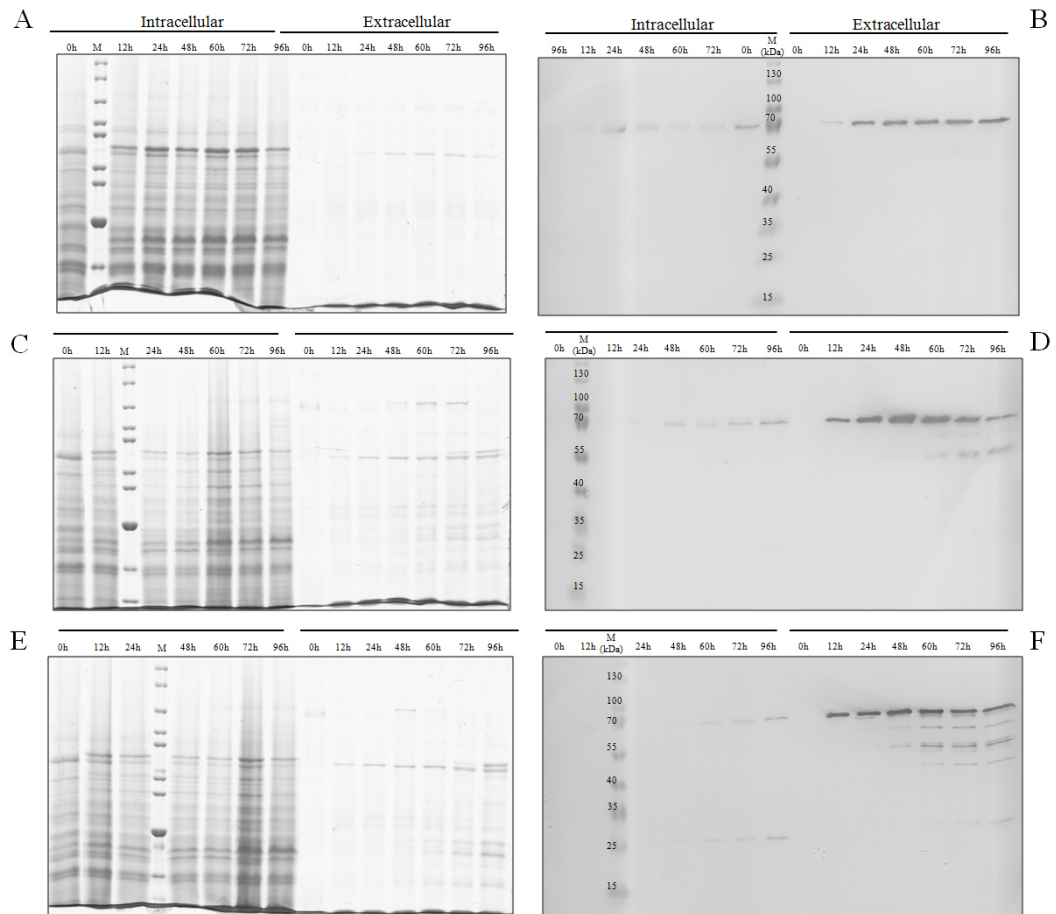


Figure 13.1.2 – SDS-PAGE and Western blot images of *Pichia pastoris* X33-IP shake flask fed-batches induced at different growth times.

Respectively, the intracellular and extracellular fractions SDS-PAGE (12 %) and Western blot (anti-HDEL) time course images employed for Kar2 relative quantification from cells harvested at exponential growth phase (A) and (B), at declining growth phase (C) and (D), at stationary phase (E) and (F). Samples were taken at the indicated time points after the start of methanol feed during shake flask fed-batch cultivations. All lysate loaded samples were normalized at OD_{600} 50 and extracellular fractions were directly applied. The M lane denotes the molecular weight marker.

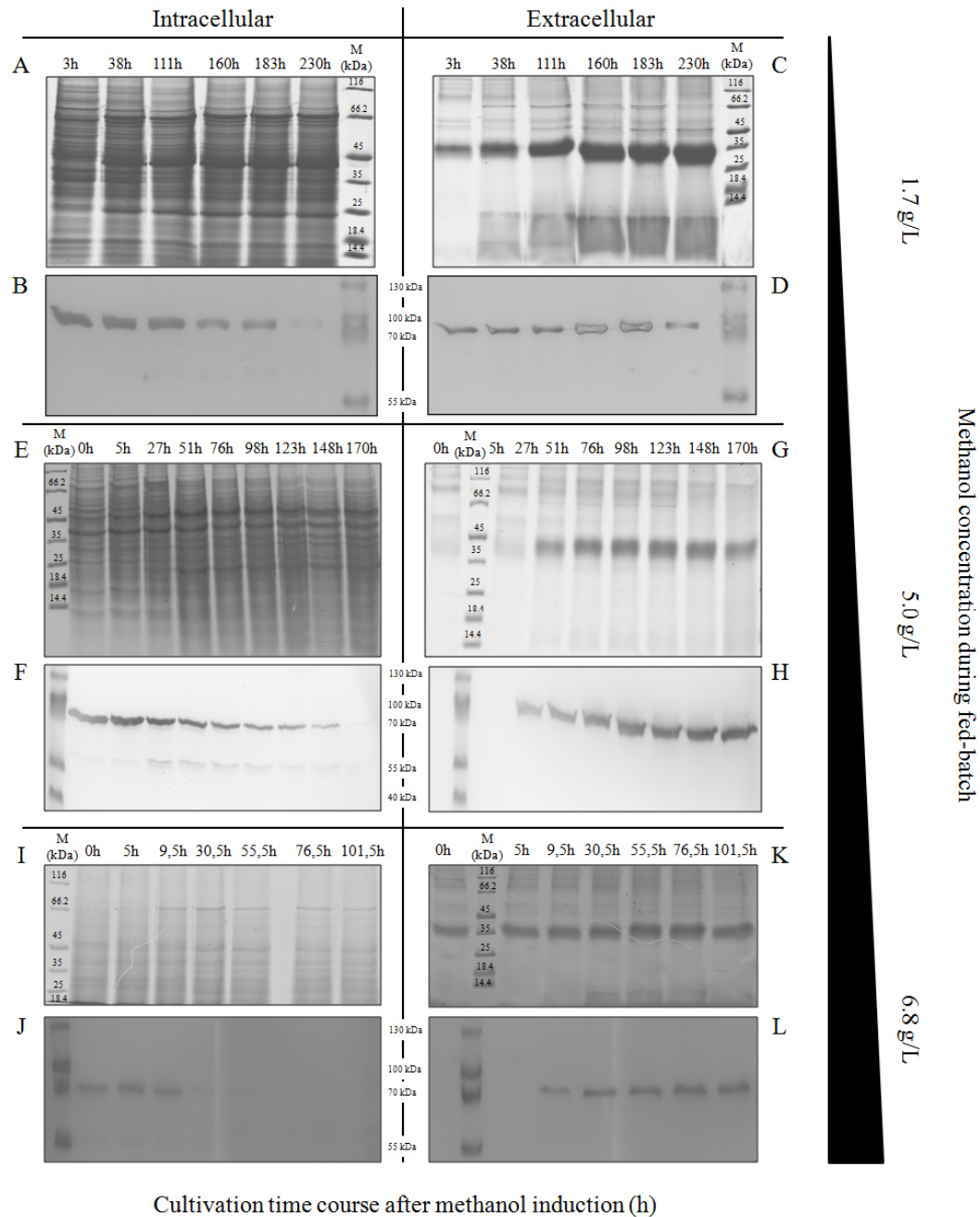


Figure 13.1.3 – SDS-PAGE and Western blot images of samples from *Pichia pastoris* X33-IP feedback controlled fed-batches.

Respectively, the intracellular and extracellular fractions SDS-PAGE (12 %) and Western blot (anti-HDEL) time course images employed for Kar2 relative quantification from feedback controlled fed-batches under: 1.7 g/L (A), (B), (C) and (D); 5.0 g/L (E), (F), (G) and (H); 6.8 g/L (I), (J), (K) and (L) methanol. Samples were taken at the indicated time points after the start of methanol feed during bioreactor fed-batch cultivations. The rectangle in the right illustrates the increase on methanol concentration from the different conditions tested. All lysate loaded samples were normalized at OD₆₀₀ 50 and extracellular fractions were directly applied. The M lane denotes the molecular weight marker.

14. Appendix VI

14.1. ROS fluorescence histograms of control experiments

Positive controls indicated that the increase in the red fluorescence intensity for propidium iodide (PI) (FL3) was negatively correlated with viable cells, and the increase of the green fluorescence intensity for 2',7'-dichlorofluorescein (DCF) (FL1) was positively correlated with intracellular ROS of yeast cells (Figure 14.1.1 – B and E, respectively). Considering that ROS is mostly generated after methanol induction, samples from the glycerol batch phase were employed as negative controls. Samples without PI and DCF staining from the glycerol batch were tested for cellular autofluorescence (Figure 14.1.1 – A and D). The indicated horizontal bar (M1) illustrated in Figure 14.1.1 – B was used to generate a gate area, which excludes the heat damaged FL3 fluorescence positive cells, allowing the qualification between viable and dead cells. Quantification of ROS was performed by the evaluation of the mean FL1 fluorescence signal intensity value for each sample incubated with DCF. Evaluation of ROS formation was performed only in viable cells through the application of the gated area in all samples. To illustrate the ROS and cellular viability quantification procedure Figure 14.1.1 – C and F are presented. Samples were double stained with PI and DCF and the fluorescence was monitored by the respective filters, FL3 and FL1. Figure 14.1.1 – F exemplifies a fluorescence histogram plot from double stained cells, harvested at glycerol exponential phase of growth, containing events gated for viable cells plotted against the DCF signal intensity (FL1). For this cultivation time point cells were 99 % viable (Figure 5.2.2 – E), according to the gate generated from the PI positive control, and presented a mean FL1 fluorescence signal intensity, which quantifies ROS formation, of 1.55 (Figure 5.2.2 – A). Curiously, the mean FL1 fluorescence signal intensity obtained for the DCF positive control, where cells were incubated for 1 h with 100 μ M DTBP, was comparable with those obtained at the end of the fed-batch cultivation.

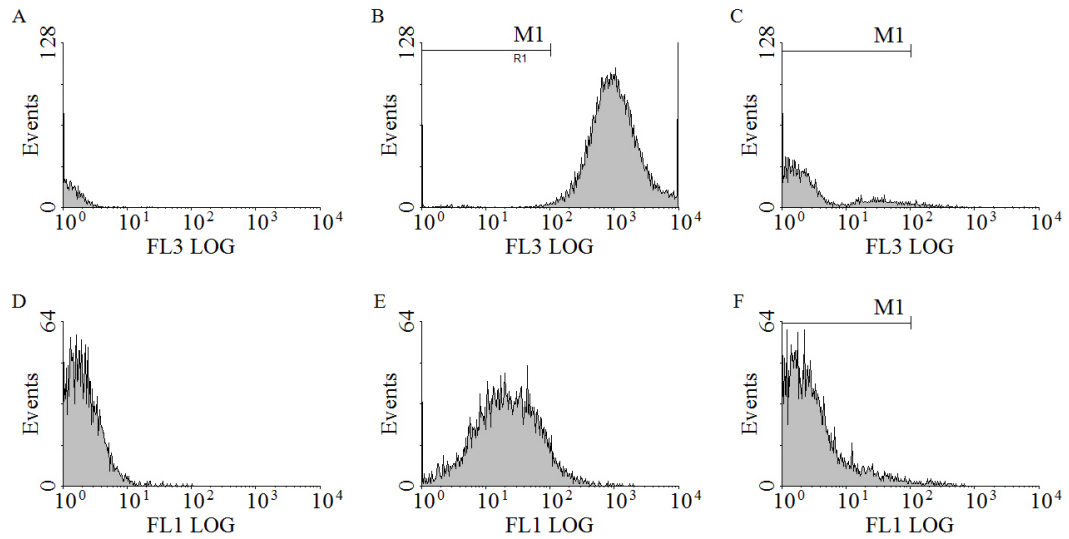


Figure 14.1.1 – Flow cytometry fluorescence histograms of control experiments.

Pichia pastoris cells viability and reactive oxygen species control experiments of (A and D) negative control, untreated glycerol batch cells without propidium iodide (PI) and 2',7'-dichlorfluorescein (DCF), (B) PI positive control, heat-killed cells, (C and F) untreated glycerol batch cells stained with PI and DCF and (E) DCF positive control, DTBP-incubated cells. FL3 LOG: fluorescence emitted by propidium iodide (PI) staining in logarithmic scale; FL1 LOG: fluorescence emitted by 2',7'-dichlorfluorescein (DCF) staining in logarithmic scale. M1 marks the gated area which represents viable cells that have not taken up PI.

15. Appendix VII

15.1. Materials

15.1.1. Strains

The *Pichia pastoris* host strain X-33 and the plasmid pPICZ α were purchased from Thermo Fisher Scientific, USA. The construction of the *P. pastoris* host strain X-33 carrying Insulin precursor gene under the control of the alcohol oxidase promoter (PAOX1) and harbouring a Mut⁺ phenotype used for this study was described previously [2].

15.1.2. Chemicals, media components, kits and other consumables

Chemicals and media components used in the present work and their sources are listed in Table 15.1.1. Pierce bicinchoninic acid (BCA) protein assay kit was obtained from Thermo Fisher Scientific, Germany. Unstained and pre-stained protein ladders were obtained from Thermo Fisher Scientific, Germany. The Streamline SPXL ion exchange resin was procured from GE Healthcare, USA. 3 μ m SUPELCOSIL™ LC-304 column (3.3 cm \times 4.6 mm) for reversed-phase high performance liquid chromatography (RP-HPLC) was purchased from Sigma-Aldrich, Germany. Aminex HPX-87H column for glycerol measurements was produced by Bio-Rad Laboratories, USA. Ethanol measurements were performed with a Supelcowax 10 column (Sigma-Aldrich, Germany). Dialysis was performed with 3 kDa molecular weight cut off Centricon tubes from Merck Millipore, Germany. Anti-HDEL (2E7 mouse monoclonal antibody was purchased from Santa Cruz Biotechnology, USA. Goat anti-mouse IgG specific peroxidase conjugate was produced by Calbiochem, USA. 3,3',5,5'-Tetramethylbenzidine (TMB) liquid substrate system for Western blot detection was obtained from Sigma-Aldrich, Germany. Polyvinylidene difluoride (PVDF) membrane for Western blotting was obtained from Bio-Rad GmbH, Germany.

Table 15.1.1 – List of chemicals used in the present work

| Chemical | Annotation | Manufacturer |
|--|--|---------------------------------------|
| Acetic acid | CH ₃ CO ₂ H | Carl Roth GmbH + Co. KG., Germany |
| Acetonitrile | CH ₃ CN | Carl Roth GmbH + Co. KG., Germany |
| Acrylamide and bisacrylamide stock solution | Rotiphorese® Gel 30 (37,5:1) | Carl Roth GmbH + Co. KG., Germany |
| Agarose | Biozym LE GP agarose | Biozym Scientific GmbH, Germany |
| Ammonia solution | NH ₄ OH (25%) | Carl Roth GmbH + Co. KG., Germany |
| Ammonium hydrogen carbonate | NH ₄ HCO ₃ | Merck KgaA, Germany |
| Ammonium persulfate | (NH ₄) ₂ S ₂ O ₈ | Sigma-Aldrich GmbH, Germany |
| Ammonium sulfate | (NH ₄) ₂ SO ₄ | Carl Roth GmbH + Co. KG., Germany |
| Antifoam Ucolub | N115 | Fragol GmbH + Co. KG., Germany |
| BD FACSTFlow Sheath Fluid | | Becton, Dickinson and Company, USA |
| D-Biotin | C ₁₀ H ₁₆ N ₂ O ₃ S | Sigma-Aldrich GmbH, Germany |
| Boric acid | H ₃ BO ₃ | Carl Roth GmbH + Co. KG., Germany |
| Bromophenol Blue | C ₁₉ H ₁₀ Br ₄ O ₅ S | Sigma-Aldrich GmbH, Germany |
| Calcium chloride dehydrate | CaCl ₂ .2H ₂ O | Carl Roth GmbH + Co. KG., Germany |
| 2',7'-dichlorodihydrofluorescein diacetate (DCFH-DA) | C ₂₄ H ₁₆ C ₁₂ O ₇ | Sigma-Aldrich GmbH, Germany |
| Coomassie Blue G250 | C ₄₇ H ₅₀ N ₃ NaO ₇ S ₂ | Merck KgaA, Germany |
| DL-Dithiothreitol (DTT) | C ₄ H ₁₀ O ₂ S ₂ | Sigma-Aldrich GmbH, Germany |
| Ethylenediaminetetraacetic acid (EDTA) | C ₁₀ H ₁₆ N ₂ O ₈ | Sigma-Aldrich GmbH, Germany |
| Ethanol (96%) | C ₂ H ₆ O | Merck KGaA, Germany |
| Formic acid | HCOOH | J.T.Baker Chemical Company, USA |
| D-Glucose | C ₆ H ₁₂ O ₆ | Carl Roth GmbH + Co. KG., Germany |
| Glycerol (86% or 99%) | C ₃ H ₈ O ₃ | Carl Roth GmbH + Co. KG., Germany |
| Glycine | C ₂ H ₅ NO ₂ | Carl Roth GmbH + Co. KG., Germany |
| Iodoacetamide | ICH ₂ CONH ₂ | GE Healthcare, United Kingdom |
| Iron(III) chloride hexahydrate | FeCl ₃ .6H ₂ O | Carl Roth GmbH + Co. KG., Germany |
| LB medium | Luria Bertani (LB) | Carl Roth GmbH + Co. KG., Germany |
| Magnesium sulphate heptahydrate | MgSO ₄ .7H ₂ O | Carl Roth GmbH + Co. KG., Germany |
| Manganese(II) sulfate | MnSO ₄ | Carl Roth GmbH + Co. KG., Germany |
| 2-Mercaptoethanol | C ₂ H ₆ OS | Sigma-Aldrich GmbH, Germany |
| Methanol | CH ₃ OH | Carl Roth GmbH + Co. KG., Germany |

| Chemical | Annotation | Manufacturer |
|--|--|------------------------------------|
| Dimethyl sulfoxide (DMSO) | $(\text{CH}_3)_2\text{SO}$ | Sigma-Aldrich GmbH, Germany |
| Peptone | Bacto™ Proteose Peptones | Difco Laboratories Inc., USA |
| Phosphoric acid | H_3PO_4 (85%) | Carl Roth GmbH + Co. KG., Germany |
| Potassium chloride | KCl | Carl Roth GmbH + Co. KG., Germany |
| Potassium iodide | KI | Carl Roth GmbH + Co. KG., Germany |
| Potassium phosphate dibasic | K_2HPO_4 | Carl Roth GmbH + Co. KG., Germany |
| Potassium phosphate monobasic | KH_2PO_4 | Carl Roth GmbH + Co. KG., Germany |
| 2-Propanol | $\text{C}_3\text{H}_8\text{O}$ | Carl Roth GmbH + Co. KG., Germany |
| Propidium iodide | $\text{C}_{27}\text{H}_{34}\text{I}_2\text{N}_4$ | Sigma-Aldrich GmbH, Germany |
| Polyvinylpyrrolidone | $(\text{C}_6\text{H}_9\text{NO})_n$ | Sigma-Aldrich GmbH, Germany |
| Silicon M100 | $(\text{C}_2\text{H}_6\text{OSi})_n$ | Carl Roth GmbH + Co. KG., Germany |
| Polydimethyl siloxane | | Becton, Dickinson and Company, USA |
| Skim milk | Skim milk | Carl Roth GmbH + Co. KG., Germany |
| Sodium chloride | NaCl | Bio-Rad Laboratories GmbH, Germany |
| Sodium dodecyl sulphate | $\text{NaC}_{12}\text{H}_{25}\text{SO}_4$ | Carl Roth GmbH + Co. KG., Germany |
| Sodium hydrogen phosphate | NaH_2PO_4 | Carl Roth GmbH + Co. KG., Germany |
| Disodium hydrogen phosphate | Na_2HPO_4 | Carl Roth GmbH + Co. KG., Germany |
| Sodium hydroxide | NaOH | Carl Roth GmbH + Co. KG., Germany |
| Sodium molybdate | Na_2MoO_4 | Carl Roth GmbH + Co. KG., Germany |
| Sulphuric acid | H_2SO_4 | Carl Roth GmbH + Co. KG., Germany |
| Tetramethylethylenediamine (TEMED) | $\text{C}_6\text{H}_{16}\text{N}_2$ | Sigma-Aldrich GmbH, Germany |
| Trifluoroacetic acid (TFA) | $\text{C}_2\text{HF}_3\text{O}_2$ | Merck KgaA, Germany |
| 3,3',5,5'-tetramethylbenzidine (TMB) | $\text{C}_{16}\text{H}_{20}\text{N}_2$ | Sigma-Aldrich GmbH, Germany |
| Tris(hydroxymethyl)aminomethane (Tris) | $\text{C}_4\text{H}_{11}\text{NO}_3$ | Carl Roth GmbH + Co. KG., Germany |
| Triton X-100 (polyethylene glycol p-(1,1,3,3-tetramethylbutyl)-phenyl ether) | $\text{C}_{14}\text{H}_{22}\text{O}(\text{C}_2\text{H}_4\text{O})_n$ | Sigma-Aldrich GmbH, Germany |
| Tween 20 (Polysorbate 20) | $\text{C}_{58}\text{H}_{114}\text{O}_{26}$ | Sigma-Aldrich GmbH, Germany |
| Yeast extract | Y.E. | Bio-Rad Laboratories GmbH, Germany |
| Yeast nitrogen base w/o amino acids and $(\text{NH}_4)_2\text{SO}_4$ | Y.N.B. | Becton, Dickinson and Company, USA |
| Zinc sulphate heptahydrate | $\text{ZnSO}_4 \cdot 7\text{H}_2\text{O}$ | Carl Roth GmbH + Co. KG., Germany |

15.1.3. Equipments and laboratory tools

| | |
|---------------------------------------|---|
| 10 L stirred tank reactor | Biostat [®] C, Sartorius AG, Germany |
| 2 L stirred tank reactor | Biostat [®] B plus, Sartorius AG, Germany |
| 5 L stirred tank reactor | Biostat [®] B plus, Sartorius AG, Germany |
| Autoclave | Systemk GmbH, Germany |
| Centrifuges | Thermo Fisher Scientific Inc., Germany Heraeus Instruments GmbH, Germany |
| Clean bench | Thermo Fisher Scientific Inc., Germany |
| Electroblot semi-dry transfer chamber | Bio-Rad Laboratories GmbH, Germany |
| Electrophoresis Chambers | Bio-Rad Laboratories GmbH, Germany |
| Flow cytometer | Epics XL-MCL, Beckman Coulter Inc., USA |
| Gas chromatograph | GC-2010 plus, Shimadzu Corp., Japan |
| Gas sensors | BlueSens GmbH, Germany |
| Glassware | Schott AG, Germany |
| HPLC system | Chromaster, Hitachi Inc., USA |
| Ice machine | Ziegrea Eismachinen GmbH, Germany |
| Incubator | Infors AG, Switzerland Certomat [®] BS-1, Sartorius AG, Germany |
| Microwave | MLS GmbH, Germany |
| Osmometer | Gonotec GmbH, Germany |
| Peristaltic pump | SciLog Inc., USA |
| Phase contrast microscope | Olympus GmbH, Germany |
| pH-electrode, inline | Hamilton Messtechnik GmbH, Germany |
| pH-meter | Deutsche Metrohm GmbH & Co. KG, Germany |
| Pipette (1000, 200, 100, 20 µL) | Eppendorf GmbH, Germany |

| | |
|------------------------------------|--|
| pO ₂ -elektrode, inline | Hamilton Messtechnik GmbH, Germany |
| Scale | Sartorius AG, Germany |
| Shake flasks 150 mL, disposable | Sigma-Aldrich GmbH, Germany |
| Spectrophotometer | Thermo Fisher Scientific Inc., Germany |
| Ultrapure water system | Sartorius AG, Germany |
| Vortex | Phoenix, Germany |

15.2. List of figures

| | |
|---|----|
| Figure 1.1 – Fellowship sponsors..... | 12 |
| Figure 2.2.1 – Amino acid sequences of human, bovine and porcine Insulin. | 14 |
| Figure 2.3.1 – <i>Pichia pastoris</i> X33-IP (A) isolated colonies grown in agar plates and (B) In situ microscopy image of high cell density culture in 10 L bioreactor. 16 | |
| Figure 2.4.1 – Schematic representation of protein folding and secretion in ER. Modified based on [35]...... | 18 |
| Figure 2.4.2 – The folding cycle of Kar2, a chaperone belonging to the Hsp70 family. Figure modified based on [47]..... | 23 |
| Figure 2.4.3 – Diagram representing the protein folding, secretion, UPR and ERAD in yeast. Modified based in [73]..... | 24 |
| Figure 2.6.1 –Oxidative protein folding in the yeast ER diagram. Modified from [97]...... | 28 |
| Figure 5.1.1 – Time course analysis of the bioreactor glycerol batch from <i>Pichia pastoris</i> X33-IP cells..... | 43 |
| Figure 5.1.2 – Media osmolarity decreases concomitant to glycerol reduction. | 44 |
| Figure 5.1.3 – Monitoring Kar2 in the intracellular and extracellular fractions of methanol fed-batch phase in shake flasks of <i>P. pastoris</i> cells harvested at different glycerol growth phase and time course analysis of secretory Insulin precursor production. | 48 |
| Figure 5.1.4 – Comparison of intracellular and extracellular Kar2 at fed-batch methanol induction time. | 49 |
| Figure 5.1.5 – Effect of different fed-batch methanol concentrations on intracellular and extracellular Kar2 and on secretory Insulin precursor production..... | 51 |
| Figure 5.2.1 – ROS, viability and optical density of 4 different <i>Pichia pastoris</i> strains. | 54 |
| Figure 5.2.2 – Methanol shake flask fed-batches time course monitoring and comparison of X33-IP cells..... | 56 |
| Figure 9.1.1 – Optical density time course comparison of <i>P. pastoris</i> X33-IP grown in different inoculum media in shake flasks. | 77 |
| Figure 9.2.1 – Schematic of a closed loop PID feedback controller applied in the fed-batches. | 79 |

| | |
|--|----|
| Figure 9.2.2 – Two-phase fed-batch cultivation of <i>P. pastoris</i> X-33 secreting Insulin precursor. | 80 |
| Figure 9.2.3 – SDS-PAGE time course analysis of <i>Pichia pastoris</i> X33-IP intracellular and extracellular fractions after methanol induction. | 81 |
| Figure 9.2.4 – SDS-PAGE and Western blot glycerol batch phase time course of the methanol feedback controlled fed-batch. | 81 |
| Figure 9.3.1 – Streamline SP XL ion exchange FPLC chromatogram and SDS-PAGE 16 % purification steps. | 82 |
| Figure 9.4.1 – Purified Insulin precursor quantification curve by RP-HPLC. | 83 |
| Figure 10.1.1 – Time course analysis of the 95 g/L bioreactor glycerol batch and shake flask fed-batch from <i>Pichia pastoris</i> X33 host cells..... | 85 |
| Figure 11.1.1 – 12 % SDS-PAGE Coomassie blue stained gel highlighting the identified protein bands..... | 87 |
| Figure 12.1.1 – Bioreactor FID feedback controlled fed-batches with different methanol concentrations. | 88 |
| Figure 12.1.2 – Relation between methanol concentration and IP volumetric productivity for <i>Pichia pastoris</i> fed-batch cultures. | 90 |
| Figure 13.1.1 – SDS-PAGE and Western blot images of <i>Pichia pastoris</i> X33-IP bioreactor batches cultivated under different initial glycerol concentrations..... | 91 |
| Figure 13.1.2 – SDS-PAGE and Western blot images of <i>Pichia pastoris</i> X33-IP shake flask fed-batches induced at different growth times..... | 92 |
| Figure 13.1.3 – SDS-PAGE and Western blot images of samples from <i>Pichia pastoris</i> X33-IP feedback controlled fed-batches..... | 93 |
| Figure 14.1.1 – Flow cytometry fluorescence histograms of control experiments. | 95 |

15.3. List of tables

| | |
|--|----|
| Table 4.6.1 – Composition of resolving and stacking SDS-PAGE gels | 36 |
| Table 5.1.1 – Comparison of <i>Pichia pastoris</i> batches with different glycerol concentrations | 45 |
| Table 12.1.1 – Parameters of <i>Pichia pastoris</i> X33-IP methanol fed-batch cultivations in 5 L bioreactor | 89 |
| Table 15.1.1 – List of chemicals used in the present work..... | 97 |

15.4. Abbreviations

| | |
|------------------------------------|--|
| % | Percent |
| [C _{co2}] _{in} | Inlet carbon dioxide concentration (%) |
| [C _{co2}] _{out} | Outlet carbon dioxide concentration (%) |
| [C _{o2}] _{in} | Inlet oxygen concentration (%) |
| [C _{o2}] _{out} | Outlet oxygen concentration (%) |
| °C | Degrees Celsius |
| μ | Specific growth rate (h ⁻¹) |
| μL | Microliter |
| μm | Micrometer |
| μ _{max} | Maximal specific growth rate (h ⁻¹) |
| μ _{s Gly} | Specific glycerol consumption rate (h ⁻¹) |
| aa | Amino acid |
| AAA | ATPases associated with diverse cellular activities |
| ADP | Adenosine diphosphate |
| Aox1 | Alcohol oxidase 1 |
| <i>AOX1</i> | Alcohol oxidase 1 gene |
| Aox2 | Alcohol oxidase 2 |
| <i>AOX2</i> | Alcohol oxidase 2 gene |
| ATP | Adenosine triphosphate |
| bar | Unit of pressure |
| BCA | Bicinchoninic acid protein assay kit |
| BiP | Immunoglobulin heavy chain-binding protein (syn. Kar2) |
| bp | Base pair |
| BSA | Bovine serum albumin |
| Cdc48 | Chaperone-like AAA ATPase in yeast |
| cm | Centimeter |
| Cne1 | Calnexin homolog in <i>S. cerevisiae</i> |
| CO ₂ | Carbon dioxide |
| CopI | Coat protein complex I |
| CopII | Coat protein complex II |
| CPR | Carbon production rate |
| Cta | Catalase |
| Dak | Dihydroxyacetone kinase |
| Das | Dihydroxyacetone synthase |
| DCF | 2',7'-dichlorofluorescein |
| DCM | Dry cell mass (g/L) |
| DHA | Dihydroxyacetone |
| DHAP | Dihydroxyacetone phosphate |
| DnaJ | Co-chaperone from <i>E. coli</i> homolog to Hsp40 |
| DnaK | Chaperone from <i>E. coli</i> homolog to |

| | |
|-----------------------|--|
| DO | Hsp70 Dissolved oxygen (%) |
| ER | Endoplasmic reticulum |
| ERAD | Endoplasmic-reticulum-associated protein degradation |
| Erd2 | Endoplasmic reticulum retention defective, ER membrane protein |
| Ero1 | Oxidoreductin 1, ER membrane protein |
| <i>ERO1</i> | Oxidoreductin 1 gene |
| ESR | Environmental stress response |
| F _{1,6} BP | Fructose 1,6-bisphosphate |
| F ₆ P | Fructose 6-phosphate |
| FAD | Flavin adenine dinucleotide |
| Fdh | NAD(+)-dependent formate dehydrogenase |
| Fgh | S-formylglutathione hydrolase |
| FID | Flame ionization detector |
| F _{in} | Inlet air flow (L/min) |
| Fld | Formaldehyde dehydrogenase |
| F _{out} | Outlet air flow (L/min) |
| <i>FPS1</i> | Plasma membrane glycerol efflux channel |
| g | Gram |
| GAP | Glyceraldehyde 3-phosphate |
| GC | Gas chromatography |
| <i>GDP1</i> | Glycerol-3-phosphate dehydrogenase |
| Grp78 | Immunoglobulin heavy chain-binding protein (syn. Kar2) |
| GS-CH ₂ OH | S-hydroxymethyl glutathione |
| GS-CHO | S-formylglutathione |
| GSH | Reduced form of glutathione |
| GSSG | Oxidized glutathione |
| h | Hour |
| H ₂ O | Water |
| Hac1 | UPR transcription factor |
| <i>HAC1</i> | UPR transcription factor gene |
| HDEL | C-terminal tetrapeptide ER retention signal in yeast |
| HOG | High osmolarity glycerol pathway |
| Hsp | Heat shock protein |
| Hsp110 | Heat shock protein/chaperone family 110 |
| Hsp40 | Heat shock protein/chaperone family 40 |
| Hsp60 | Heat shock protein: family 60; tetradecameric mitochondrial chaperonin |
| Hsp70 | Heat shock protein/chaperone family 70 |

| | |
|-------------------|--|
| Hsp82 | Heat shock protein/chaperone family 90 |
| Hsp90 | Heat shock protein/chaperone family 90 |
| HspA5 | Immunoglobulin heavy chain-binding protein (syn. Kar2) |
| IgG | Immunoglobulin G |
| Ire1 | Serine-threonine kinase and endoribonuclease, transmembrane protein |
| Kar2 | Immunoglobulin heavy chain-binding protein |
| <i>KAR2</i> | Immunoglobulin heavy chain-binding protein gene |
| kDa | Kilodalton |
| KDEL | C-terminal tetrapeptide ER retention signal in mammals |
| Kg | Kilogram |
| L | Liter |
| mAU | Milliabsorbance units |
| MF α | <i>Saccharomyces cerevisiae</i> α -mating factor pre-pro-peptide signal leader sequence |
| min | Minute |
| mL | Milliliter |
| mm | Millimeter |
| <i>MM</i> | Molecular mass (g/mol) |
| mmol | Millinumber of atoms 6.0221415×10^{23} |
| mol | Number of atoms 6.0221415×10^{23} |
| mRNA | Messenger RNA |
| mS | Millisiemens |
| Mut ⁻ | Methanol utilization minus <i>P. pastoris</i> strain |
| Mut ⁺ | Methanol utilization plus <i>P. pastoris</i> strain |
| Mut ^s | Methanol utilization slow <i>P. pastoris</i> strain |
| NEF | Nucleotide exchange factors |
| nm | Nanometer |
| O ₂ | Oxygen |
| OD ₆₀₀ | Optical density measured at 600 nm |
| osmol | osmotic active units (in mol) |
| OUR | Oxygen uptake rate |
| PAOX1 | Alcohol oxidase promoter |
| PBS | Phosphate buffered saline solution with 1 % (v/v) Tween 20 |
| PBS | Phosphate buffered saline solution |
| PDI | Protein disulfide isomerase |
| <i>PDI</i> | Protein disulfide isomerase gene |

| | |
|----------------------|---|
| pH | pH value, negative log of the activity of the hydrogen ion in an aqueous solution |
| PI | Propidium iodide |
| PPI | Peptidyl prolyl isomerase |
| PVDF | Polvinylidene fluoride |
| QC | Quality control |
| Rgl1 | Transfer RNA ligase |
| ROS | Reactive oxygen species |
| RP- HPLC | Reversed-phase high performance liquid chromatography |
| rpm | Rotations per minute |
| RQ | Respiratory quotient |
| SDS-PAGE | Sodium dodecylsulfate polyacrylamide gel electrophoresis |
| Sec61 | Translocon pore complex |
| Ssa3 | Heat shock protein/chaperone family 70 |
| Ssa4 | Heat shock protein/chaperone family 70 |
| Ssb1 | Heat shock protein/chaperone family 70 |
| Sso2 | Plasma membrane t-SNARE involved in secretion |
| T | Temperature |
| TEMED | N, N, N', N'- Tetramethylethylenediamine |
| TMB | 3, 3', 5, 5'- Tetramethylbenzidine |
| UGGT | (UDP)-glucose:glycoprotein glucosyltransferase |
| UPR | Unfolded protein response |
| v/v | Volume per volume |
| V_m | Ideal gas molecular volume (L/mol) |
| V_R | Bioreactor volume (L) |
| vvm | Volume of medium per volume of air ($L_{\text{medium}}/L_{\text{air}}$) |
| w/v | Weight per volume |
| w/w | Weight per weight |
| X33 | <i>Pichia pastoris</i> host strain |
| X33-IP | <i>Pichia pastoris</i> secretory Insulin precursor producing strain |
| Xu ₅ P | Xylulose 5-phosphate |
| $Y_{\text{DCM/Gly}}$ | Conversion of glycerol in biomass ($g_{\text{DCM}}/g_{\text{Gly}}$) |
| YNB | Yeast nitrogen base without amino acids and ammonium sulfate |
| YTM | Yeast trace metal solution |

16. Curriculum Vitae

Personal information

Name: Gustavo Roth
Date of Birth: 25.09.1986
Place of Birth: Caxias do Sul/RS, Brazil
Nationality: Brazilian and Italian

Education

Sep/2012 – Sep/2015 **PhD student**

Biochemistry
Institute of Technical Chemistry
Leibniz Universität Hannover (LUH), Germany
Advisors: Prof. Dr. Thomas Scheper and
Prof. Dr. Ursula Rinas

Jan/2010 – Apr/2012 **Mestre em Biologia Celular e Molecular**

Master in cellular and molecular biology
Pontifícia Universidade Católica do Rio Grande do Sul
(PUC-RS), Porto Alegre, Brazil
Advisors: Prof. Dr. Diógenes S. Santos and
Prof. Dr. Luiz A. Basso

Mar/2004 – Dez/2010 **Engenheiro Químico**

Chemical engineer degree
Pontifícia Universidade Católica do Rio Grande do Sul
(PUC-RS), Porto Alegre, Brazil

Publications

Roth, G., Nunes, J. E. S., Rosado, L. A., Bizarro, C. V., Volpato, G., Nunes, C. P., Renard, G., Basso, L. A., Santos, D. S., & Chies, J. M. (2013). **Recombinant *Erwinia carotovora* l-asparaginase II production in *Escherichia coli* fed-batch cultures.** *Brazilian Journal of Chemical Engineering*, 30, 245–256.

Posters

Vanz AL, Lünsdorf H, **Roth G**, Nöhren G, Rinas U. Autophagy in recombinant *Pichia pastoris*: adaptation response to nutrient conditions. 7th Conference on Recombinant Protein Production – RPP7 (Laupheim, 2013).